MOLECULAR STRUCTURE ANALYSES OF ASYMMETRIC HYDROCARBON LIQUID COMPOUNDS IN THE GAS PHASE USING CHIRPED-PULSE FOURIER TRANSFORM MICROWAVE SPECTROSCOPY: ACYL CHLORIDES AND PERFLUORINATED ACYL CHLORIDES

Robert A. Powoski, B.S.

Thesis Prepared for Degree of

MASTER OF SCIENCE

UNIVERSITY OF NORTH TEXAS

August 2011

APPROVED:

Stephen A. Cooke, Major Professor
Teresa Golden, Committee Member
William E. Acree, Jr., Chair of the Department of Chemistry
James D. Meernik, Acting Dean of the Toulouse Graduate School

Powoski, Robert A. Molecular Structure Analyses of Asymmetric Hydrocarbon Liquid Compounds in the Gas Phase Using Chirped-pulse Fourier Transform Microwave Spectroscopy: Acyl Chlorides and Perfluorinated Acyl Chlorides. Master of Science (Chemistry-Analytical Chemistry), August 2011, 106 pp., 25 tables, 12 illustrations, references, 89 titles.

Examinations of the effects of (a.) alkyl carbon chain length and (b.) perfluorination of acyl chlorides; propionyl chloride, butyryl chloride, valeroyl chloride, and perfluorinated acyl chlorides; perfluoropropionyl chloride and perfluorobutyryl chloride, are reported and compared using CP-FTMW spectroscopy. All of these molecules are already published in various journals except for valeroyl chloride. The chapters are organized by molecule alkyl chain length and include some background theory. Conformational stability, internal rotation, helicity, and ionic character of the C-Cl bond via the nuclear electric quadrupole coupling constant (χ_{zz}) are analyzed. Results show syn, syn-anti/syn-gauche, and syn-anti-anti/syn-gauche-anti stable conformations. Internal rotation was only seen in propionyl chloride. Helicity was not observed. (χ_{zz}) was observed to be inert to alkyl chain length, ~ 60 MHz and ~ 65 MHz for the nonfluorinated and fluorinated acyl chlorides. Partial fluorination and varying functional groups are recommended.

ACKNOWLEDGEMENTS

I would like to thank the Department of Chemistry at the University of North Texas (UNT) and the National Science Foundation (NSF) for financial support as a NSF-REU undergraduate student and as a graduate student. The NSF-REU funding gave me the opportunity to do research as an undergraduate student, which persuaded me to get my Master's degree. Without these sources of funding, such as the UNT startup fund and the National Science Foundation Research Grant for Dr. Stephen Cooke, purchase of the necessary chemicals, instrument components, and therefore the opportunity to do research would not have been possible. I would also like to thank Dr. G.S. Grubbs II for letting me include his data on perfluorobutyryl chloride into my thesis for comparison purposes. I would especially like to thank Dr. Stephen Cooke for his time spent mentoring and advising me throughout my career as an undergraduate and graduate student.

TABLE OF CONTENTS

Page

CHAPTER 1

BACKGROUND, MOTIVATION, AND APPLICATION OF MOLECULES

1.1 Acyl Chloride Background

In this work, a series of acyl chlorides and perfluorinated acyl chlorides were studied. Namely, the molecules in this study are propionyl chloride (CH_3CH_2COCl), butyryl chloride ($CH_3CH_2CH_2COCl$), valeroyl chloride ($CH_3CH_2CH_2CH_2COCl$), perfluoropropionyl chloride (CF_3CF_2COCl), and perfluorobutyryl chloride ($CF_3CF_2CF_2COCl$). Of this list of acyl chlorides, all of them are corrosive, and most are liquids at standard temperature and pressure (STP). Acyl chlorides have a very characteristic odor that are identifiable from far distances and react readily with water to produce a carboxylic acid and hydrochloric acid. Some of their chemical properties can be found in material safety data sheets (MSDS) and chemical supply company catalogs but not all of them. There is limited information on the chemical properties of these molecules in MSDS databases. Table 1.1 lists some of the properties that were gathered for the acyl chlorides and their perfluoroinated counterparts. In this table, there is a trend of increasing boiling point with increasing parent chain length and a decreasing boiling point with perfluorination of the parent chain. Also, there is a decreasing vapor pressure with increasing parent chain length. The fact that not all of the properties are known or reported for these molecules in the MSDS sheets highlights the importance of quantifying and reporting as much information about them as possible. This is one of the motivations of the study. However, there are a manifold of reasons and motivations for choosing to examine acyl chlorides and perfluorinated acyl chlorides using chirped-pulse Fourier transform microwave (CP-FTMW) spectroscopy.

Acyl chlorides have many different synonyms based on different naming conventions. For example, valeroyl chloride is synonymous with pentanoyl chloride or valeryl chloride.

However, the names of the acyl chlorides used in this study are propionyl chloride, butyryl chloride, and valeroyl chloride. Perfluoropropionyl chloride is synonymous with pentafluoropropionyl chloride. The naming system chosen for the perfluorinated acyl chlorides were as follows: perfluoropropionyl chloride, perfluorobutyryl chloride, and perfluorovaleroyl chloride to ease the comparison of molecules. All of these molecules have been experimentally studied directly by me with the exception of perfluorobutyryl chloride done by Dr. Gary S. Grubbs II, which I gratefully acknowledge. Perfluorobutyryl chloride was included in this study to further complete the series of the molecular structure and electronic structure of acyl chloride and perfluoroacyl chloride trend.

1.2 Literature Search of Published Related Work

The following are a list of references that use microwave spectroscopy methods applied to acyl halide related molecules. [1, 2, 3, 4 , 5, 6, 7, 8, 9, 10, 11] Some of the microwave spectroscopy studies that have methyl internal rotation include the following references. [3, 12, 13, 14, 15, 16] Of the studies that had internal rotation, most consisted of small alkane related molecules with no more than 3 carbons in the parent chain, even with an OH or C=O functional group. However, butyronitrile had internal rotation while butyryl chloride did not according to the low resolution FTMW study by Mata, and another by Vorman. [3, 17]

Helicity has been explored slightly for alkane and alkenes and some of their perfluorinated counterparts by Bohn et al. and others. [18, 19, 20]. There is more than one method to measure helicity, such as electron diffraction (ED) spectroscopy, circular dichroism (CD) spectroscopy, and Fourier transform microwave (FTMW) spectroscopy.

Table 1.1: Chemical properties of acyl chlorides and perfluorinated acyl chlorides

	Propionyl Chloride	Butyryl Chloride	Valeroyl Chloride	Perfluoropropionyl Chloride	Perflurorobutryl Chloride	Perfluorovaleroyl Chloride
Molecular Formula	CH_3CH_2COCl	$CH_3CH_2CH_2COCl$	$CH_3CH_2CH_2CH_2COCl$	CF_3CF_2COCl	$CF_3CF_2CF_2COCl$	$CF_3CF_2CF_2CF_2COCl$
Boiling Point (^{0}C)	77-79	98-102	125-129	7-9	38	67-68
Flash Point (^{0}C/^{0}F)	6/43 [a]	18/64	32/90	-	38-39 [c]	-
Vapor Pressure	-	39 mmHg @ 20 °C [b]	8.6 mmHg @ 20 °C [b]	1291 mmHg @ 20°C [a]	-	Evaporates quickly
Vapor Density vs Air	3.19	3.7	-	-	-	-
pH	7	-	-	-	-	-
Phase	Liquid (Clear)	Liquid (Clear)	Liquid (Clear)	Gas@ 20°C	Liquid(clear)	Liquid (Clear)
mp (^{0}C/^{0}F)	-94/-137	-89/-129	-	-	-	-
Source	MSDS-Aldrich	Aldrich Catalog	Fluka bottle	Synquest Catalog	Synquest Catalog	Synquest Catalog

[a] Sigma Aldrich catalog
[b] http://www.shivapharmachem.com/msds
[c] http://www.chemicalbook.com/ChemicalProductProperty_EN_CB8126331.htm

CD spectroscopy identifies helicity of liquids using circularly polarized radiation while CP-FTMW spectroscopy uses linearly polarized radiation. The circularly polarized radiation enables detection of the difference between absorption of left-handed circularly polarized light (L-CPL) and right-handed circularly polarized light (R-CPL) when a molecule contains one or more chiral light-absorbing group. [21] In CD spectroscopy methods, the molecules are measured over a range of wavelengths and are often used to explore a helical molecule's secondary conformation as its environment is changed where structural, kinetic and thermodynamic information about macromolecules can be derived. [21] In other words, exploring the secondary structure utilizes helicity modulation (HM) of circularly polarized light to measure circular dichroism in soft X-ray absorption. [21] However, CP-FTMW spectroscopy simply uses linearly polarized radiation to characterize the exact bond lengths, bond angles, and dihedral angles that enable helicity to be easily calculated. [21] For example, Fournier et al. (2009) [18] thoroughly define helicity in two perspectives, the helical perspective and the molecular perspective. [18]

The helical perspective measures helicity as function of the following molecular parameters: helical angle made about the helical axis, Θ, the CCCC dihedral angles, τ, and the CCC angles, φ, as defined in the Fournier et al. study. [18] The molecular perspective similarly measures helicity, but as function of the following helical parameters: the C-C bondlengths, r; CCC bond angles, φ; and CCCC dihedral angles, τ. [18] This helical axis is near co-axial with the a-axis when in principal coordinate notation. When looking down the principal a-axis in principal coordinate notation, a staggered orientation of the hydrogens exists for pentane. [18] However, a more helical orientation of the fluorines in perfluoropentane results in about a 17^0 from 180^0 dihedral angle twist. [18] For polytetrafluoroethylene (PTFE) below 19^0 C, the chain twists 180^0 every 13 carbon atoms, which has helical angles of 13.8^0 or ~163^0 dihedral angle. [18]

The higher the temperature, the less twisting is observed. Knowing this, it would be interesting to compare the role of perfluorination on helicity of alkanes to alkanes that have different functional groups attached.

The ab initio computational work on polytetrafluoroethylene (Teflon®) related compounds done by D. Dixon (1988) suggested that the helicity begins with four carbons according to perfluorinated butane and suggest that the perfluorination is what causes the helicity.[20] Specifically, the reason given for the helicity is due to the electronic properties of the isolated chains and not to crystal packing forces.[20] Other microwave spectroscopy studies performed on related alkanes, alkenes, and alkynes include the following:[18, 19, 20, 22, 23, 24, 25, 26, 27, 28, 29, 30, 3, 16]. Alkyl chains with CN and CCH substituent's prefer gauche conformations, which is another reason why studying acyl chlorides would be important in comparing their Newman projections to this trend with CN and CCH functional groups.[23] It is predicted that the acyl chloride group will also have gauche conformations because of the study by Restrepo and Bohn (2007).[23] Literature searches[31] also show that there is interest and room for further contribution in the area surrounding the several effects of perfluorination on hydrocarbons[18, 22] and functionalized hydrocarbons.[8, 32, 33] The structural effects of perfluorination include (i) differing lowest energy conformations and (ii) reduced conformational flexibility of perfluorinated compounds compared to the hydrogenated analogues.

1.3 Motivation and Application

The first motivation and reason for choosing to study acyl chlorides and perfluorinated acyl chlorides is because the molecular and electronic structure of these molecules using microwave spectroscopy have either never been reported at all or were reported with minimal information that used low resolution Fourier transform microwave (FTMW) spectroscopy

methods. [2, 1, 4, 3] The resolution of the 1978 study on butyryl chloride, butyryl bromide, and butyryl fluoride and the 1984 butyronitrilevs butyryl chloride study were labeled "low" resolution because they had a resolution range of 5,000 – 25,000 kHz. [4, 3] This resolution is significantly limiting in resolving hyperfine structure frequencies and other details. On the other hand, the 1976 and 1979 studies are accurate within 0.05 MHz of the observed frequency unless stated otherwise translating into an approximate resolution of 50 kHz. [1] This is the same official resolution of the CP-FTMW in its current arrangement at the University of North Texas (UNT). Although the CP-FTMW spectrometer at UNT in its current arrangement has the same official resolution of 50 kHz, it has the additional advantage of providing correct line intensities with a significantly larger bandwidth by about 2000 MHz more than the cavity FTMW spectrometer. This enabled a more exhaustive examination of these molecules and therefore it is reported in this study. Therefore, one of the motivations of this study is to provide an opportunity to compare low resolution FTMW spectroscopy from the 1970s to high resolution studies using cavity FTMW in the 1980's and CP-FTMW spectroscopy currently at the University of North Texas (UNT). All data can be found at the end of each of the molecule chapters 4, 5, and 6 for reference and examination.

Secondly, the main goal of this study is to compare and examine how molecular structure and electronic of a series of acyl chlorides are affected by (a.) increasing the length of and (b.) perfluorinating the alkyl hydrocarbon parent chain. Examining this trend for a series of acyl chlorides has great potential and provides a better understanding of hydrocarbon related molecules.

Thirdly, the goal of this study is to quantify the chemical properties of acyl chlorides relative to molecular structure and electronic sturcture. Knowing the molecular and electronic

structure enables a thorough understanding of the connection between the structure of a molecule and the chemical properties reported on MSDS sheets and in literature. For example, some of these properties include the following: boiling point, melting point, flash point, and other properties. Some other properties that are desirable to be quantified include conformational stability, internal rotation, helicity, reactivity, acidity, and asymmetry. Identifying how many stable conformations there are and what they are is useful in explaining chemical properties. Once there is verification that there is more than one stable conformation for acyl chlorides, then the question of why can better be addressed. Other studies indicate that internal rotation exists for some acyl chlorides but not for others. [2, 1, 3, 4] Therefore, this study will help further identify when internal rotation exists as parent chain length increases and the possible affects of perfluorination. In addition, quantifying the nuclear electric field gradient (q) along the carbon-chlorine bond through the nuclear electric quadrupole coupling constant (eQq) can better measure the acidity or reactivity of these compounds quantitatively instead of just qualitatively. The nuclear electric quadrupole coupling constant (eQq) is commonly reported as a χ symbol. This quadrupole coupling constant can better explain the observed inductive effect of the perfluoroalkyl effect with quantitative values. The quantitative values for acidity or stability are something that is lacking in literature, which FTMW spectroscopy can make a contribution to. Another motivation for quantifying the electric quadrupole coupling constant, χ, would be to compare the role of oxygen and the fluorines on the χ-tensor for acyl chlorides as the parent chain increases. This would be determined by measuring the quadrupole coupling constant χ-tensor along the z-axis. If the χ-tensor along the z axis (χ_{zz}) were inert as the parent chain length increased, then this would indicate that there is a stabilization effect from the oxygen. If the (χ_{zz}) varied as the parent chain increased, then it would imply little to no stabilization from the oxygen

atom. In addition, quantifying the asymmetry of the molecule parameter or the symmetry of the χ-tensor would help describe the molecular and electronic structure of the molecule. Inertial defects calculations would provide planarity information as well.

Fourthly, acyl chlorides are important to study because they are of value to the petroleum, fragrance, organic synthesis, and academic industries. The petroleum industry could use acyl chloride molecular structural information because they involve hydrocarbons. The fragrance industry could use information on acyl chloride molecular structures because of the connection of the odor to the molecular structure. The organic synthesis industry could use acyl chloride molecular structural information because of the organic nature of these molecules and because acyl chlorides are frequently studied in organic chemistry lectures and labs throughout the world. Lemal (2004) provides a very thorough explanation of the many applications and uses of fluorocarbons for industrial purposes. [31] For any of these industries, the molecular and electronic structural information of these molecules will aid in understanding the stable conformations and kinetics of hydrocarbon related compounds. For example, IUPAC [34] published steady state photolysis data on some of the kinetic information of molecules related to acyl halides using Fourier transform infrared (FT-IR) spectroscopy and flash photolysis time-resolved UV absorption methods. Therefore, FTMW methods could further assist with those initiatives done by IUPAC. Moreover, acquiring high resolution rotational frequency data on these molecules can be used by NASA to determine if these molecules exist in interstellar media or outer space. Last but not least, these industries would be interested in having accurate experimental molecular structure parameters to incorporate into their programming of computational quantum mechanical code for predicting chemical properties and modeling chemical species.

CHAPTER 2

THEORY AND EQUATIONS

2.1 Fundamentals and Theory of Microwave Spectroscopy

Microwave (MW) spectroscopy is unique from all other spectroscopic methods simply because the microwave energy is of the amount to induce a rotational energy level transition within a molecule. Therefore, (MW) spectroscopy is often considered to be synonymous with rotational spectroscopy. No established convention for the division of regions of the electromagnetic spectrum exists but Brown and Carrington use 10 cm to 1 cm, 0.1 cm^{-1} to 1 cm^{-1}, 3 GHz to 30 GHz convention for the microwave region. [35] However, Gordy and Cook cite a range of 30 cm to 0.03 cm. According to Shou-Yuan et al., [36] it is 0.1 cm -100 cm, 300 MHz to 300 GHz. The main point is that the region is of low energy and therefore requires high resolution to resolve the rotational energy transitions within this region. Fourier Transform Microwave (FTMW) spectroscopy is very capable of doing just that and will be demonstrated in this study.

Spectroscopy methods fall under three main categories of techniques: absorption, emission, or resonance. Fourier transform microwave (FTMW) spectroscopy, similar to nuclear magnetic resonance (NMR) spectroscopy, usually is classified as a resonance technique. All of these techniques involve interaction of radiation from a certain range of the electromagnetic spectrum, via absorption or transmission, through a sample. This interacted radiation then continues through a series of circuit components and ultimately reaches a detector to provide unique information about the properties of the molecular composition. Further detail on how FTMW spectrometers work is provided in chapter 3.

The moment of inertia of a molecular system is the fundamental property that enables the mathematical description of a rotating molecule. Therefore, its geometric structure**,** such as bond angles, bond-lengths, atomic coordinates, among many other parameters, are able to be identified within a high level of certainty. This is because all identical molecules have a common unique distribution of mass and therefore a unique moment of inertia. This means that when the molecules rotate, they will do so in a manner according to their unique moment of inertia.

To better explain the behavior of rotating molecules, a classical point of view can be used to imagine quantum mechanical molecules. If a molecule is assumed to be a freely rotating rigid body experiencing no molecular collisions, and none of its components are spinning, then moment of inertia (I) can exclusively provide accurate geometric parameters. Furthermore, even if its inner components are spinning, such as the nuclei or an internal functional group, the moment of inertia is still heavily involved in obtaining the geometric structure through coupling of the rotational angular momentum (J) with any of the internal spinning components. [35] This coupling of two types of spin or angular momentum usually causes hyperfine splitting of frequency spectral lines. Electronic structural information can be evaluated through hyperfine splitting when the second spin category comes from nuclear spin or any spin involving the electronic distribution. Coupling could also occur between internal rotation of functional groups within the molecule and molecular angular momentum. Section 2.6 further discusses hyperfine splitting from internal rotation and nuclear spin coupling.

Also, rotational constant, F, is reported frequently with internal rotation energy barriers. The rotational constant, F, is essentially the rotational constant for the molecule with the principal axis being along the axis of the internal rotor.

2.2 Moment of Inertia

Moments of inertia, a mass distribution property, for a linear diatomic molecule is classically defined as the sum of the masses of each atom multiplied by the square of its distance from the rotational axis through the center of mass of the molecule where (r_i) is the perpendicular distance of the atom (i) from the axis of rotation.[37] For a diatomic molecule, the moment of inertia is simply as follows:

$$I = \sum_{i}^{Natoms} \mathrm{m_i}\, r_i^{\,2}$$

Non-linear molecules have more involved expressions to describe their moment of inertia but the expressions still involve mass (m) and distances (r_i) from the axis of rotation. Classically, linear momentum (ρ) of anything is defined as the product of its mass (m) and velocity (ν). Similarly, angular momentum (P) of a system is the product of its mass-related moment of inertia (I) and angular velocity (ω) .Therefore, the angular momentum (P) is directly related to the moment of inertia (I) by definition.

$$P = I \cdot \omega$$

Moment of inertia (I) applied specifically to a molecule is usually expressed about each of the three perpendicular axes (x, y, z) assigned to the molecule with the origin set center of mass (C.O.M.). The molecular system is then rotated until all of the off-diagonal components of its inertial tensor are zero at which the three (x, y, z) axes consequently are then termed principle axis coordinates (a, b, c). Mathematically, this is achieved by diagonalizing inertial tensor matrices. Of the moments of Inertia (I_a, I_b, I_c), convention usually has (I_c) selected to have the largest magnitude while (I_a) is selected to have the smallest magnitude, ($I_c \geq I_b \geq I_a$). Since moment of inertia (I_a, I_b, I_c) and rotational constants (A, B, C) are inversely proportional, this

gives rotational constants in order of ($A \geq B \geq C$) with the largest magnitude for the A-rotational constant. Therefore, the rotational constants (A, B, C) are magnitudes that indicate the three dimensional distribution of atomic mass and hence the general shape of a molecule. A Watson-A Hamiltonian is usually used for asymmetric molecules, which employs a I_r representation of the coordinate system where the x, y, z, system corresponds to rotational constants (B, C, A).[38] This is the coordinate representation used in this study. These constants can be determined when approximated constants are fitted to microwave spectroscopy rotational energy transition frequencies using software of the AABS package created by Pickett obtainable from the Programs of Rotational Spectroscopy (PROSPE) website.[39] The main programs in this package are SPFIT and SPCAT. SPCAT displays the predicted spectra with the ASCP program using approximated rotational constants as the bare minimum requirement. SPFIT quantum mechanically fits quantum numbers for energy transitions assigned to experimental spectral frequencies displayed in the SVIEW program using an appropriately chosen Hamiltonian, usually Watson A for asymmetric molecules. Ultimately, the moment of inertia is what enables these rotational constants and other constants to be calculated.

The moment of inertias (I) applied specifically to a molecule can be calculated in the following series of steps. First, an arbitrary system of coordinates created for a molecular distribution in terms of mass and location coordinates (x, y, z) for each atom needs to be determined. This can be done through constructing Cartesian coordinates. The origin must be converted into a center of mass (COM) origin system so that the total kinetic energy can be written as a sum of the kinetic energy of translational motion of the (C.O.M.) plus the kinetic energy of motion relative to the COM. This is beneficial because then the kinetic energies can be treated separately. Thankfully, many computational programs already output the coordinates

having a (C.O.M.) origin. Ultimately, the (C.O.M.) coordinate is calculated by multiplying each arbitrary coordinate by its atomic mass, summing the results for each of the x, y, or z axis systems and dividing the axis system sum by the molar mass of the molecule.

$$(COM\ coordinate) = (\frac{\sum_{x,y,or\ z}(atomic\ mass * arbitrary\ coordinate)}{MMmolecule})$$

The difference between the (COM) coordinate and the original arbitrary axis system coordinates produces an adjusted (C.O.M.) coordinate for each atom in the x, y, z axis system. Finally, these adjusted (C.O.M.) coordinates can be used to calculate the moments inertia in all three dimensions of the principals axis system and their products (I_{xx}, I_{yy}, I_{zz}, I_{xy}, I_{xz}, and I_{yz}) using the following formulas:

$$I_{xx} = \sum_i m_i(y^2 + z^2) \quad | \quad I_{xy} = I_{yx} = -\sum_i m_i xy$$

$$I_{yy} = \sum_i m_i(z^2 + x^2) \quad | \quad I_{zx} = I_{xz} = -\sum_i m_i xz$$

$$I_{zz} = \sum_i m_i(x^2 + y^2) \quad | \quad I_{yz} = I_{zy} = -\sum_i m_i yz$$

The above moments of inertia are put into a moment of inertia tensor via a three-by-three matrix of the form following form where the diagonal components are considered to be moments of inertia in all three dimensions and the off-diagonal components are the products of moment of inertia.

$$I = \begin{vmatrix} I_{xx} & I_{xy} & I_{xz} \\ I_{yx} & I_{yy} & I_{yz} \\ I_{zx} & I_{zy} & I_{zz} \end{vmatrix}$$

Again, when the molecule is rotated in the (C.O.M.) axis system so that all of the off-diagonal products are zero, the diagonal components become termed principal axis components (I_a, I_b, I_c). This is done mathematically by diagonalizing the moment of inertia tensor (I) where the moment of inertia tensor becomes:

$$I = \begin{vmatrix} I_a & 0 & 0 \\ 0 & I_b & 0 \\ 0 & 0 & I_c \end{vmatrix}$$

2.3 Moment of Inertia Applied to the Energy of a Rotating Body

Another important property that can be examined with rotational or (FTMW) spectroscopy is the energy of the molecule. There are three main types of energy level transitions that can be accounted for in molecular spectroscopy: electronic, vibrational, and rotational. (FTMW) spectroscopy usually focuses on the rotational energy level transitions that are within a given vibrational level, which are within a given electronic energy level.

Furthermore, there are two kinds of energy, potential and kinetic, where kinetic energy can include translational, electronic, vibrational, and rotational energy. The total energy, kinetic and potential, of a rotating molecule can be solved for quantum mechanically using calculus-based methods with the Schrodinger equation:

$$\hat{H}\psi = E\psi$$

However, an alternative method is possible by evaluating/diagonalizing matrices that are formulated to describe molecules. The diagonalized components are equivalent to the eigen-

values solved via calculus using the Schrodinger equation. The $\hat{H}$ is an operator known as the Hamiltonian that operates on the mathematical wavefunction ψ. The Hamiltonian usually accounts for kinetic and potential energy with kinetic energy having three main possible energy contributions given in the general form:

$$\hat{H} = \hat{H}_{electonic} + \hat{H}_{vibrational} + \hat{H}_{rotational} + \hat{H}_{translational}$$

For FTMW spectroscopy, the rotational Hamiltonian is what is wanted for solving the Schrodinger equation. When this operation of Hamiltonian ($\hat{H}$) on the wavefunction (ψ) produces a value multiplied by the original wavefunction, the value is said to be an eigenvalue. The eigenvalue produced in this way is said to be the energy (E) property of this molecule. However, the rotational energy of a molecule can be very much simplified by identifying the classical energy expressions for rotating bodies, adjusting it to display it in terms of angular momentum, and then plugging back into the equations for quantum mechanical properties. [37] For example, classical motion of a rigid rotating molecule's energy is directly related to its linear momentum, which is related to its angular momentum (P) = I·ω. It is useful to compare this to the kinetic energy. If the kinetic energy can be assumed to be the rotational energy, then $E_{rotational}$ is defined as follows:

$$E_{rotational} = (½)\, m\, v^2$$

or

$$= (½)\frac{\rho^2}{I}$$

However, (½) mv^2 is for linear momentum, rotating bodies also have angular momentum (P) defined as P = I·ω. The kinetic energy in terms of angular momentum will be as follows:

$$E_{rotational} = \left(\frac{1}{2}\right) I\omega^2 = \left(\frac{1}{2}\right)\frac{P^2}{I}$$

Applying this to all three principal axes gives the following for $E_{rotational}$:

$$E_{rotational} = \left(\frac{P_a^2}{2I_a}\right) + \left(\frac{P_b^2}{2I_b}\right) + \left(\frac{P_c^2}{2I_c}\right)$$

In summary, this classical expression of a rigid body without centrifugal distortion is the fundamental rotational energy expression used as a Hamiltonian operator in the Schrödinger equation to calculate accurate rotational energies quantum mechanically. Section 2.7 discusses the approximation of assuming that the rotating body is rigid and without vibration or centrifugal distortion. It is known as the rigid rotor approximation and the requirement to account for centrifugal distortion will be discussed further in section 2.7. For example, the energy of a spherical rotating body is a special case of the above $E_{rotational}$ equation. This is because the moment of inertia is identical for all three axes, this makes the above equation become as follows:

$$E_{rotational} = \frac{(J_a^2 + J_b^2 + J_c^2)}{2I}$$

$$= \frac{J^2}{2I}$$

J is the angular momentum. The quantum mechanical expression for this energy can easily be expressed simply by replacing the J^2 with the operator $J(J+1)\hbar^2$ that happens to satisfy the Schrodinger equation. This gives the new equation for a linear molecule:

$$E(J) = \frac{\hbar^2 J(J+1)}{2I} \qquad J = 0,1,2 \ldots$$

$$= \frac{(h^2)\, J(J+1)}{4\,\pi^2\, I}$$

The expression for the energy is then E(J) = hcBJ(J+1) and because hcB = $\frac{\hbar^2}{2\,Ib}$, the rotational constant B is defined as

$$B = \frac{\hbar}{4\pi C\, I} = \frac{h}{8\ \pi^2\, I}$$

$$\nu = \frac{2\ h\ (J+1)}{8\ \pi^2\ I}$$

$$= 2B(J+1)$$

Harmonic frequencies of different J energy levels are generally separated by 2B for linear molecules but for asymmetric molecules the separation becomes more accurately identified by (B+C). Selection rules fall out of the Hamiltonian operation, which is evidenced by the (J+1) and results in an expression that only allows ΔJ= (0, +/- 1) transitions. This gives the separation of 2B for linear diatomic molecules. However, technically ΔJ = 0 is not allowed for linear shaped molecules. Although energy and the angular momentum quantum number J are proportional, ΔE_J' - ΔE_J" gives the frequency of the transition frequency while ΔJ only shows what quantized values are allowed for the transition.

The Hamiltonian above is more efficient if algebraically rearranged whenever applied to a symmetric or spherical mass distribution classification. This highlights the importance of how the Hamiltonian is significantly affected by the way the mass, and therefore the moment of inertia tensor, is distributed. Spectroscopists have determined four categories to consider that are based on the mass distribution or moment of inertia tensor related to its symmetry around

principal axis. The four categories are spherical rotors, linear rotors, symmetric rotors, and asymmetric rotors (See Table 2.1).

Table 2.1: Classifications of rotors based on inertial symmetry.

Spherical rotor	$I_c = I_b = I_a$	CH_4, SF_6
Linear rotor	$I_a = 0$, $I_b = I_c$	AlF, OCS, C_3O_2
Symmetric rotor (a) prolate	$I_a < I_b = I_c$ $I_\parallel < I_\perp$	CH_3Br, CH_3-C≡C-H
(b) oblate	$I_a = I_b < I_c$ $I_\perp < I_\parallel$	$Mn(CO)_5H$, NH_3, C_6H_6
Asymmetric rotor	$I_a < I_b < I_c$	H_2O, NH_2D, C_6H_5F

2.4 Molecular Shape Classification of Rigid Rotors

Spherical rotor molecules have all three principal moments of inertia equal to each other ($I_c = I_b = I_a$), which results in a dipole moment of zero for the overall dipole moment. Electric dipole moments allow rotation functionally due to oscillating charge. However, dipole moments determine how fast the molecule rotates. A dipole moment is required to rotate a molecule in (FTMW) Spectroscopy according to dipole matrix elements and therefore cannot be analyzed using (FTMW) methods unless a dipole is induced.

Symmetric rotors have two principal moments of inertia equal to each other and one unique moment of inertia. The two equal moments of inertia can either be $I_a = I_b$, or $I_b = I_c$. The unique moment of inertia usually coincides with the principal axis. Linear rotor molecules are a special kind of symmetric rotor whose one unique moment of inertia specifically equals zero. This is the moment of inertia that is about the molecular axis. Examples of this are usually diatomic molecules. Moreover, symmetric rotors can further be classified into a sub category of oblate (disc-shaped) with $I_a < I_b = I_c$ or prolate (cigar shaped) with $I_a = I_b < I_c$. Some sources

clarify the unique moment of inertia that is about the principal axis as ($I_{\parallel}$) and the other two moments of inertia to be ($I_{\perp}$). [37] Under this classification, oblate molecules have $I_{\perp} < I_{\parallel}$, and prolate molecules have $I_{\perp} > I_{\parallel}$ (See table 2.1).

Asymmetric rotors have no moments of inertia equal to each other, $I_a < I_b < I_c$, and have the most number of molecules classified in it. Three examples of this category are thoroughly explored in chapters 4, 5, and 6. Ray's asymmetry parameter, κ, described by Ray in the 1920s, is used as a model or system for quantifying the degree or amount of asymmetry in a molecule and will be discussed in further detail later in section 2.8. [40]

2.5 Rigid Rotor Approximation for Molecular Shape

2.5.1 Symmetric Rigid Rotor

As mentioned earlier, the symmetric rotor has two identical moments of inertia and one unique moment along the principal axis. This enables the Hamiltonian to be manipulated to show this. Remembering that the unique moment of inertia that is about the principal axis is labeled ($I_{\parallel}$) and the other two moments of inertia to be ($I_{\perp}$), the Hamiltonian energy then becomes as follows: [37]

$$E = \frac{J_b^2 + J_c^2}{2I_{\perp}} + \frac{J_a^2}{2I_{\parallel}}$$

We know that the numerator of the first term is $j^2 - J_a^2$ by rearrangement of $j^2 = j_a^2 + J_b^2 + J_c^2$.

$$E = \frac{j^2 - J_a^2}{2I_{\perp}} + \frac{J_a^2}{2I_{\parallel}}$$

Extracting or un-distributing J_a^2 gives the following equation:

$$E = \frac{j^2}{2I_{\perp}} - \left(\frac{1}{2I_{\perp}} + \frac{1}{2I_{\parallel}}\right) J_a^2$$

Generation of the necessary quantum expression is done by replacing the j^2 with $J(J+1)\hbar^2$ and J_a^2 with $k^2(\hbar)^2$. Angular momentum quantum theory identifies that the angular about any axis is restricted to values kħ where k = 0, +/-1..+/-J. Therefore, J_a^2 is replaced with $k^2(\hbar)^2$. After making the above replacements the $\frac{\hbar^2}{2I}$ simply to rotational constant B, and the k^2 simplifies to (A-B) to give the following expression of energy to be as follows:

(Prolate): $F(J,K) = BJ(J+1) + \mathbf{(A-B)}k^2$ for $J= 0,1,2\ldots k=0,+/-1\ldots+/- J$

The previous equation is for a prolate rotor evidenced by the (A-B) constant for change the k quantum number term. To apply this same equation for an oblate molecule would simply change the k constant to (C-B) which yields the contrasting results:

(Oblate) $F(J,K) = BJ(J+1) + \mathbf{(C-B)}k^2$ for $J= 0,1,2\ldots k=0,+/-1\ldots+/- J$

The rotational constant A correlates to $I_{\parallel}$ and rotational constant B correlates to $I_{\perp}$for the prolate scenario. The second quantum number, κ, arises from the fact that symmetrical rotors allow for rotation about the angular momentum axis P at the same time about the symmetrical a-axis. However, when k = 0, there is no angular momentum about the principal axis, and the molecule is mostly dependant on ($I_{\perp}$). When K = +/-1, then all angular momentum arises from the rotation about the principal axis being mostly dependant on $I_{\parallel}$. The +/- sign of the quantum number k only indicates the direction of rotation about the axis.

2.5.2 Asymmetric Rigid Rotor

Asymmetric rotors are best described by comparison to symmetric rotors. The main difference is that this category has no moments of inertia equal to each other, $I_a < I_b < I_c$, and symmetrical rotors have two equal to each other, $I_a = I_b < I_c$ or $I_a < I_b = I_c$. However, whenever

rotational constants B and C differ by a small amount, the molecule is said to be near oblate. Whenever rotational constants A and B differ by a small amount the molecule is said to be near prolate. As mentioned earlier, there is more than one way to indicate the degree of asymmetry in a molecule. Ray's Asymmetry parameter (κ) of a molecule is defined in terms of rotational constants as:

$$\kappa = \frac{2B-A-C}{A-C}$$

The most asymmetric rotor will have a k value of zero.[40] As further review, for a prolate symmetric rotor (B = C), k becomes -1. For an oblate symmetric rotor (B = A), k becomes 1. Therefore, for an asymmetric category, the κ value will range anywhere in between -1 and 1, hence giving an indication of how prolate or oblate it really is or not and its degree of asymmetry relative to how close it is to zero.

Moreover, for symmetric rotors, the quantum number k is defined as a "good" quantum number but it is not for an asymmetric molecule. This is because asymmetric molecules have no components of the angular momentum that are constant along any direction in the rotating asymmetric molecule, which is where the quantum number k comes from. In other words, quantum number k is a projection of J on the symmetry axis, which is no longer the case for an asymmetric molecule.[41] However, the total angular momentum J and its projection M on the axis fixed in space are "good" quantum numbers because they are still constants of the motion for asymmetric molecules.

The importance in describing the asymmetric shape effect on quantum number k is to better interpret the quantum numbers assigned in spectral analysis. The k quantum numbers assigned in spectra are based on the asymmetry parameter. The energy levels may be specified using this quantum number. This is done by labeling the magnitudes of the rotational quantum

numbers J with its corresponding quantum number k as either k_{-1} or k_{1}. The subscripts -1 and 1 are simply the designated asymmetry parameter and indicate oblate or prolate character. However, it is important to realize that the asymmetry parameter for these subscripts is not -1 or 1 exactly but is somewhere in between. This is yet another way of explaining how the quantum number k is a "bad" quantum number for asymmetric rotors but is more ideal for near oblate and near-prolate asymmetric scenarios as k → 1 for an oblate molecule and as k→ -1 for a prolate molecule. Therefore, whenever a data table lists k_{-1}, it indicates the molecule's oblate character and whenever the data table displays k_1, it indicates the molecule's prolate character. An example of this format or labeling system as it would be displayed in data tables is of the following form:

$$J_{K\text{-}1,K1} \leftarrow J_{K\text{-}1,K1}$$

Moreover, asymmetric rotors have (2J+1) individual rotational sublevels for each J while symmetric rotors have only (J+1) sublevels for each J. This is because symmetric molecules have κ-levels of -κ and +κ that are of the same energy for symmetric molecules but split separately for asymmetric molecules, which creates the (2J+1) sublevels instead of the (J+1) sublevel.

Townes and Schalow [41] describe the method of providing a general picture of the behavior of the energy levels of an asymmetric rotor by examining how the rotational behavior changes from the prolate to the oblate extreme symmetries. They define the energy in terms of (W) to still be as follows:

$$W = \left(\frac{P_a^2}{2I_a}\right) + \left(\frac{P_b^2}{2I_b}\right) + \left(\frac{P_c^2}{2I_c}\right)$$

This quantum mechanical Hamiltonian for an asymmetric rigid rotating molecule under the rigid rotor approximations is no different than the fundamental energy equation listed above because

none of the moments of inertia are the same. Re-writing the Hamiltonian in terms of rotational constants instead of moments of inertia yields the following:

$$\hat{\mathrm{H}} = AP_a^2 + BP_b^2 + CP_c^2$$

This Hamiltonian equation can be algebraically rearranged by substituting ray's asymmetry parameter into the Hamiltonian in terms of A and C using the equation that $p^2 = P_a^2 + P_b^2 + P_c^2$ to yield the following: [40]:

$$\hat{\mathrm{H}} = \left(\frac{1}{2}\right)(A + C)P^2 + \left(\frac{1}{2}\right)(A - C)H(k)$$

The reduced Hamiltonian H(K) is defined as such: [40]

$$H(k) = P_a^2 + kP_b^2 + P_c^2$$

The significance of this is that the reduced Hamiltonian H(K) for the hypothetical rotor with A=1, B=k, C=-1 produces reduced energies that are eigen values of H(k) that depend only on the inertial asymmetry parameter (k) instead of on rotational constants evidenced by the absence of rotational constants in the reduced Hamiltonian expression above. A consequence of this asymmetry is that the Hamiltonian operator for asymmetry is no longer directly solvable but common methods include linear combinations of symmetric rotor functions of the following Schrödinger equation form: [40] $\psi_{J\tau M} = \sum_{J,K,M} a_{J,K,M}\, \psi_{J,K,M}$. The symmetric rotor wavefunctions are orthonormal $\psi_{J,K,M}$, which produce 0 and 1 answers when both upper and lower energy level quantum numbers J,K,M in a transition are identical or not. The above Hamiltonian produces rotational energies of the following form:

$$E = \left(\frac{1}{2}\right)(A + C)J(J + 1) + \left(\frac{1}{2}\right)(A - C)\mathrm{E}_{J_\tau}(k)$$

E_{J_τ} is defined as $\mathrm{E}_{\text{k-1}\,-\,\text{k1.}}$ In general, the selection rules are the same as the symmetric rotor at:

$$\Delta J = 0, +/- 1$$

2.6 Internal Rotation

Internal rotation refers to one or more of the functional groups internally within the molecule, that rotate simultaneously with the total angular momentum of the molecule. The FTMW spectrometer is able to resolve internal rotation frequency splitting in some molecules but not in others mainly due to the potential energy barrier of the internal rotor. Internal rotation occurs generally through a tunneling phenomenon specifically whenever the potential energy barrier for a n-fold axis of rotation is low enough to split energy states, such as rotational energy states, into two states, namely A and E states. Fundamentally, these A and E states arrive from the mixing, via addition or subtraction, of two wavefunctions in a n-fold potential energy well. [40]

The potential energy barrier V of the internal rotor functional group is the main factor that determines whether or not internal rotation of a molecule is observable in rotational spectra. For a CH_3 or CF_3 function group, there is a three-fold axis and thus the potential energy barrier is called the V_3 potential energy barrier of internal rotation. With higher (V_3) barriers, the lesser probability of resolving internal rotation exists in rotational spectra. In most molecules, the V_3 barrier is around the value of 1000 cm^{-1} or $4.7478*10^{-24}$ kcal or $1.2398*10^{-1}$ eV. Although there is a potential energy barrier V_3 for internal rotation, the effect of tunneling is observable where internal rotation energy transitions tunnel through the V_3 barrier. Therefore, the result is that some internal rotation energy transitions mix up and others mix down with the wavefunction describing the transition. This then yields what are called A and E states where one includes the mixing up state and the other includes the mixing down state.

2.7 Centrifugal Distortion

Centrifugal distortion occurs in molecules because molecules are not rigid and have the

ability to stretch or vibrate while rotating. A centrifugal force is the force that pushes atoms away from each other as the angular velocity increases, which results in a stretching of the bond. However, the restoring force pulls the atoms back together causing a cycling stretching and contracting of the bonds. Therefore, it is a weak assumption to assume that rotational constants can purely be used to predict rotational spectra. For example, centrifugal distortion for a symmetric molecule has relatively little effect on the molecular spectra, changes on the order of only one megacycle. [41] However, for asymmetric molecules, such as those in this study, centrifugal constants can change the frequencies many hundreds of megacycles. [41] The greater importance of centrifugal motion on asymmetric molecules is mainly because the transitions that occur in asymmetric molecules usually have larger angular momentum and therefore large rotational constants. Therefore, if the transitions involve larger rotational constants, then centrifugally distorting them would mean bigger changes in those larger transitions. Correction terms that are added to the Hamiltonian to account for centrifugal motion are called centrifugal distortion terms that contain centrifugal distortion constants (D). Centrifugal distortion constants (D) are directly proportional to the ability to stretch or inversely proportional to rigidity of the bonds. For example, large (D) values indicate large stretching ability. (D) constants are usually on the order of kHz, which is closer to symmetric rather than asymmetric changes.

There are two types of notations for reporting centrifugal distortion constants. They are based on if a Watson A or a Watson S Hamiltonian was used in the analysis when constructing the Hamiltonian to save time. With modern computer abilities, this is not as important any more. The Watson A notation is used when the molecule is asymmetric, and a Watson S notation is used when the molecule is only slightly asymmetric. The following table demonstrates that by looking at the notation of the constants reported in data tables, it can tell you what Hamiltonian

was used. This table also shows that centrifugal distortion constants have a dependence on J and K or both as follows: [40]

Watson S notation	Watson-A notation
D_J	Δ_J
D_{JK}	Δ_{JK}
d_K	δ_K

The energy equation for a transition frequency of a linear rotor including centrifugal distortion is defined as [40]

$$\nu = 2B_\nu(J+1) - 4D_\nu(J+1)^3 + Higher\ order\ centrifugal\ terms$$

$$B_\nu = \beta_e - (\nu + \frac{1}{2}) + \gamma_e + (\nu + \frac{1}{2})^2$$

$$D_\nu = D_e + \beta_e (\nu + \frac{1}{2}) + \cdots$$

The expressions get much more complex for non-linear molecules as more vibrational modes become possible for non-linear rotors.

2.8 Nuclear Electric Quadrupole Coupling

Nuclear quadrupole coupling is a source of one type of hyperfine splitting that provides electronic structural information about a molecule termed hyperfine structure. Hyperfine splitting is defined as splitting of spectral frequencies due to changes in energy levels caused by coupling of angular momentum of two sources. It is misleading to assume that all molecules have spherically symmetric nuclei with no nuclear spin (I). Molecules have a quadrupole moment if any of its atoms have a nuclear spin (I) greater than ½. This is because molecules with nuclear spins greater than ½ have large enough non-spherical charge distributions arising from the

nuclear spin (I) that are able to couple with the total angular momentum (J), which changes the energy levels for transition frequencies. A Clebsch-Gordon series can describe the hyperfine components that give rise to splitting of spectral frequencies. It is usually of the following form:

$$\mathrm{F} = I + J, J + I - 1, J + I - 2 \ldots [I - J]$$

From the Clebsch-Gordon Series, one is able to better explain why resolving higher J levels in a molecule is increasingly more difficult as the number of F states increase dramatically when J increase. The Hamiltonian that accounts for rotation, centrifugal distortion, and quadrupole coupling is in the form given as follows:

$$H = H_{rot} + H_{cd} + H_{quad}$$

Gordy and Cook cite it in compact form as follows:

$$\mathrm{H} = \frac{eQq}{(2J\ (2J-1)I\ (2I-1)}[2(\mathrm{I}.\mathrm{J})^2 + \frac{3}{2}I.J - \mathrm{I}^2\mathrm{J}^2]$$

In this study, electric dipole moments instead of magnetic dipole moments are examined. Therefore, quadrupole moments are usually reported as nuclear electric quadrupole constants (eQq) where e is the charge on the electron, Q is the quadrupole moment, and q is the electric field gradient tensor at the nucleus with the nuclear spin. The nuclear electric quadrupole coupling constant is reported as a tensor quantity either as (eQq) or (χ) according to most literature sources. The significance of (χ) is that it involves the electric field gradient tensor (q) which can be used to interpret the electronic environment around any given nucleus that has significant nuclear spin. For example, molecules with spherical electric field gradients (q) are equal to zero. This means the (χ) is also equal to zero at this point. As the electric field gradient becomes more non-spherical, the eQq should become larger in magnitude. When a molecule is rotated into its principal axis system, the electric field gradient of a bond between two atoms may be very near coaxial with the principal axis. If this is the case, then information about the

electronic structure of the atoms involved can be deduced. The electronic structure usually involves p-orbitals for atoms having electrons involved in bonding located in p-orbitals near the nucleus. P-orbitals are also possibly involved because they have non-spherical shape, which non-zero eQq values indicate.

Furthermore, one is able to acquire information about the ionic character of a bond by examining the eQq or q value along a bond using the Townes Daley Model. This model compares the eQq values to the unbounded non-spherical electric field gradient of the single atom that has the nuclear spin. In this study, this atom happens to be atomic chlorine. For example, according to Townes and Schawlow, atomic chlorine has an eQq value of -109.6 MHz. [41] Covalent molecules usually have higher eQq values than ionic molecules. The very covalent FCl molecule has an eQq around -146 MHz and the very ionic Nail has an eQq value around < 1 MHz. Therefore, if the eQq is anywhere in between these two values then one is able to quantify the ionic character of a bond in a molecule, assuming the role of the electrons in certain orbitals are consistent for comparison. Townes and Schawlow describe the importance of considering hybridization when interpreting and comparing eQq values.

Nuclear electric quadrupole coupling constants can also be used to determine some degree of asymmetry of the χ-tensor. This is done by reporting the asymmetry parameter (η), which is best reported for slightly asymmetric molecules. When the asymmetry parameter (η) has the most symmetric axis set as the z-axis (c-axis in principal axis coordinates), then the asymmetry parameter (η) is defined as follows:

$$\eta = \frac{\chi_{xx} - \chi_{yy}}{\chi_{zz}}$$

or

$$\eta = \frac{\chi_{aa} - \chi_{bb}}{\chi_{cc}}$$

This is because setting the χ-tensor in the denominator to the most symmetric axis results in an asymmetry parameter (η) that is lowest. This equation is a Laplace equation where $\chi_{aa} + \chi_{bb} + \chi_{cc} = 0$. Therefore, there are two independent coupling parameters χ_{zz} and η. The off-diagonal components can be determined with perturbation theory but are unnecessary when written in principal axis notation because they then become zero in that notation. Ultimately, the lower the magnitude of the asymmetry parameter (η), the more asymmetric the χ-tensor. (η) is a measure of the cylindrical symmetry along the bond containing the atom with nuclear spin when rotated into the principal axis system.

There is another way to indicate the degree of asymmetry for a molecule instead of the χ-tensor. It is termed Ray's Asymmetry parameter (κ) defined in terms of rotational constants:

$$\kappa = \frac{2B - A - C}{A - C}$$

The most asymmetric rotor will have a κ value of zero.[40] For a prolate symmetric rotor (B = C), k becomes -1; for an oblate symmetric rotor (B = A), k becomes 1. Therefore, for an asymmetric category, the κ value will range anywhere in between -1 and 1, hence giving an indication of how asymmetric it really is or not and whether or not it is prolate or oblate.

2.9 Inertial Defect

The inertial defect (Δ) is essentially a calculation of quantifying how planar or non-planar a molecule is based on its moments of inertia in three dimensions. Mathematically it is defined as follows:

$$\Delta = I_{cc} - I_{aa} - I_{bb}$$

The moments of inertia are assigned according to convention where $\Delta = I_{aa} \leq I_{bb} \leq I_{cc}$. Planar molecules will have inertial defects (Δ) = zero. Non-planar molecules will have inertial defects (Δ) = negative values. In this convention, there will never be an inertial defect (Δ) that is positive. As Oka (1995) 42 summarizes, moment of inertia is defined as follows:

$$I_{\alpha\alpha} = \sum_i m_i (\beta_i^2 + \gamma_i^2)$$

2.9.1 Planar Moments

The planar moment is very similar to the moment of inertia. It is sometimes termed the second moment. Gordy and Cook [40] define it as such:

$$P_{\alpha\alpha} = \sum m_i (x_{\alpha\alpha}^2)$$

$$P_{xy} = \sum m_i x_i y_i$$

The two matrices (I) and (P) are related by the matrix equation that involves dE where $d = \sum_i m_i (x_i^2 + y_i^2 z_i^2))$ and E = 3 x 3 unit matrix to give the following relation:

$$I = dE - P$$

Gordy and Cook go on to inform that this relation can reduce to the form $I_x = d - P_x$. They also express the planar moment as follows:

$$P_x = \frac{1}{2}(-I_x + I_y + I_z)$$

and

$$I_x = (-I_x + I_y + I_z)$$

2.9.2 Kraitchman Isotopic Substitution

Kraitchman substitution is a method that allows one to calculate the position of an atom in a molecule by utilizing the changes in the moments of inertia resulting from a single isotopic substitution of the atom.[40] An accurate structure of the molecule is possible to be determined without computational calculation once an adequate number of coordinates from at least two different isotopes along the principal axis have been determined.[40] This is because one is able to calculate how the geometric structure changes when a different isotopic mass is accounted for relative to another isotopic mass. This is enabled by the effects of the Born-Oppenheimer Approximation where it is assumed the nuclear position did not change with mass changes. This enables specification of spatial orientation of certain atoms in a molecule relative to each other and therefore it's exact geometry. Therefore, multiple isotopic substitution methods require spectroscopic constants for multiple isotopic species along the principal axis system throughout the molecule in order to determine the exact geometry of a molecule.

Single Isotopic substitution is needed sometimes when only one isotopic atom exists in a molecule. This limits the exact determination of the overall molecular geometry but still provides insightful information about the location of the atoms near the single isotopically substituted atom. A computational calculation is able to provide re-assurance of the molecular geometry when the predicted constants match the calculated spectroscopic constants. In the following study the kraitchman substitution coordinates are in units of angstroms.

CHAPTER 3

INSTRUMENTATION

Microwave spectroscopy can be used to study many different types of molecules. However, there are some requirements in choosing a molecule to study via current microwave spectroscopy methods. Some of these requirements include having a dipole moment and the ability to get the molecule(s) into the gas phase. The majority of molecules have a dipole moment, which makes microwave spectroscopy a useful method in determining molecular and electronic structure. However, in the rare case that a non-polar molecule is to be studied, methods of inducing a dipole moment in a molecule using double resonance techniques with microwave spectroscopy methods exist at other research labs. Moreover, not all molecules exist naturally in the gas phase under standard temperature and pressure. Therefore, various methods of changing solids and liquids into the gas phases have been developed. For metals, laser ablation techniques have been used at the University of North Texas (UNT) to ablate metal atoms into a gas phase while simultaneously combining with other gas species. For liquids, the simplest technique is to bubble a carrier gas through the liquid that has sufficiently high enough vapor pressure to carry gas phase vapor into the microwave spectroscopy chamber. This is the case for most of the molecules in this study. However, even if the vapor pressure is very low for a sample, it is plausible that some methods are capable of obtaining gas phase molecules from low vapor pressure liquids, such as heating the liquid sample into the gas phase just prior to entering the microwave spectroscopy chamber.

Rotational spectra were recorded using a chirped pulse Fourier Transform Microwave (CP-FTMW) spectrometer located at the University of North Texas. The circuit for this spectrometer is located in Figure 3.1 and it has been described in detail elsewhere.[6] The

inspiration for this technique came mainly from Brown et al. (2008). [43]

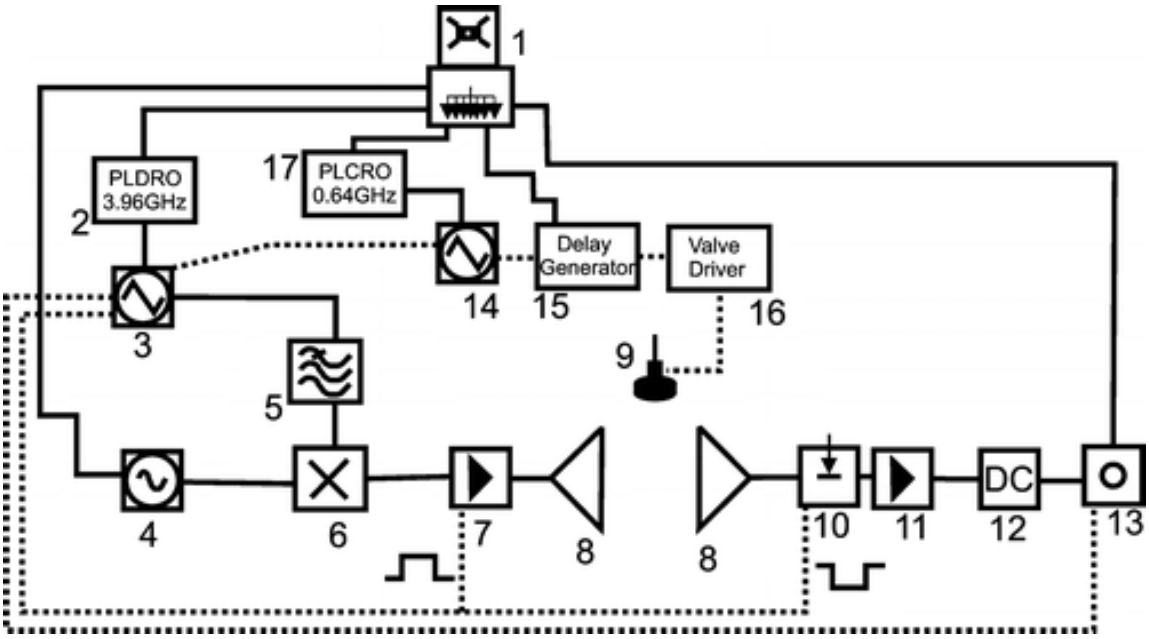

Figure 3.1: Circuit of the chirped-pulse Fourier transform microwave spectrometer and experimental summary. [6] 1, Rb atomic clock, SRS FS725, and distribution amplifier, Wenzel Associates; 2, 3.96 GHz PLDRO Nexyn Corp. NXPLOS-0396-2381; 3, Tektronix AWG 710B; 4, MW synthesizer HP 8341A; 5, low pass filter, Minicircuits; 6, mixer, Miteq DB0418LW1; 7, power amplifier, Microwave Power, L0818-37; 8, horn antenna, Amplifier Research AT 4004; 9, series 9 solenoid valve, Parker-Hannefin; 10, SPST pin diode switch ATM S1517D; 11, LNA Miteq AMF-6F-06001800-15-10P; 12, dc block; 13, O-scope Tektronix TDS 6124C; 14, Tektronix AWG 2041; 15, BNC 505-8C; 16, Iota One valve driver, Parker Hannefin; 17, PLCRO 0.64 GHz Nexyn Corp. NXPLOS-0064-2381. Dotted lines show TTL pulse timing communication lines.

The general function and summary of the circuit sequence of the chirped-pulse Fourier Transform Microwave Spectrometer at the University of North Texas is as follows. CP-FTMW spectrometers can be summarized relative to the vacuum chamber in three stages of the circuitry: pre-chamber, inside the chamber, and post chamber. During pre-chamber circuitry, a chirped-pulse is synthesized simultaneously as a sample is pulsed. Inside the chamber, molecular rotational excitation from the interaction of the chirped pulse and the sample occurs. During post chamber circuitry, free induction decay (FID) data of the sample is collected. The circuitry is explained more specifically as follows. A microwave synthesizer outputs a chosen frequency

while simultaneously mixing with an arbitrary waveform generator output that is filtered by a low pass filter. In this study, an arbitrary waveform generator AWG710B is used to create the fast linear frequency sweep in 5 μs duration between the frequency limits of DC− 1 GHz. In other words, this linear frequency sweep signal is mixed with a center frequency, *v*, from the monochromatic output of a 8341A Synthesized Hewlett Packard microwave synthesizer producing a fast linear frequency sweep spanning approximately *v* -1 GHz to *v* +1 GHz. This means that if the center frequency of the microwave synthesizer generated is 9 GHz, then the frequency sweep would include 9 (+/-)1 GHz making a pulse of 8-10 GHz. This is one of the main components that makes the (CP-FTMW) a fast passage chirped pulse technique instead of a regular FTMW technique because this arbitrary waveform generator produces the linear frequency sweep at a sufficient rate (5μs), which enables the collection of a large range of spectrum within a short amount of time. The linear frequency sweep is called "chirped pulse" because it is analogous to scaling up a series of notes to a high pitch chirp in a musical instrument. The linear frequency sweep signal is amplified by a 5 Watt power amplifier that is rated for the 8-18 GHz range before being broadcast into a high vacuum, ~10^{-6} Torr, cavity chamber modified with an emitting and receiving standard gain horn antenna. The standard gain horn antennae are placed in a perpendicular arrangement relative to the gas entrance.

Inside this high vacuum chamber, a gas sample is supersonically expanded from a series-9 solenoid valve at room temperature. The molecules interact with the linear frequency sweep and become polarized. Because the molecules in the sample have the same dipole moments, all of the molecules rotate in phase when stimulated by the microwave signal (linear frequency sweep ν +/-1 GHz). When the microwave signal is turned off, free induction decay (FID) occurs

as the molecules decay from their macroscopically polarized condition and move toward random orientations.

The circuit continues outside of the chamber beginning with the receiving horn antenna where the FID data in the time domain is collected, amplified with a low noise amplifier, directly digitized, and fast Fourier transformed into the frequency domain using a 12 GHz bandwidth, 40 GS/s, TDS6124C digital storage oscilloscope. The low noise amplifier that is used to amplify the FID is a Miteq AMF-6F-06001800-15-10P amplifier. The circuit timings are controlled through a switch using an inverse logic between polarization of the sample via synthesized microwave radiation and collection of the molecular FID at the oscilloscope. Specifically, this inverse logic is controlled by a single pole single throw (SPST) pin diode switch located right before the low noise amplifier so that only properties of the molecules are being studied and not the synthesized microwave frequencies. When microwaves are pulsing, the pin diode switch is open to stop data collection. When the microwaves are not pulsing, the switch is closed to allow for FID data collection.

The fast Fourier transformations in this experimental study were performed such that line widths obtained were approximately 80 kHz (FWHM) and were given a generous uncertainty of 25 kHz, which is an approximate deviation measurement of the line centers. However, whenever certain spectra frequencies were relatively broader than usual, > 80 kHz, and the predicted spectra showed more than one frequency line in that region, it was assumed that the resolution was too poor to resolve the multiple frequencies. Therefore, the uncertainty was slightly increased, no greater than 50 kHz, to better assign the multiple frequencies. When working with liquid samples, approximately 2-3 milliliters of the liquid sample is all that is usually needed to bubble through 1/4” polyethylene tubing using argon backing gas at a backing pressure of

approximately 2 atm. The spectra frequency data for each of the 2-3 scans of the same 2 GHz linear frequency sweep spectrum can be deep averaged by adding them together to enhance the intensities of the spectra allowing sufficient fitting of the molecular structural parameters. Multiples scans were averaged in this study.

3.1 Analytical Applications

Efficiently applying older methods of FTMW spectroscopy to analytical or quality control applications was inhibited largely by the time-consuming spectral acquisition process and the small 1 MHz instrumental bandwidth limit for each scan to be of sufficient resolution. [43] For example, the older regular cavity FTMW, such as at the University of Virginia, required 14 hours to acquire a 11 GHz bandwidth when automated to sum up a series of frequency steps consisting of ten signal averages each at 500 kHz. For the CP-FTMW method, it took almost half that time. [43] Brown et al. (2008) state that the basic CP-FTMW spectrometer is capable of acquiring full rotational spectra approximately 50 times faster than the Balle-Flygare cavity with accurate spectral intensities to greatly assist with spectral assignment. [43] Therefore, the advantage of CP-FTMW spectroscopy is that it greatly increases the acquisition time, the experimental bandwidth, and accurate relative intensities. However, the goal is, without significantly sacrificing resolution, to acquire the best sensitivity in the shortest amount of time. Sensitivity refers to signal intensity but more important is increasing the signal-to-noise ratio (S/N) to enhance resolution. The sensitivity for the CP-FTMW at UNT for OCS is usually around a magnitude of 40 mV, but 60 mV has been achieved with fresh diffusion pump oil and other fine tuning of circuit timings. This translates into a (S/N) of about 10,000:1. The CP-FTMW at UNT typically

achieves 80 kHz resolution with 2GHz bandwidth in only about 2-3 hours when only 20 μs of FID are sampled.

The CP-FTMW spectrometer used an automation process for some of the molecules in this study. This process saves user time and moves the CP-FTMW closer to becoming an analytical technique. The automation feature is explained as follows and is described elsewhere in the Grubbs II et al study [6]. The oscilloscope used has hardware limited to 10,000 permissible averaging cycles. A National Instruments LabView code has been written to overcome this limitation by controlling the instrument through GPIB connections. An unlimited amount of 10,000 averaged scans can now be saved to an external hard drive and the software can automatically step up the frequency. For example, the software can run multiple 10,000 acquisitions at 9−11 GHz, then step up and collect multiple 10,000 acquisitions at 11−13 GHz and so forth. This allows the instrument to run uninterrupted for several days and the data can be extracted, and "averaged" or "pieced together" in preparation for analysis.

3.2 Resolution Limitations

Resolution is defined as the smallest observable separation between two closely spaced spectral bands or frequencies. [37] There are three main sources that affect the resolution of spectral frequencies in CP-FTMW spectroscopy, namely in order of decreasing importance: 1.) instrumental limitations, 2.) doppler broadening, and 3.) lifetime broadening. [44]

Instrument circuit components significantly limit the resolution of a CP-FTMW spectrometer. The oscilloscope programming is what affects it the most. In regards to the fit, resolution is defined as follows:

$$Resolution = (number\ of\ points * (\frac{time}{point})^{-1})$$

The sampling rate used with the oscilloscope in this study is 25 ps/point and since only 20 μs of the FID is collected, there are 800,000 points sampled during the time collecting FID. Therefore, the calculated resolution of the CP-FTMW spectrometer is officially 50 kHz. The linewidths are typically about 80 kHz when sampling 20 μs of FID. An 80 kHz resolution(one linewidth) approximation is able to resolve most if not all rotational spectra. Therefore, 80 kHz is the resolution commonly approximated in this study. Furthermore, if 40 μs of the FID were sampled, the resolution would increase dramatically to about 25 kHz (FWHM) resolution with linewidths closer to 40 kHz. Since the oscilloscope is programmable to control the amount of time spent sampling the FID, resolution is affected most significantly by the oscilloscope.

Doppler broadening affects resolution. Doppler broadening is defined as an effect caused by the fact that, relative to the source of radiation, motion of molecules move in a range of speeds in different directions according to a Maxwell distribution,whereby some move toward the source and others move away from the source. Blue shifts move toward the source; red shifts move away from the source. This causes emission or absorption at different frequencies which when all of the individual wavelength doppler shifts are summed up, a Gaussian curve results. In other words, the doppler line width or shape is the absorption or emission profile arising from all of the doppler shifts, which increases the full width half maximum (FWHM) width of the frequency spectra and therefore the resolution. [44] Doppler broadening increases at higher temperatures because the molecules acquire a wider range of speeds. [37]

Lifetime broadening, also known as uncertainty broadening, affects the resolution of CP-FTMW the least since the samples are not transient species and have a large lifetime. The larger the lifetime of a molecule, or quantized state, the more narrow the frequency. [37] Lifetime broadening is defined as the effect of the finite lifetime of the energy level due to emission,

dissociation, or other processes giving rise to a width in accordance to the uncertainty principle $\Delta E \Delta t \sim \hbar$. [44]. Lifetime broadening is evident especially when doppler broadening is quenched as much as possible through low temperatures, and yet infinitely sharp lines are still not observed. Lifetime broadening is mainly due to quantum mechanical effects where it is impossible to specify the exact energy levels. nergy levels of a system are blurred to an order of δE when the average lifetime τ of a system exists for time τ according to the relation $\delta E \sim \hbar/\tau$. Lifetimes are finite mainly because of collisional deactivation and the rate of spontaneous emission. Collisional deactivation occurs mainly from molecular collisions making lifetime proportional to pressure. The rate of spontaneous emission is unique to an energy level transition and therefore it is a natural linewidth affecting the resolution. For example, at lower frequencies, more narrow linewidths of rotational energy transitions exist, which allows for doppler broadening to dominate resolution. This is probably the case in the Brown et al. (2008) [43] study where Doppler doubling was dominating for the CP-FTMW spectrometer working in a lower 7.5 – 18.5 GHz bandwidth range. The highest resolution is obtainable when the molecules are either gaseous or at low enough pressure so that molecular collisions are infrequent or non-existent. However, all of the instrument components still have to be optimized to obtain the best sensitivity.

3.3 Bandwidth Instrumental Limitations

Instrumental components significantly affect the bandwidth of spectrometers, especially Fourier transform spectrometers. For example, the regular FTMW spectrometers have two mirrors that act as a bandpass or bandwidth, but CP-FTMW spectrometers do not have this. CP-FTMW spectrometers instead have standard gain horn antenna. Although other components within the circuit limit the bandwidth the most, the antennae partially limit the size of the

microwaves able to be collected based on the size of the horn antenna. The CP-FTMW method provides separation between bandwidth and pulse generation making it possible to separately control the frequency range of the excitation and the amount of energy delivered to the sample. [43] The CP-FTMW spectrometer at the University of Virginia has a 7.5-18.5 GHz bandwidth with a FID that decays according to a Gaussian profile, where it takes 10 μs to reach half of the maximum amplitude, which is dominated by doppler broadening. [43] There are other forms of bandwidth in a spectrometer instrument circuit, such as unity gain bandwidth of amplifiers or a pin diode switch. Unity gain bandwidth is a defined as a frequency range from dc to the frequency at which A=1 (0 dB). [45] The gain of the 8-18 GHz rated power amplifier is 37 dB. The gain on the Low Noise Amplifier (LNA) is 45 dB. Furthermore**,** the oscilloscope has a bandwidth limitation of 12 GHz mainly due to the 3 dB gain drop off that occurs for each GHz beyond the 12 GHz mark, thus making the sensitivity weaker and weaker with higher frequencies.

3.4 Calibration

Calibration is especially important with CP-FTMW spectrometry since CP-FTMW spectrometry is likely to eventually become a standardized analytical technique. For example, before an unknown sample is run on a FTMW or CP-FTMW spectrometer, the instrument is calibrated with carbonyl sulfide (OCS). OCS is chosen mainly because it exists as a gas naturally, it has rotational transition frequencies within the bandwidth limits of the CP-FTMW spectrometer, and it has very intense lines that are predictably spaced out because of its linear shape. The timings of the width of the gas pulse into the chamber and the timings of the delay between pulses of gas are optimized to OCS to achieve the greatest signal-to-noise ratio (S/N)

possible. Typically, the best sensitivity is maximized at a magnitude of 40 mV, but 60 mV has been achieved with fresh diffusion pump oil and other fine tuning of circuit timings. The (S/N) is usually about 10,000:1. The assumption is that if OCS circuit timings are maximized, the unknown sample circuit timings will be maximized as well and yield maximum sensitivity and (S/N). Brown et al. (2008) show their dynamic range by comparing the (S/N) for OCS collected on a CP-FTMW spectrometer equipped with a 50 G sample/s oscilloscope and a 20 GS/s arbitrary waveform generator (AWG). The dynamic range results of this consist of a (S/N) of 3500:1 after 1 shot or average and 200,000:1 after 4000 domain averages.

Calibration of the frequency standard is one of the most important components to calibrate in the entire CP-FTMW circuit. The frequency standard used at UNT is a 10 MHz frequency standard, model FS725. It enables the CP-FTMW circuit to function reliably by providing a 10 MHz standard reference frequency to all electronic components transmitting frequency. This 10 MHz reference frequency ensures that all frequency signals in the entire circuit are in sync without destructive interference destroying the transmission of frequency data from component to component. This component is usually calibrated by an outside source, such as NIST, every 5- 10 years.

Another component worth calibrating is the standard pressure gauge for the gas sample tanks and the thermocouple vacuum gauge for the microwave chamber. The pressure gauge for the gas sample tanks in this study was calibrated at about 1500 units / 760 Torr referenced to a thermocouple ion gauge. With 760 Torr being one atmosphere, this means that values displayed are approximately at 2 atmospheres of pressure in units of Torr. Again, pressure is important because pressure directly affects lifetime broadening, which is proportional to molecular collisions that create collisional deactivation and therefore affect the full width half maximum

(FWHM) resolution of the frequency. The thermocouple vacuum gauge for the vacuum chamber was also calibrated referenced to a high precision thermocouple ion gauge directly in terms of units of millitorr.

Other components, such as amplifiers, are periodically checked to ensure that their operation are within their specification via a voltmeter or analysis of the frequencies displayed on an oscilloscope.

3.5 Quality of Parameter Fit

The statistical quality of the fit between the experimental frequencies and the predicted frequencies that give structural constants of a molecule are commonly determined by root-mean-square (RMS) values. The lower the RMS of the fit, the more certainty there is in the accuracy of the spectroscopic constants. There are two different notations of reporting RMS, one without units and the other with units. They are termed the statistical RMS (σ_{rms}) and microwave RMS (σ) accordingly. They are used in this study and are mathematically defined as follows:

$$\sigma_{rms} = \sqrt{\frac{\sum(\frac{\text{obs} - \text{calc}}{\text{error}})^2}{N}}$$

$$\sigma = \sqrt{\frac{\sum(\text{obs} - \text{calc})^2}{N}}$$

N_i is the number of lines. A statistical RMS is usually less than 1. For assigning spectra using the CP-FTMW used at UNT, it is often significantly lower than 1. If the statistical RMS is above 1, the fit is no longer reliable because the error between the observed frequency and the calculated frequency is greater than the uncertainty or error set for the observed line. For example, the statistical RMS has been as low as << 0.2 for many molecular studies on the CP-FTMW at UNT.

For these molecules, 25 kHz uncertainties were generously attributed to the line centers of spectral frequencies as an approximation. Since the statistical RMS is so much lower than 1, the uncertainty can technically be decreased to give a statistical RMS closer to 1. This is what has been done for all of the microwave RMS data fitted thus far for the CP-FTMW instrument at UNT in order to determine the accuracy of the line centers for the CP-FTMW spectrometer. The results demonstrated that the generous uncertainty of 25 kHz is allowed to be lowered to about 6 kHz and still have the statistical RMS below 1. Therefore, the 25 KHz uncertainty attributed to the line centers is considered generous since theoretically it can be set to 6 KHz and still provide high quality of fitted spectral frequencies. The microwave RMS is very similar to the statistical RMS except that it has units and it does not include the error set for each predicted line in it. This allows the RMS to be above 1 because the difference in the observed frequency and the calculated frequency are not divided by an error value. Also, worth noting is that all of the frequencies in this study report error values in parentheses that are 1 standard deviation, 67% confidence level, in units of the least significant figure. This gives a sense of how confident the fits of the assigned frequency are to the predicted spectra in terms of standard deviation from the recorded line centers.

CHAPTER 4

MOLECULAR STRUCTURE ANALYSES OF PROPIONYL CHLORIDE AND PERFLUOROPROPIONYL CHLORIDE*

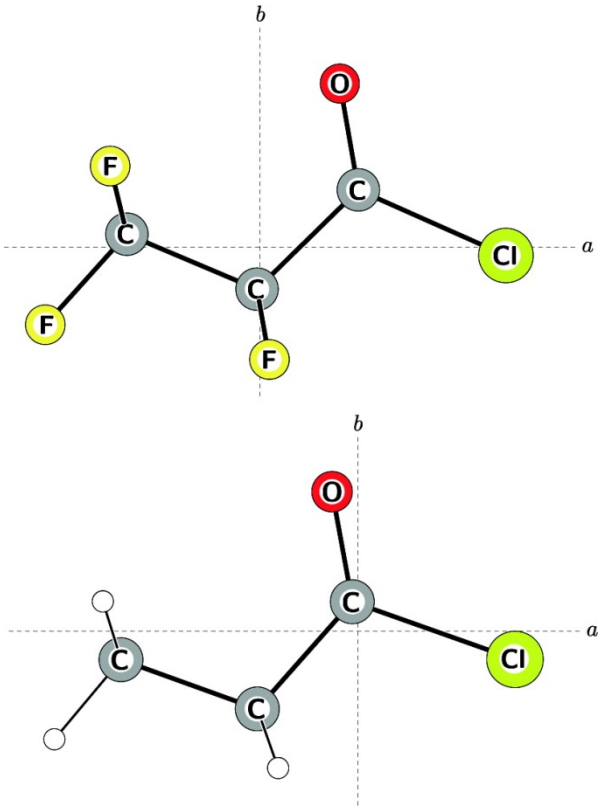

Figure 4.1: The M06-2X/6-311G** calculated structures of propionyl chloride and perfluoropropionyl chloride.[6]

4.1 Introduction and Review

As further review from chapter 2, there are many different motivations and applications for studying propionyl chloride and perfluoropropionyl chloride via microwave spectroscopy. Motivation for studying the series of acyl chlorides was catalyzed from curiosity of three main effects: (i) the effect of varying the alkyl chain length (ii) the effect of perfluorinating the acyl

* All tables and figures in this chapter, as well as major parts of Sections 4.2, 4.3.1, 4.3.2, 4.4.1, and 4.4.2, and minor parts of other sections, have been reproduced from G. S. Grubbs II, R. A. Powoski, D. Jojola, and S. A. Cooke, Journal of Physical Chemistry A, 114, (2010). Reproduced with permission from the American Chemical Society.

chloride hydrocarbon chain; and (iii) the effect of eventually partially perfluorinating the acyl chloride hydrocarbon parent chain. The first two effects will be reported in this study, but the latter is still in progress at the University of North Texas (UNT). Perfluorination is defined as saturating all hydrogen atoms in a molecule with fluorine atoms. [6] The main purpose and motivation for this study is to explore the molecular and electronic structure of a series of acyl chlorides by obtaining and assigning as many spectroscopic parameters pertaining to the geometric and electronic properties as possible. Some of these parameters reported in this study consist of calculated data such as Cartesian coordinates in the a, b, c axis system; calculated equilibrium rotational constants and dipole moments; numerous ground state spectroscopic constants; internal rotation parameters; and kraitchman substitution coordinates. Other parameters were determined experimentally, such as experimentally derived geometric parameters; second moments and related quantities; and chlorine nuclear quadrupole coupling tensors in the principal axis system for some similar acyl chlorides.

In this study, the "perfluoroalkyl effect" is defined as the structural effects of perfluorination. This study allows the perfluoroalkyl effect to be further understood beyond the general belief that steric reasons cause the "perfluoroalkyl effect", such as electronic properties via the χ-tensor. Also, the structural effects of perfluorination relate to the kinetic and thermodynamic stabilizing effect that fluorination contributes to a carbon framework. [46] Moreover, the role of alkyl chain length is important for studying helicity, a structural feature evident in the polymer Polytetrafluoroethylene, (Teflon) [20] yet not present in hydrogenated carbon chains. [6] Examining the molecular structure of hydrocarbons with a different functional group, such as the carbonyl chloride functional group, may provide greater understanding for the requirements for helicity in molecules.

A perfluorination-initiated destabilizing effect of the carbonyl group, termed perfluoro-destabilizing effect, is commonly observed for molecules that have a carbonyl group. [47, 48] It is one of the main goals of this study to help provide a means of quantifying this perfluoro-destabilizing effect because no experimental methods have done this so far. For example, numerous perfluoroenols resist ketonization in the presence of acids whereas nonfluorinated enols will easily undergo ketonization. [49] One current way to study this destabilizing effect consists of using a fluorine-19 nuclear magnetic resonance (^{19}F NMR) method, which usually involves measuring the equilibrium constant between the ketone and the enol.

CP-FTMW spectroscopy offers a different method of quantifying this perfluoro-destabilizing effect. This method consists of measuring the difference in the electric field gradient at the chlorine nucleus, derived from χ, for an acyl chloride. Comparing this χ to a perfluoroacyl chloride would be useful if the χ-tensor was in the plane of the carbon-chlorine bond. This is nearly the case for χ_{zz} where the χ_{zz} tensor is nearly co-axial with the carbon-chlorine bond. The nuclear electric quadrupole coupling constants express the magnitude for the electric field gradient at the chlorine nucleus (See Table 9). Since this magnitude at the chlorine is different for the perfluorinated species, the fluorines must be affecting the electric field gradient. Examining perfluorobutyryl chloride, the longer version of perfluoropropionyl chloride will either confirm or refute this chemical behavior.

The perfluoro-destabilizing effect may be explained by this possible trend of greater χ-tensor magnitude felt at the chlorine nucleus for perfluorinated acyl chlorides. The explanation is possibly as follows. Lemal (2004) states that electron withdrawal by the fluorines strengthens the carbon-carbon bonds in the parent chain framework by as much as 7 kcal/mole greater in hexafluoroethane relative to ethane. C-F bonds are highly polar, which contributes to their

strength. The fluorines might have an electron-withdrawing effect when in close proximity to the carbonyl group, which results in a less partial positive carbonyl carbon. Therefore, a destabilizing effect occurs in the molecule. Ultimately the χ(Cl) has a greater electric field gradient at the chlorine nucleus due to the fluorines. Moreover, the fluorine atoms may resist the pull of electrons by the carbonyl oxygen. This normally causes substantial positive charge on the carbonyl carbon but instead may increase the negative charge on the carbonyl carbon and hence the increase in eQq at the chlorine nucleus. In addition to examining the χ_{zz}-tensors to explain the destabilizing effect, Table 1 shows decreasing magnitudes for the Cartesian coordinates in the a and b-axis systems and increasing magnitudes for the Cartesian coordinates in the c-axis system, which may further support somewhat of a destabilization effect. Further discussion of fluorocarbons is included in the Lemal et al. study. [31]

This chapter focuses primarily on characterization of propionyl chloride and perfluoropropionyl chloride done by Grubbs II et al. [6] The propionyl chloride contribution was a more exhaustive re-visitation using CP-FTMW methods instead. [6] There were a total of two prior FTMW spectroscopic studies on propionyl chloride that had been previously studied in the late 1970's. The first was done by Karlsson[1] and a second by Mata and Alonso. [2] The older FTMW studies provide spectral data found in the ground vibrational state, two excited states, and agree that the cis-conformer was the only conformer observed. Its dihedral angle was determined to be < CCCO = 0°. However, there was insufficient sensitivity for the assignment of the carbon-13 isotopologue species. [1, 2] The 1979 study by F. Mata [2] further improved upon the 1976 study by H. Karlsson [1] by improving the assignment in the K-band and the components of the quadrupole multiplets. Again, the previous FTMW and the 2010 CP-FTMW propionyl chloride study [6] all identify the cis-isomer of propionyl chloride as the lowest energy conformer. The rotational

spectra in the older studies were recorded in the vibrational ground state and two vibrationally excited states.[6] After transforming χ_{aa}, χ_{bb}, χ_{cc} into the principal axis of the quadrupole tensor assumed to be along the C-Cl bond, propionyl chloride's π-bonding character, π_c, was reported to be 0.104 or ~10% and it's ionic character, i_c, to be about 36%.[1] The C−Cl bond length was determined to be 1.789 Å.[1] Both of the π-character and bond length indicate high ionic character of the C−Cl bond in agreement with the 36% calculated value. π-character is calculated using the following formula where eQq is for the chlorine-35 nucleus with a value of -109.74 MHz, and χ_{zz} and χ_{yy} were taken from the Karlsson study.[1]

$$\pi_c = \frac{\frac{2}{3}(\chi_{zz} - \chi_{yy})}{-eQq(35_{Cl})}$$

Internal rotation for propionyl chloride was observed in the spectra of this 2010 study and partially in the Karlsson (1976) study.[1] In the Karlsson study, the V_3 barrier to internal rotation of the terminal methyl group was estimated to be 867(14) cm^{-1} or ~2480 cal/mole.[1] However, the resolution used in the 1976 study was less than that which was needed to resolve A-E internal rotation splitting in the ground state. This was solved with the resolution used at UNT in the 2010 study.[6] The V_3 barrier to internal rotation of the terminal methyl group is now measured to be about 853 cm^{-1} or ~2440 cal/mole (See Table 6).[6]

A CP-FTMW spectrometer[43] was used in all experiments in this study. Propionyl chloride and perfluoropropionyl chloride were experimentally done with a new automation program feature. This differs from the butyryl chloride experiment, which was run manually. The automated modifications of the CP-FTMW experiment done at UNT were used in this chapter and are described in chapter 3 as well as the Grubbs II et al study.[6] Everything else was done the same way as described in chapter 3 with a gas pulsing rate of 4 Hz. The experiment was set to

collect 20 μs durations of the free induction decay (FID) at 25 ps/point that are fast Fourier transformed to give usual line widths of approximately 80 kHz full width at half-maximum height (fwhm). [6]

In this study, the liquid propionyl chloride was purchased from Sigma-Aldrich and was sampled by pulsing argon gas through a $^1/_4$ in. tube filled with approximately 5 mL of liquid about 40 cm up stream of the solenoid valve. Propionyl chloride is a volatile liquid, bp = 77−79 °C. Perfluoropropionyl chloride was purchased from Synquest Laboratories as a gas with a bp of 7−9 °C. The gas sample was made by dissolving the gas in argon at about 3% by volume in a gas tank held at approximately 4−5 atm. [6]

4.2 Quantum Chemical Calculations

The GAMESS software package [50] Version 12 January 2009 (R1) was used to calculate the Quantum chemical calculations. The purpose of these calculations was to help identify the dipole moments and useful structures for propionyl chloride and perfluoropropionyl chloride, which is extremely helpful in assigning quantum energy transitions to experimental spectral frequencies. The calculations utilized a density functional method, M06-2X [51, 52] with 6-311G** basis sets. [53, 54.] The basis sets were not modified when used in the calculation and were acquired from the EMSL Basis Set Library. [55, 56] Table 1 and Table 2 of this chapter report the results of these calculations produced for propionyl chloride and perfluoropropionyl chloride. The calculations included in these tables consist of Cartesian coordinates, calculated rotational constants, and dipole moments. [6]

4.3 Experimental Results and Assignment

4.3.1 Assignment

Both molecules were assigned in a related way. This is most likely because of two reasons (i) both molecules are asymmetric rotors based on ray's asymmetry parameter value of, $\kappa \approx -0.87$, and (ii) the principal components of the electric dipole moment are, in both cases, aligned only along the a and b axes, despite having different magnitudes. [6] The chlorine-35 and chlorine-37 isotopologues of a straight parent chain conformation were both assigned. The strategy used was to first assign the harmonic sequences of $^{a}R_{0,\,1}$-type transitions with the chlorine-35 parent isotopologue being identified first. An approximately 100 MHz portion of the observed propionyl chloride spectrum is shown in Figure 3. [6]

After the $^{a}R_{0,\,1}$-type transitions were assigned, ^{a}Q-, ^{b}P-, ^{b}Q-, and ^{b}R-type transitions were assigned next. An all inclusive list of the quantum number assignments correlated to their observed frequencies can be found with the originally published article. [6] The AABS package, [57] obtained freely from the PROSPE Web site, [58] was used to make assignments of the spectra for these molecules. The programs of this package created by Pickett, namely, SPFIT and SPCAT, [39, 59] enable one to predict and make spectral assignments through a fitting process that uses different Hamiltonians. For example, one can use a Watson-A or a Watson-S Hamiltonian. In this experiment, a Watson A Hamiltonian, $\hat{H}$, was constructed in the coupled basis $I + J = F$ where I is a nuclear spin parameter, J is a rotational angular momentum parameter, and the coupled sum of the two parameters being the total angular momentum. The Hamiltonian used was sufficient to include two main terms, mainly the semi rigid rotor approximation rotational term ($\hat{H}_R$) and a nuclear quadrupole coupling of the nuclear spin ($\hat{H}_Q$) term having the following form:

$$\hat{H} = \hat{H}_Q + \hat{H}_R \qquad (1)$$

Furthermore, the $\hat{H}_Q$ term is the usual operator describing the interaction of chlorine quadrupole and framework angular momentum vectors I and J, respectively. [6] The Watson-A reduction in the Ir representation contribution is found in the H_R term. [60] The details of these forms of terms as well as other terms, such as centrifugal distortion, are discussed in Gordy and Cook (1984) [40] The fitted constants for propionyl chloride and perfluoropropionyl chloride constants are presented in Table 3 and Table 4, respectively. The strategy of assignment began with assignment of the parent chlorine-35 species of both molecules, propionyl chloride and perfluoropropionyl chloride, which were readily assigned. Propionyl chloride spectra were of sufficient intensity to assign carbon-13 transitions, but the carbon-13 isotopologues for perfluoropropionyl chloride were not. It is somewhat expected that perfluoropropionyl chloride did not have carbon-13 spectra assigned because it has a significantly smaller dipole moment component compared to propionyl chloride, see Table 2. Furthermore, propionyl chloride carbon-13 isotopomer spectra for the chlorine-35 parent isotopologues of all three carbon-13 isotopes were rapidly identified. [6]

4.3.2 Unique Lines Assigned

Although previous studies performed with the CP-FTMW spectrometer at UNT show that structureless lines are usually about 80 kHz wide (fwhm), several unique broadened b-type transitions were observed with line widths of ≈100 kHz (fwhm) or greater. In addition, four rotational transitions were clearly observed as distinct doublets and were later supported with calculation to be due to internal rotation of the terminal methyl group. Specifically, these transitions were the $J_{k-1k+1} = 4_{32} \leftarrow 5_{23}$, the $5_{32} \leftarrow 6_{25}$, the $7_{43} \leftarrow 8_{36}$, the $9_{27} \leftarrow 8_{36}$, and are listed

in Table 5 minus the transition frequencies calculated using parameters in Table 6. Moreover, these four transitions in Table 5 are considered tentative quantum number assignments. Further analysis of the doublet lines using the extended internal axis method with the XIAM software [61] was undertaken because these four lines provide only a limited data set. [6] Hyperfine structure suspected to be caused by internal rotation produced from the $J_{k-1k+1} = 4_{32} \leftarrow 5_{23}$ transition is shown in Figure 4. The barrier height, V_3, and methyl axis rotational constant, F, in propionyl chloride have been determined using centrifugal distortion and hyperfine constants held fixed at those values given in Table 3 and holding $\delta_{i,a}$, the angle between the methyl rotor and the a-axis fixed at a calculated value of 19.85°. [6] Table 6 shows the determined parameters and one notices that the value of F seems very reasonable at 160(7) GHz when compared to similar molecules. Highlighting that other rotational constants were held fixed, the error on the V_3 value is likely greatly larger than stated. However, the internal rotation splitting on the observed a-type and many of the b-type transitions are predicted to be below the ≈80 kHz resolution of our instrument in its current configuration. [6]

4.4 Discussion

4.4.1 Geometric Structures

Kraitchman substitution is a method that allows one to calculate the position of an atom in a molecule by utilizing the changes in the moments of inertia resulting from a single isotopic substitution of the atom. [40] An accurate structure of the molecule is possible to be determined without computational calculation once an adequate number of coordinates from at least two different isotopes along the principal axis have been determined. [40] In Table 7 of this study, a partial Kraitchman substitution structure [62] for both molecules has been started. Table 8 includes

Ray's asymmetry parameters [40] and experimental second moments along with inertial defects that have been evaluated for each isotopologue of each molecule. Upon doing a kraitchman substitution calculation and other calculations, the C−Cl bond length in both perfluoropropionyl chloride and propionyl chloride is established "to be shorter than that previously assumed for propionyl chloride, where r(C−Cl) was evaluated to be 1.789 Å." [1, 6]

There are five main sources of compelling evidence to support that the cis conformer is observed in this work with both propionyl chloride and perfluoropropionyl chloride having a cis dihedral angle of approximately ∠CCCO = 0°. They are as follows: (i) agreement between the calculated rotational constants, Table 2, and observed rotational constants, Table 6; (ii) zero magnitudes of the c principal axes Cartesian coordinates for the CCC(═O)Cl backbone in the calculated structures of these molecules, Table 1; (iii) the trans conformation has very poor agreement between calculated rotational constants A = 5036.76 MHz, B = 3745.70 MHz, and C = 2209.14 MHz for the trans conformer of propionyl chloride with the observed rotational constants; (iv) the kraitchman substitution structural properties of propionyl chloride and perfluoropropionyl chloride show nearly zero magnitudes in the c-plane, Table 7; and (v.) the relative inertness or invariance of the second moment, P_{cc}, to substitution of Cl (perfluoropropionyl chloride) and Cl, C(1), C(2), and C(3) (propionyl chloride), Table 8, confirm the cis conformation for both molecules. [6]

When examining the calculated molecular structure of these two molecules, one notices the distribution of nuclear masses in propionyl chloride differs from perfluoropropionyl chloride. Propionyl chloride has less parent chain mass along the a-axis. Perfluroropropionyl chloride slightly rotates the common backbone CCC(═O)Cl clockwise in the ab plane when compared to propionyl chloride. The angle between the C−Cl bond and the a-axis is 19.5°, and the angle of

the C═O bond with the b-axis is 31° for the calculated structures for propionyl chloride, Table 9. The analogous angles in perfluoropropionyl chloride are respectively 24° and 30°. The fact that μ_b is slightly larger in magnitude than μ_a for perfluoropropionyl chloride, whereas the reverse is true for propionyl chloride, can be partially explained by this subtle difference in the angle between the C-Cl bond and the (a-b axis), see Table 2.[6] Moreover, at least two studies by Fouriner et al. [18]and Dewberry et al. [63] have demonstrated that perfluoro-induced helicity of alkyl chains requires a chain length of at least four or five carbons. The results of this study further support this when examining the molecular structure helical angles or Newman projections and will be further discussed and magnified in chapter four and five on analogous butyryl chloride and valeroyl chloride molecules.

4.4.2 Electronic Structure: Chlorine Nuclear Quadrupole Coupling Tensors and the Destabilizing Effect of Perfluorination on the Carbonyl Group

Components of the chlorine nuclear quadrupole coupling tensor, χ, can be reported in terms of either a reduced mass fixed principal axis (a, b, c) or a spaced fixed principal axis usually labeled (x, y, z). This study, similar to the Karlsson [1] study, has had the inertial axes of (χ_{aa}, χ_{bb}, χ_{cc}) transformed into their principal axes of the quadrupole tensor assumed to be along the C-Cl bond for propionyl chloride, perfluoropropionyl chloride, and even later molecules. Specifically, the chlorine nuclear quadrupole coupling tensors for several other acyl halides, also rotated into their principal axes, are reported in Table 9. The assumption that this transformation results in a quadrupole tensor along the C-Cl bond is based on the fact that most of the mass lies along the principal a-axis, which gets rotated into the new principal z-axis somewhat along the C-Cl bond. However, one must be careful when comparing these values to ensure that he or she is comparing "apples to apples." For example, when comparing χ_{zz} from one molecule to another,

the angle between the principle z-axis and the C-Cl bond may not be exactly aligned with the C-Cl bond. With this clarified, this study reports observation in all cases that the angles between the z and a-axes as well as between the C-Cl bond and a-axis are very close and thus a fair comparison can be made between the different chlorine χ_{zz} values. As reported in Table 9, hydrocarbon parent chain series HCOCl, CH_3COCl, CH_3CH_2COCl, and syn−anti $CH_3CH_2CH_2COCl$, the magnitude of the chlorine χ_{zz}(Cl) value of ≈−59 MHz, is relatively inert to the alkyl chain length.[6] This "standard" acyl chloride χ_{zz}(Cl) value is perhaps explained best by the idea that the neighboring carbonyl group affects the Cl center local electronic environment, in a manner that hides the effect of the alkyl chain on the other side of the carbonyl group. It is less important, but perhaps still useful information, to point out that the χ_{xx}(Cl) and χ_{yy}(Cl) values are also somewhat unchanging with varied chain length. In fact, variation only occurs at about 10% or less across the series of nonfluorinated hydrocarbon parent chain species shown in Table 9.[6]

Moreover, perfluorinated acyl chlorides appear to show a different "standard" for χ_{zz} (Cl). There are two perfluoroacyl chlorides to compare to date for a seemingly "standard" perfluoroacyl chloride χ_{zz} (Cl) value of ≈−65 MHz. This difference of the χ_{zz} (Cl) between hydrocarbon-based acyl chlorides and perfluorinated acyl chlorides demonstrates that the electronic structure is significantly affected by perfluorination. A proposed explanation for this difference may be explained in the following way: Nuclear electric quadrupole coupling (eQq) values may act as a quantitative measure of the electric field gradient in a certain plane. When the electric field gradient is co-axial with a certain bond such as the C-Cl bond, then better assumptions can be made about electronic structural effects occurring along that bond. Due to the spherically symmetric electron distribution about the Cl nuclei due to the full valence shell,

the electric field gradient, $\partial^2V/\partial z^2$, at the nucleus in an isolated chloride ion, Cl^-, will be zero. Similar to the Townes-Dailey model, this zero value of $\partial^2V/\partial z^2$ translates to a zero value for the Cl nuclear quadrupole coupling component χ_{zz} in Cl^-. As in the Townes-Dailey model, any deviations from zero may be interpreted in terms of the decreasing ionicity or increasing covalency of the C−Cl bond. Larger positive magnitudes of eQq usually indicate larger ionic character along that bond based on this simple model. The Cl center in the perfluoroacyl chlorides has a more negative eQq and therefore appears to be in a slightly more covalent environment than in the acyl chlorides. In the specific case of the propionyl chlorides, this suggests that the difference in electronegativity of Cl and that of the $CF_3CF_2C(=O)-$ group is smaller than the difference between Cl and that of the $CH_3CH_2C(=O)-$ group. In short, $CF_3CF_2C(=O)-$ is more electronegative than $CH_3CH_2C(=O)-$. The smaller calculated dipole moments for perfluoroprionyl chloride compared to propionyl chloride provide further agreement for this correlation, see Table 2. These findings are fully consistent with the perfluoro-destabilizing effect of the carbonyl groups and provide a new way of looking at the effect. [6]

It is interesting to point out that Table 9 shows that the electronegativity of $C_nF_{2n+1}C(=O)-$ is greater than that for $C_nH_{2n+1}C(=O)-$, and both are little affected by varying the chain length n. Chapter five will further explore this effect of increasing the hydrocarbon and perfluorinated alkyl chain length.

4.5 Propionyl Chloride Methyl Group Internal Rotation

The results of this study show that there is evidence of internal rotation for propionyl chloride. However, there is no evidence of internal rotation for perfluoropropionyl chloride. The terminal methyl group on propionyl chloride produces a threefold barrier to internal rotation, V_3,

for propionyl chloride of 853(35) cm^{-1} or 2440(100) cal mol^{-1}. This is the first determination of the methyl torsional barrier height for propionyl chloride data in the pure ground vibrational state. The V_3 barrier appears to be reasonable when compared to related molecule V_3 barriers and when considering the error is within the 80 kHz (fwhm) resolution of the spectrometer as currently arranged. As discussed above in the unique lines assigned section 3.5, the observed splittings in four of the rotational transitions for propionyl chloride have been analyzed, see Table 5 and Figure 4. Karlsson [1] and Mata [2] in late 1970's reported a barrier to methyl group internal rotation of 867(14) cm^{-1} or 2480(40) cal mol^{-1} using their splittings in spectral transitions for propionyl chloride in excited vibrational states. Table 10 lists and compares magnitudes of determined V_3 barriers to methyl internal rotation for several related molecules, of which include the Karlsson's [1] barrier. [6]

The quantum mechanical calculations for the V_3 barriers agree well with experimental observation. For example, Table 5 reports the B3LYP/6-31+G calculated barriers to terminal methyl group internal rotation in propionyl chloride and perfluoropropionyl chloride with propionyl chloride having a barrier of 817 cm^{-1}. This is in near agreement with the 853(35) cm^{-1} experimental value for this work. As expected, A−E internal rotation splitting in the perfluoropropionyl chloride rotational spectrum is not observed for the trifluoromethyl group internal rotation in perfluoropropionyl chloride because a significantly higher barrier of 1120 cm^{-1}, or 3200 cal mol^{-1} is measured. This difference in barrier height is better compared in Figure 5. [6]

As a review, this chapter demonstrates that internal rotation exists for propionyl chloride but not for perfluoropropionyl chloride. A χ_{zz} is about -60 MHz for the propionyl chloride and -65 MHz for the perfluorinated counterpart. There is only one stable conformation observed for

each of the compounds, and it seems to be straight in its geometric shape. Chapter 5 and 6 provide comparison of these molecular and geometric properties, along with other structure, and will continue to show how increasing parent chain length affects these properties. All data and assigned frequencies can be found in the following tables.

Table 4.1: M06-2X/6-311G** Calculated Cartesian coordinates in units of angstroms in the principal inertial axis system for propionyl chloride and perfluoropropionyl chloride.[6]

	CH_3CH_2COCl			CF_3CF_2COCl		
atom	a	b	C	a	b	c
C	−2.486	−0.300	0.0000	−1.450	0.141	0.0000
C	−1.054	−0.816	0.0000	−0.033	−0.457	0.0000
C	−0.057	0.31	0.0000	1.069	0.624	0.0000
O	−0.269	1.466	0.0000	0.868	1.781	0.0000
Cl	1.652	−0.296	0.0000	2.676	−0.091	0.0000
H/F	−0.836	−1.437	−0.874	0.102	−1.224	−1.090
H/F	−0.836	−1.438	0.872	0.102	−1.223	1.091
H/F	−2.677	0.315	−0.880	−1.631	0.882	−1.084
H/F	−2.677	0.313	0.882	−1.631	0.883	1.083
H/F	−3.186	−1.135	0.0000	−2.337	−0.845	0.0000

Table 4.2: M06-2X/6-311G** Calculated equilibrium rotational constants and dipole moments for propionyl chloride and perfluoropropionyl chloride.[6]

parameter	CH_3CH_2COCl	CF_3CF_2COCl
A/MHz	8956.98	2035.79
B/MHz	2368.72	847.3
C/MHz	1917.39	759.74
μ_a/D	−2.29	0.29
μ_b/D	−2.10	−0.54
μ_c/D	0	0

Table 4.3: Ground state spectroscopic parameters for propionyl chloride.[6]

parameter	$CH_3CH_2CO^{35}Cl$	$CH_3CH_2CO^{37}Cl$	$CH_3CH_2{}^{13}CO^{35}Cl$	$CH_3{}^{13}CH_2CO^{35}Cl$	$^{13}CH_3CH_2CO^{35}Cl$
A_0/MHz	8854.7845(14)[a]	8828.0790(21)	8840.9115(74)	8755.7361(49)	8841.1905(51)
B_0/MHz	2377.94361(37)	2320.2750(12)	2378.1111(29)	2365.7836(17)	2311.1544(16)
C_0/MHz	1918.68343(24)	1879.7511(13)	1918.1392(20)	1906.1228(13)	1874.3562(13)
Δ_J/kHz	0.3016(98)	0.237(18)	0.23(12)	0.320(73)	0.282(73)
Δ_{JK}/kHz	1.335(66)	1.09(12)	1.335[b]	1.335[b]	1.25(18)
Δ_K/kHz	13.83(25)	12.06(14)	14.7(27)	13.8(20)	13.7(18)
δ_J/kHz	0.0591(16)	0.0488(42)	0.0591[b]	0.0591[b]	0.0591b
δ_k/kHz	0.788(67)	0.28(55)	0.788[b]	0.788[b]	0.788b
χ_{aa}/MHz	−49.0673(37)	−38.9625(51)	−49.133(29)	−48.747(35)	−48.814(14)
χ_{bb}/MHz	26.4986(55)	21.1725(80)	26.448(47)	26.165(39)	26.215(24)
χ_{cc}/MHz	22.5687(40)	17.7900(61)	22.685(37)	22.582(34)	22.599(19)
$\lvert\chi_{ab}\rvert$/MHz	29.94(57)	23.75(40)	33.2(28)	29.6(25)	30.8(18)
N[c]	125	92	22	24	31
σ_{rms} [d]	0.227	0.27	0.467	0.345	0.319
σ/kHz [e]	5.67	6.74	11.67	8.62	7.98

[a] Numbers in parentheses give standard errors (1σ, 67% confidence level) in units of the least significant figure.
[b] Fixed at the parental isotopologue value.
[c] Number of observed transitions used in the fit.
[d] The root-mean-square deviation of the fit is unitless and equal to $\sqrt{\frac{\Sigma[((obs-calc)/error)^2]}{N}}$
[e] This quantity is equal to $\sqrt{\frac{\Sigma[(obs-calc)^2]}{N}}$.

Table 4.4: Ground state spectroscopic parameters for perfluoropropionyl chloride. [6]

parameter	^{35}Cl	^{37}Cl
A_0/MHz	2025.71840(19)[a]	2025.58453(37)
B_0/MHz	842.99816(13)	823.58204(35)
C_0/MHz	755.97374(14)	740.30668(35)
Δ_J/Hz	28.9(11)	26.6(21)
Δ_{JK}/Hz	290.7(30)	292(10)
Δ_K/Hz	−227.2(57)	−224(14)
δ_J/Hz	4.07(23)	2.7(10)
δ_k/Hz	−340(23)	−381(98)
χ_{aa}/MHz	−49.7148(61)	−39.256(11)
χ_{bb}/MHz	25.4688(90)	20.147(16)
χ_{cc}/MHz	24.2460(66)	19.109(12)
$\lvert\chi_{ab}\rvert$/MHz	37.77(21)	29.84(13)
N[b]	402	232
σ_{rms}[c]	0.296	0.348
σ/kHz[d]	7.4	8.71

[a] Numbers in parentheses give standard errors
(1σ, 67% confidence level) in units of the least significant figure.

[b] Number of observed transitions used in the fit.

[c] Root mean square deviation of the fit, $\sqrt{\frac{\Sigma[((obs-calc)/error)^2]}{N}}$

[d] This quantity is equal to $\sqrt{\frac{\Sigma[(obs-calc)^2]}{N}}$

Table 4.5: Observed transitions frequencies for those propionyl chloride transitions observed as doublets due to methyl group internal rotation. [6]

$J'_{K-1K+1} \leftarrow J''_{K-1K+1}$	$2F'-2F''$	Symmetry	Frequency/ MHz	(obsd-calcd) /kHz[a]
$5_{32}-6_{25}$	7−9	A	8077.5732	−5.3
	13−15	A	8079.2326	−35.6
	11−13	A	8086.6362	−33.1
	7−9	E	8077.5011	15.7
	13−15	E	8079.1608	−14.4
	11−15	E	8086.5598	−16.4
$9_{27}-8_{36}$	19−17	A	9885.0316	−5.4
	17−15	A	9885.4381	2.6
	21−19	A	9888.5241	3
	15−13	A	9888.9286	−0.9
	19−17	E	9885.16	3.9
	17−15	E	9885.5606	5.9
	21−19	E	9888.6554	2.6
	15−13	E	9889.0544	−6.8
$4_{32}-5_{23}$	5−7	A	11367.4579	−10.3
	11−13	A	11371.113	−14.9
	7−9	A	11379.3949	−14.9
	9−11	A	11383.0529	−17.1
	5−7	E	11367.2202	−1.7
	11−13	E	11370.8833	1.7
	7−9	E	11379.159	−4.4
	9−11	E	11382.8281	4.5
$7_{43}-8_{36}$	11−13	A	12248.4677	29.8
	17−19	A	12249.4821	26.1
	13−15	A	12254.4064	28
	15−17	A	12255.4202	23.7
	11−13	E	12248.5879	13.4
	17−19	E	12249.5948	2.1
	13−15	E	12254.5091	−6.1
	15−17	E	12255.5243	−9.0

[a] The observed transition frequencies minus those transition frequencies calculated using those parameters in Table 6.

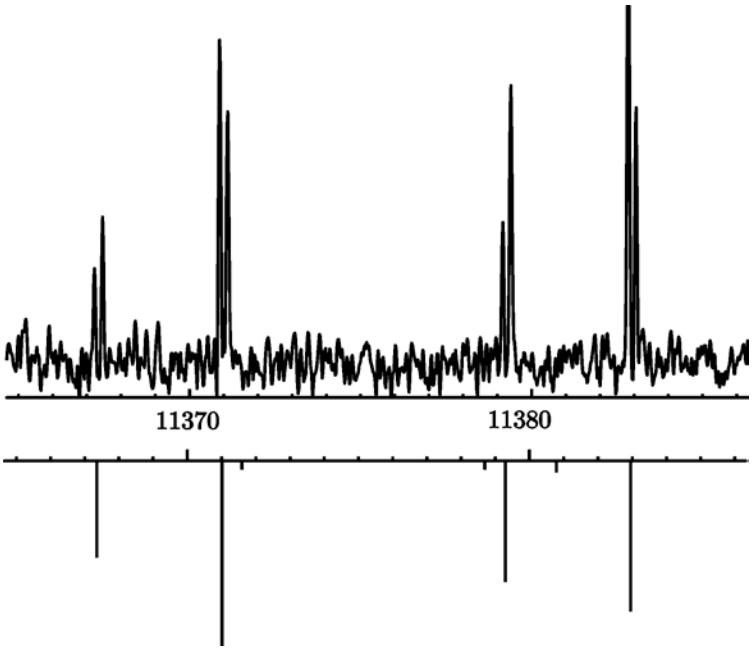

Figure 4: The $4_{32} \leftarrow 5_{23}$ transition. The upper figure shows the observed spectrum the lower figure shows the spectrum produced using the constants in Table 4.3. The transition is clearly doubled. [6]

Table 4.6: Internal rotation parameters related to the internal methyl rotor in propionyl chloride[a, 6]

parameter	Value
A/MHz	8854.7062(30)
B/MHz	2377.9342(38)
C/MHz	1918.6425(43)
F/GHz	160(7)
V_3/cm^{-1}	853(35)
$\delta_{i,a}$ /deg	19.85[b]
N[c]	30
σ/kHz[d]	15.7
σ_{rms}[e]	0.628

[a] The centrifugal distortion parameters and Cl nuclear quadrupole coupling tensor values were held fixed to those values given in Table 3.
[b] This parameter, the angle between the symmetry axis of the methyl rotor and the a axis, was held fixed at this value, obtained from the calculated structure.
[c] Number of observed transitions in the fit.
[d] This quantity is equal to $\sqrt{\frac{\Sigma[(obs-calc)^2]}{N}}$
[e] Root mean square deviation of the fit, $\sqrt{\frac{\Sigma[((obs-calc)/error)^2]}{N}}$

Table 4.7: Kraitchman substitution coordinates[a] and experimentally derived geometric parameters for propionyl chloride and perfluoropropionyl chloride. [6]

	CH_3CH_2COCl			CF_3CF_2COCl		
	A	*b*	*c*	*a*	*b*	*C*
Cl	1.6430(9)	−0.302(5)	0[b]	2.6747(6)	−0.09(2)	0.02(6)
C(1)	0[b]	0.300(5)	0[b]			
C(2)	−1.046(2)	−0.809(2)	0.03(4)			
C(3)	−2.4868(6)	−0.303(5)	0.0(1)			
r(C(1)−Cl)/Å		1.750(3)			1.777(3)[c]	
r(C(1)−C(2))/Å		1.525(5)				
r(C(2)−C(3))/Å		1.527(3)				
<(Cl−C(1)−C(2))/deg		113.2(3)				
<(C(1)−C(2)−C(3))/deg		114.0(3)				
D(Cl−C(1)−C(2)−C(3))/deg		180				

[a] In units of angstroms. Signs have been added on the basis of the calculated structures. C(1) is the carbon closest to the acyl chloride group.
[b] An imaginary value was obtained which is indicative that the value is very close to zero.
[c] This value best reproduces the determined rotational constants for both isotopologues given in Table 4.4.

Table 4.8: Second moments and related quantities for propionyl chloride and perfluoropropionyl chloride. [6]

Parameter	P_{aa}/u Å^2 [a]	P_{bb}/u Å^2	P_{cc}/u Å^2	Δ/u Å^2 [b]	K [c]
$CH_3CH_2CO^{35}Cl$	209.4262	53.9726	3.1015	−6.2030	−0.8676
$CH_3CH_2CO^{37}Cl$	214.7087	54.1455	3.1013	−6.2025	−0.8732
$CH_3CH_2{}^{13}CO^{35}Cl$	209.4113	54.0622	3.1014	−6.2029	−0.8671
$CH_3{}^{13}CH_2\ CO^{35}\ Cl$	210.5175	54.6171	3.1027	−6.2053	−0.8658
$^{13}CH_3CH_2CO^{35}Cl$	215.5678	54.0602	3.1017	−6.2033	−0.8746
$CF_3CF_2CO^{35}Cl$	509.2673	159.2467	90.2347	−180.4693	−0.8629
$CF_3CF_2CO^{37}Cl$	523.3996	159.2621	90.2357	−180.4714	−0.8704

[a] The second moment, $P_{aa} = \sum_i m_i a_i^2$, and similarly for P_{bb} and P_{cc}.
[b] $\Delta = I_c - I_a - I_b$ is the inertial defect.
[c] κ is the asymmetry parameter and is equal to $(2B - A - C)/(A - C)$.

Table 4.9: The chlorine nuclear quadrupole coupling tensor in the principal axes system for various acyl chlorides. [6]

parameter	HCOCl[a,b]	CH_3COCl[a,c]	C_2H_5COCl	C_2F_5COCl	syn−anti-C_3H_7COCl[d]	syn−anti-C_3F_7COCl[e]	$(CH_3)_3CCOCl$[f]
χ_{zz}/ MHz	−59.8(7)[g]	−59.486	−59.49(35)	−65.41(15)	−59.22(21)	−65.427(18)	−60.05(22)
χ_{xx}/ MHz	39.0(2)	37.542	36.92(35)	41.17(15)	36.73(21)	41.129(19)	37.56(22)
χ_{yy}/ MHz	20.8(2)	21.944	22.569(4)	24.246(7)	22.485(6)	24.298(13)	22.4864(50)
η_z[h]	−0.303(2)	−0.2622	−0.2413(61)	−0.2587(24)	−0.2406(36)	−0.2572(4)	−0.2510(40)
η_{za}[i]/ deg	17.5	5.16	19.20(27)	22.569(81)	32.082(60)	33.185(8)	31.64(7)
$\theta_{(C-Cl),a}$/ deg[i]	17.5k	5.16[k]	19.5[k]	24.0[k]	32.8[k]	34.68[k]	

[a] Obtained from a first-order perturbation analysis. No off-diagonal χ components determined. No uncertainties given.
[b] Reference [9].
[c] Reference [10].
[d] Reference [5].
[e] Reference [64].
[f] Reference [11].
[g] Standard errors (1σ, 67% confidence level) in units of the least significant figure.
[h] The asymmetry of the χ tensor in the principal axes system, $\eta_x = (\chi_{xx} - \chi_{yy})/\chi_{zz}$.
[i] The angle between the z and a axis.
[j] The angle between the Cl−C bond axis and the (a,b) axes.
[k] Taken from the calculated structure.

Table 4.10: Methyl group internal rotation barrier heights in related molecules. [6]

molecule	V_3/ cal mol^{-1}	Ref
ethanoyl chloride	1269(10)	10
cis-propanal	2280(100)	65
cis-propionic acid	2340(30)	13
cis-propionyl fluoride	2400(60)	66
cis-propionyl chloride	2440(100)	this work.
cis-propionyl chloride[a]	2480(40)	1
Trans-1-chloropentane	2760(20)	67
[a] Determined from the molecule in an excited vibrational state.		

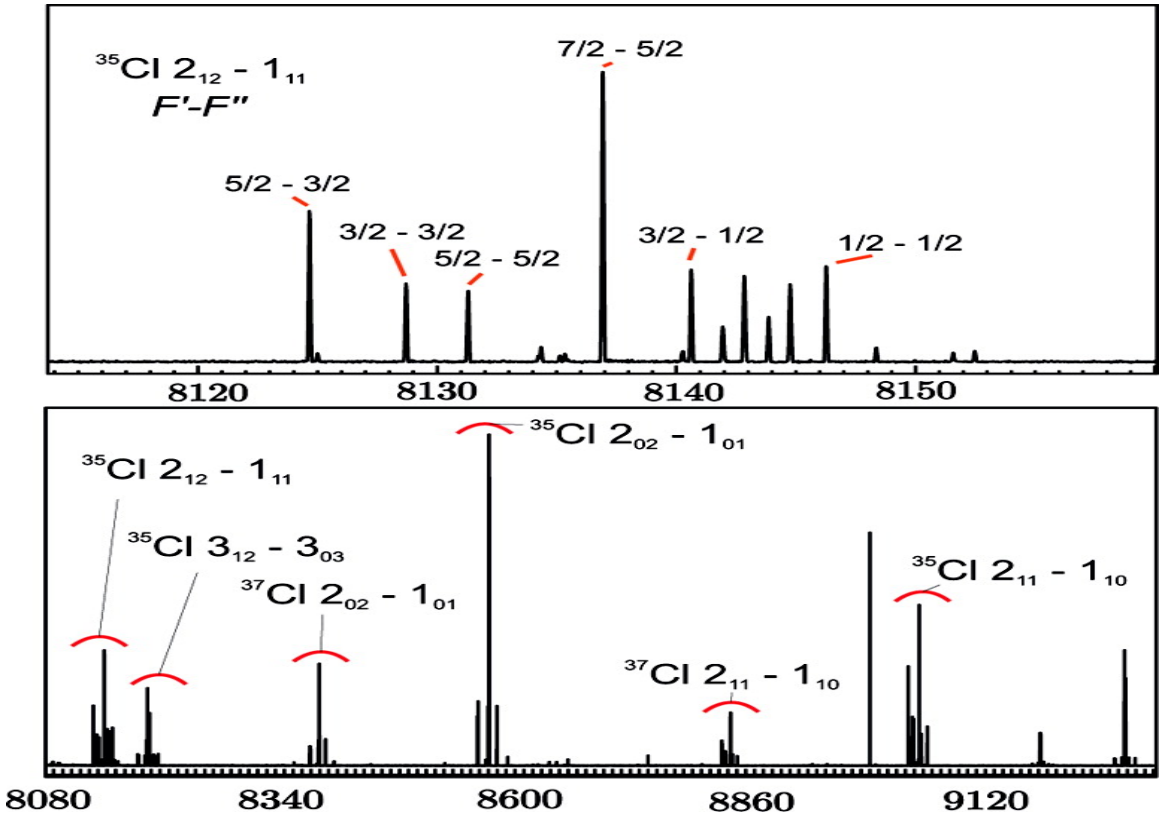

Figure 4.5: A 1000 MHz portion and a subsection of spectra collected for propionyl chloride. The lower figure shows a broad scan (30000 averaging scans). The upper figure shows a blow up of a small region. Several transitions have been labelled. All transitions shown may be identified by consulting the supporting information. [6]

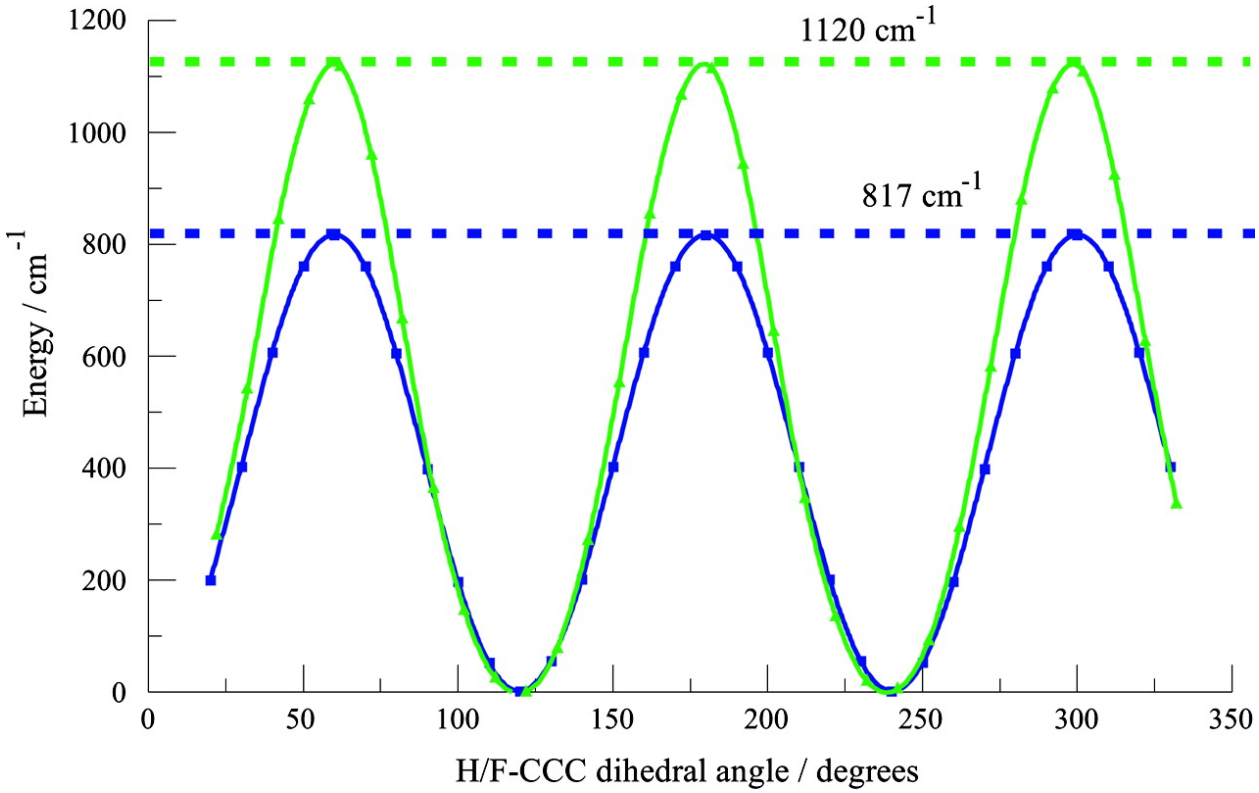

Figure 4.7: The B3LYP/6-31+G calculated barrier to methyl and trifluoromethyl group internal rotation in propionyl chloride (blue line) and perfluoropropionyl chloride (green line).[6]

CHAPTER 5

MOLECULAR STRUCTURE ANALYSES OF BUTYRYL CHLORIDE AND PERFLUOROBUTYRYL CHLORIDE[†]

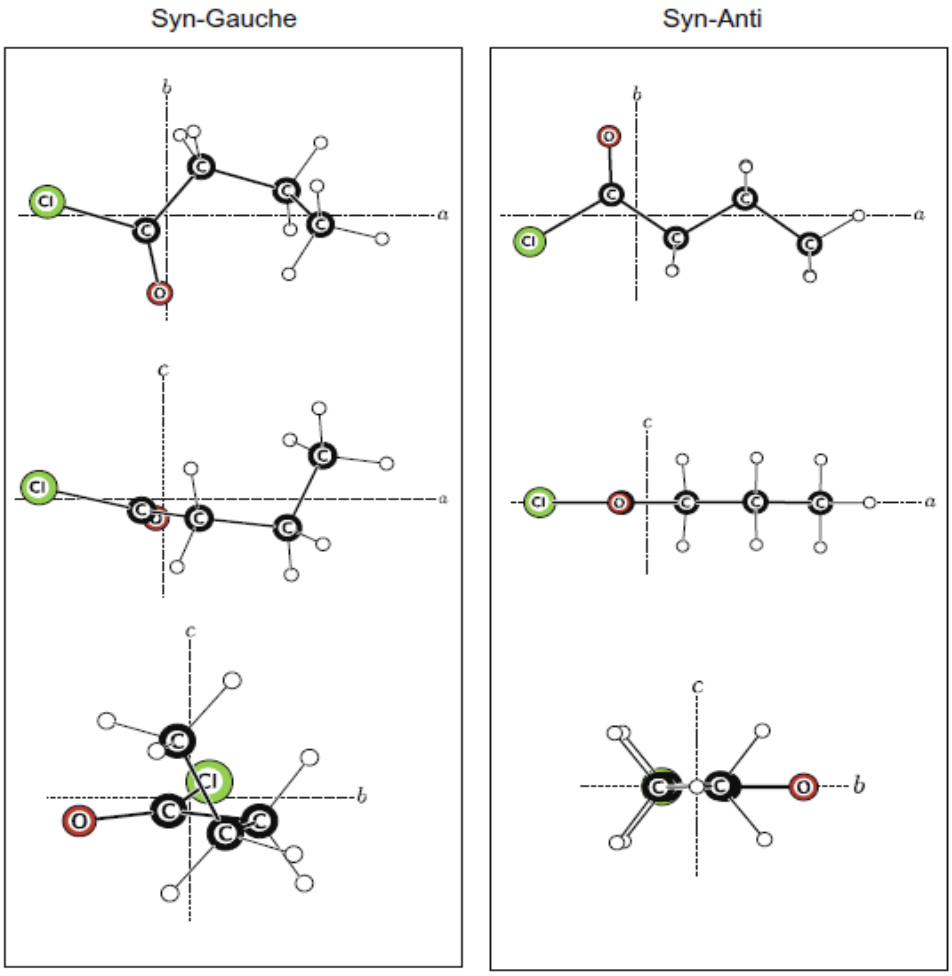

Figure 5.1: The MP2/6-311G** calculated structures of the syn-gauche and syn-anti conformers of butyryl chloride in the *ab*, *ac* and *bc* planes of the principal inertial axes systems. 5

5.1 Introduction and Review

This chapter focuses on the characterization of two molecules, butyryl chloride and perfluorobutyryl chloride, for the purpose of continuing exploration of the molecular and

[†] All tables and figures in this chapter, as well as major parts of Sections 5.1, 5.2, 5.3, 5.4, 5.4.1, 5.4.2, and minor parts of other sections, have been reproduced from R.A. Powoski, G.S. Grubbs II, S.A. Cooke, Journal of Molecular Structure, Volume 963, Issues 2-3, 29 January (2010). Reproduced with permission from Elsevier.

electronic structure of acyl chlorides and their perfluorinated counterparts. Two molecular studies will be the main source of the focus of this chapter, the perfluorobutyryl chloride 2009 study by Grubbs II et al. [64] and the butyryl chloride 2010 study by Powoski et al. [5] Up until the Powoski et al. study [5], butyryl chloride had been the subject of two prior microwave spectroscopic investigations, one by Thomas et al. [4] and a second by Mata and Pérez [3]. In both cases, low resolution microwave spectroscopy was used in which 5–25 MHz uncertainties on measured line centers were ascribed depending upon the line shape observed.

> When considering the structure of butyryl chloride one must consider two dihedral, or torsional, angles namely that between the CCCO centers and a second between the CCCC centers. Of the five postulated conformers for butyryl chloride two were observed in the low resolution work by Mata et al. and Thomas et al. [3, 4] Although exact geometries were not tractable by kraitchman substitution methods, the experimentally obtained *B*+*C* rotational constant for the syn-anti form were consistent with the dihedral angles of τ_1(CCCO) ≈ 0^0 and τ_2(CCCC) ≈180^0, and *B*+*C* for the syn-gauche form were consistent with τ_1(CCCO) ≈ 0° and τ_2(CCCC) ≈70^0. The ratio of the intensity of the syn-gauche rotational transitions to those of syn-anti was observed as approximately the same at 25 and −63 °C indicating that the difference in energy between the two conformers was very small. [5]

"With the exception of monofluorinated ethanoyl chloride (CH_2FCOCl), perfluorobutyryl chloride was the first acyl chloride study to have a fully perfluorinated carbon backbone." [64] This created further motivation to later study perfluoropropionyl chloride (CF_3CF_2COCl), propionyl chloride (CH_3CH_2COCl), and valeroyl chloride ($CH_3CH_2CH_2COCl$). As for internal rotation, the CF_3 barrier, V_3, to internal rotation in CF_3COCl is determined to be less than the barrier to CH_3

internal rotation in CH_3COCl.[64] "However, the CF_3 internal rotation stopped being observed for perfluoropropionyl chloride (CF_3CF_2COCl), but CH_3 internal rotation was observed for propionyl chloride (CH_3CH_2COCl)."[6] This is likely that the CF_3 V_3 barrier is smaller than the CP-FTMW sensitivity. As for butyryl chloride and perfluorobutyryl chloride, no internal rotation was observed. This indicates that the trend for the CF_3 internal rotation barrier V_3 for acyl chlorides is too small to be observed beyond a 2 carbon backbone, and the CH_3 internal rotation is too small to be observed beyond a 3 carbon backbone with the CP-FTMW spectrometer. Further comparison of this trend with spectroscopic studies of alkanes, alkynes, and related molecules[26, 19, 20, 18, 25, 69, 28, 22, 23, 24] would be of interest to the general perspective of hydrocarbons as a whole but will not be focused on in detail for this study. Overall, the microwave spectrum of butyryl chloride and perfluorobutyryl chloride at higher resolution further contributes to the structure of the molecule and adds to the existing microwave spectroscopic studies on other acyl halides[9, 70, 10, 66, 1, 71, 68].

5.2 Experiment

Samples of liquid butyryl chloride (Sigma–Aldrich >98%) and perfluorobutyryl chloride (Synquest Inc. > 90%) were used without further purification.[8, 6] Rotational spectra were recorded using a Chirped-pulse Fourier Transform Microwave (CP-FTMW) spectrometer located at the University of North Texas. Again, this instrument has been described in detail in chapter 3 and elsewhere[72, 6] with inspiration for this technique coming from Brown et al.[43] The fast Fourier transformations in our experiment were performed such that line widths obtained were approximately 80 kHz (FWHM), and an uncertainty of 25 kHz is attributed to the location of recorded line centers. The backing gas used was

argon, and the backing pressure was approximately 2 atm. One experimental difference is that this data was not collected using the automated Labview program. [5] However, 10,000 shots were still run at a time and averaged manually. The high resolution, about 80 kHz, of the (CP-FTMW) technique at (UNT) improved the spectroscopic data that had only been done with low resolution of 5,000-25,000 kHz in the studies by Thomas et al. [4] and by Mata and Pérez. [3]

5.3 Quantum Chemical Calculations

Quantum chemical calculations were performed using the GAMESS software package [50], Version 12 January 2009 (R1). Similar quantum calculation strategies were employed on these molecules, as done on the molecules as described in Chapter 4, in order to obtain a good initial guess using a personal computer. The same two computational methods; an ab initio 2nd order Møller–Plesset [73]and a density functional method, M06-2X, were used. [51, 52] with 6-311G** basis sets [53, 54]. [5]

5.4 Experimental Results

The spectroscopic results for the butyryl chloride were relatively unique from chapter four because two stable conformations instead of just one, were assigned: syn-anti and syn-gauche, each with separate chlorine-35 and chlorine-37 isotopologues being assigned. This is significant because it suggests that the alkyl chain length requires four carbons or greater to observe more than one measureable stable conformation. However, only one stable syn-anti conformation for the chlorine-35 isotopologue was assigned for perfluorobutyryl chloride. [8] A similar straight or syn-anti single conformation was assigned for both propionyl chloride and

perfluoropropionyl chloride shown in chapter 4. Moreover, sensitivity was not sufficient to observe and assign carbon-13 spectra.

Cartesian coordinates of the MP2, instead of M06-2X, calculated structures of two conformers of butyryl chloride are given in Table 1 for the syn-gauche conformer and in Table 2 for the syn-anti conformer. Internal rotation was not observed for either molecule, which suggests that internal rotation may not occur beyond 3 carbons in acyl chlorides. The calculated structures of the two conformers drawn in the principal inertial planes are given in Figure 5.1. Newman projections and relative energies for the two conformers are presented in Fig. 5.2 and Table 5.3. Calculated rotational constants and dipole moments are also given in Table 5.3.

5.4.1 Assignment

As for spectral assignment, a 500 MHz portion of the observed spectrum is shown in Fig. 5.3. Transitions were assigned using the calculated spectroscopic constants. Similar to the chapter 3, the fitting of spectra utilized the AABS package [57, 58]. The assigned transition frequencies can be found in the originally published articles. [5, 64] The beginning assignment strategy was the same as chapter 4 where reliable values of the rotational constants A, B, C along with components of the chlorine nuclear quadrupole coupling tensor were possible once $^{a}R_{01}$ type transitions were assigned first. These constants then facilitated assignment of *b*-type transitions, but no *c*-type transitions were observed for either conformer. A Watson-A reduced Hamiltonian [74] in the I^{r} representation was again used. The spectroscopic parameters of the type $\hat{H} = \hat{H}_r + \hat{H}_{cd} + \hat{H}_Q$ were allowed to vary when using programs by Pickett. [59, 39] The results of this procedure are given in Table 5.4.

5.4.2 Unique Lines Assigned

There were some special assumptions or strategies used in assigning certain spectroscopic parameters for these molecules. For example, the centrifugal distortion constant Δ_{JK} was not determinable for the syn-anti ^{37}Cl species for butyryl chloride. The solution utilized was to simply hold it fixed at the value for the ^{35}Cl isotopologue to assist with assignment. Also, χ_{bc} was not determinable for the ^{37}Cl species, and so this term was held fixed at the scaled value of the ^{35}Cl isotopologue, using $Q(^{35}\text{Cl})/Q(^{37}\text{Cl}) = 1.2688$ [75]. Lastly, although the signs of the off-diagonal components of the Cl nuclear quadrupole coupling tensor are not determinable, an improved RMS for the fit of the syn-gauche data was obtained when the sign of the product of the off-diagonal components was negative.

5.5 Discussion

5.5.1 Geometric Structure

For the syn-gauche conformer, the dipole moment is increased along the c-plane. Therefore, if c-type transitions were to be observed, the syn-gauche conformer is anticipated to have the largest c-type transitions because of the increased dipole moment along the c-plane. However, despite successful assignment of *a*-type and *b*-type transitions, attempts at observing *c*-types were unsuccessful for either conformer, which was not surprising for the syn-anti conformer since its dipole moment in the c-plane was much smaller. Table 3 lists the calculation of the dipole moments, and it does indicate that μ_c is fairly small, 0.3 D. Presumably this is believed to be the main reason for failing to observe *c*-type transitions in the microwave spectroscopy experiments.

As mentioned in section 5.1, two conformations were observed for butyryl chloride and one for perfluorobutyryl chloride. Their bond angles and bond lengths are calculated and reported in Table 7 and Table 8. Both butyryl chloride and perfluorobutyryl chloride demonstrate the syn-anti being stable conformations with the syn-gauche being similar in stability. The τ_2(CCCC) $\approx 70^0$ unique stability may possibly be explained by the terminal methyl group having somewhat of an attraction for the carbonyl group while still maintaining repulsion from the gauche orientations for the hydrogens on the carbon backbone. Figure 2 shows the Newman projections of this.

There are a few main sources of evidence that indicate the cis conformer is observed in this work for butyryl chloride and perfluorobutyryl chloride possessing an approximate cis dihedral angle of, ∠CCCO = 0°. They are as follows: (i) agreement between the calculated rotational constants, Table 2, and observed rotational constants, Table 3, and (ii) near zero magnitudes of the c principal axes Cartesian coordinates for the CCC(=O)Cl backbone in the calculated structures of these molecules, Table 1.

The pseudo-inertial defects for both conformers, presented with the experimentally derived moments of inertia and planar moments in Table 5, are consistent with the calculated structures. When examining inertial defects, the magnitude is directly proportional to the mass in the plane. [40] Therefore, the 6 out-of-plane hydrogens make it not surprising to find a small value of the pseudo inertial defect for the syn-anti conformer, Table 5.

Kraitchman substitution coordinates for the chlorine atom in both conformers have been determined and are presented in Table 5.5. Again, evidenced by similar magnitudes for the chlorine atom, Tables 5.1 and 5.2, very good agreement is found when comparing the substitution coordinates of the Cl atom with the calculated Cartesian coordinates in Table 5.1 and

Table 5.2. However, no other substitution coordinates were able to be calculated because the spectral intensity was not large enough for assignment of the carbon-13 transitions.

Breaking the trend from the work on propionyl chloride [1] where evidence of internal rotation was found in the ground state spectrum, no evidence of methyl-group internal rotation was observed in the butyryl chloride or perfluorobutyryl chloride spectra. On the other hand, it is somewhat surprising given the observation of internal rotation in butyronitrile [17]. A- and E-splitting were on the order of 300 kHz for butyro nitrile and a barrier height to internal rotation, V_3, was determined to be ≈13 kJ mol^{-1} for both *trans* and *cis* conformers. Failure to observe internal rotation in butyryl chloride indicates that the acyl chloride group produces a significantly higher barrier to methyl-group rotation than that determined in butyronitrile.

In regards to the relative energies of the syn-anti and syn-gauche conformers, the quantum chemical calculations performed indicate that the syn-gauche conformer is marginally more stable than the syn-anti. This agrees with the Bohn et al. study where the effects of CN and CCH functional groups instead of the COCl acyl chloride functional group were explored on alkyl chains. [23]

Further evidence for the syn-gauche conformer being more stable than the syn-anti is also present in the observed spectrum. For example, in the low resolution microwave spectra, *a*-type transitions were observed with an intensity ratio of 1:0.4, syn-anti:syn-gauche. The observed ratio was the same at 25 and −63 °C indicating that the conformers were very close in energy. In our experiments, we estimate a rotational temperature of about 4 K or -269 ^{0}C in the supersonic expansion. The ratio of *a*-type transitions in our experiments was found to be about 1:0.8, syn-anti:syn-gauche. In absorption experiments, the signal intensity is proportional to the dipole moment; in Fourier transform microwave spectroscopy, the intensity is proportional to the square

of the dipole moment. Using the calculated μ_a component of the dipole moments for syn-anti and syn-gauche butyryl chloride, Table 3, and assuming that the syn-anti and syn-gauche conformers are of equal energy, then the 1:0.4 ratio previously observed in the absorption experiments can be extrapolated to an anticipated ratio of 1:<0.4 syn-anti:syn-gauche in the Fourier transform experiments. The observed ratio of 1:0.8 at our lower experimental temperature provides some evidence that the syn-gauche is indeed the more stable. However, the difference in intensity increased at the colder experimental conditions for the syn-anti but fell short of the syn-gauche. It is important to consider that this increase from 0.4 to 0.8 for the syn-anti may be partially due to the spectrometer studies in 1978 [4] and 1984 [3], as well as the higher resolution CP-FTMW spectrometer used in the Powoski et al. study in 2010. [5]

5.5.2 Electronic Structure: Quadrupole Coupling Tensor & Effect of Perfluorination on the Carbonyl Group

For butyryl chloride and perfluorobutyryl chloride, the experimentally determined complete ^{35}Cl nuclear quadrupole coupling tensors in Table 5.4 have been rotated into the *x*, *y*, *z* axis system enabling comparison of this quantity with related species just as was done and explained previously in chapter 3 and chapter 1. This comparison is presented in Table 5.6. In all cases, the *z*-axis lies very close to the axis of the C-Cl bond, Table 5.6. One notices a continuation of the invariance of the magnitude of χ_{zz} to the length of the carbon chain, branching of the carbon chain, and an invariance trend beginning for the fluorination of the carbon chain. Upon a current literature search for hydrocarbon acyl chlorides, a $\chi_{zz}\approx$-60 MHz for all the acyl chloride species is measured and a $\chi_{zz}\approx$-65 MHz invariant trend for perfluorinated acyl chlorides is measured. Therefore, the electric field gradient at the Cl center is dominated heavily by the local effects of

the carbonyl group. Further exploration of increasing the length of the carbon backbone chain in acyl chlorides is studied in chapter 6.

Table 5.1: MP2/6-311G** calculated Cartesian coordinates in units of Ångstroms in the principal inertial axis system for butyryl chloride (syn-gauche) and (syn-anti). [5]

	Butyryl Chloride (syn-gauche)			Butyryl Chloride (syn-anti)		
Atom	*a*	*b*	*C*	*a*	*b*	*c*
C	2.623	−0.128	0.791	3.218	−0.571	−0.000
C	2.044	0.436	−0.506	1.996	0.346	0
C	0.589	0.875	−0.358	0.7	−0.458	0
C	−0.358	−0.286	−0.183	−0.530	0.412	0
H	0.234	1.423	−1.239	0.633	−1.116	−0.875
H	0.458	1.55	0.494	0.633	−1.116	0.875
H	2.626	1.307	−0.822	2.012	0.1	−0.877
H	2.116	−0.308	−1.305	2.012	0.999	0.877
H	2.083	−1.023	1.107	4.143	0.011	−0.001
H	2.562	0.614	1.593	3.224	−1.215	0.885
H	3.674	−0.398	0.662	3.223	−1.214	−0.885
O	−0.116	−1.446	−0.308	−0.576	1.603	−0.000
Cl	−2.024	0.263	0.215	−2.042	−0.563	−0.000

Table 5.2: Calculated equilibrium rotational constants and dipole moments for butyryl chloride. [5]

Parameter	MP2/6-311G**		M06-2X/6-311G**	
	Syn-gauche	Syn-anti	Syn-gauche	Syn-anti
Relative energy/ kJ mol^{-1} [a]	0	0.013	0	0.49
A_e/MHz	6281.53	6807.61	6394.48	6868.09
B_e/MHz	1476.61	1315.3	1473.17	1282.71
C_e/MHz	1349.26	1125.26	1346.28	1102.83
μ_a/D	1.97	2.54	2.22	2.81
μ_b/D	2.05	−1.54	2.21	−1.66
μ_c/D	−0.30	0	−0.28	0
μ_{total}/D	2.86	2.97	3.15	3.27

[a] Relative energies within each method. Zero point energies have not been taken into account.

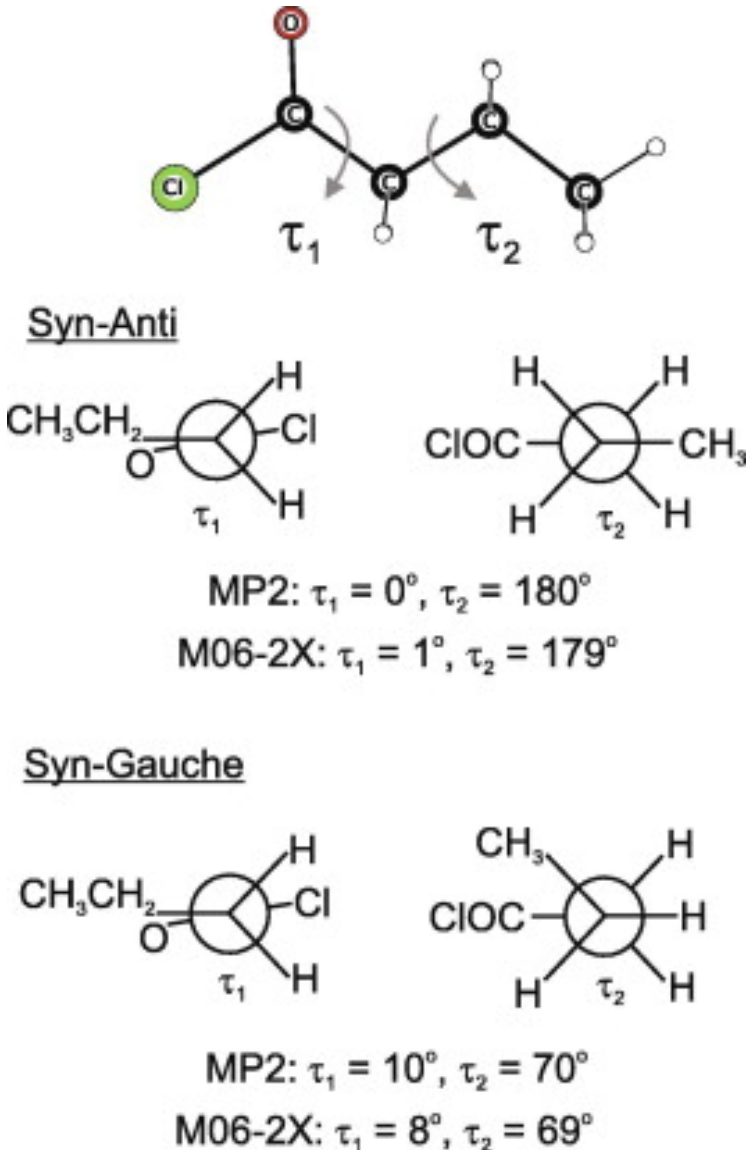

Figure 5.2: Newman projections for the syn-anti and syn-gauche conformers of butyryl chloride. The syn conformer refers to the dihedral angle between the ethyl group and the carbonyl group, $\tau_1 \approx 0°$. The anti and gauche conformers refer to the dihedral angle between the methyl and acyl halide groups, $\tau_2 \approx 180°$ and $\approx 70°$, respectively. [5]

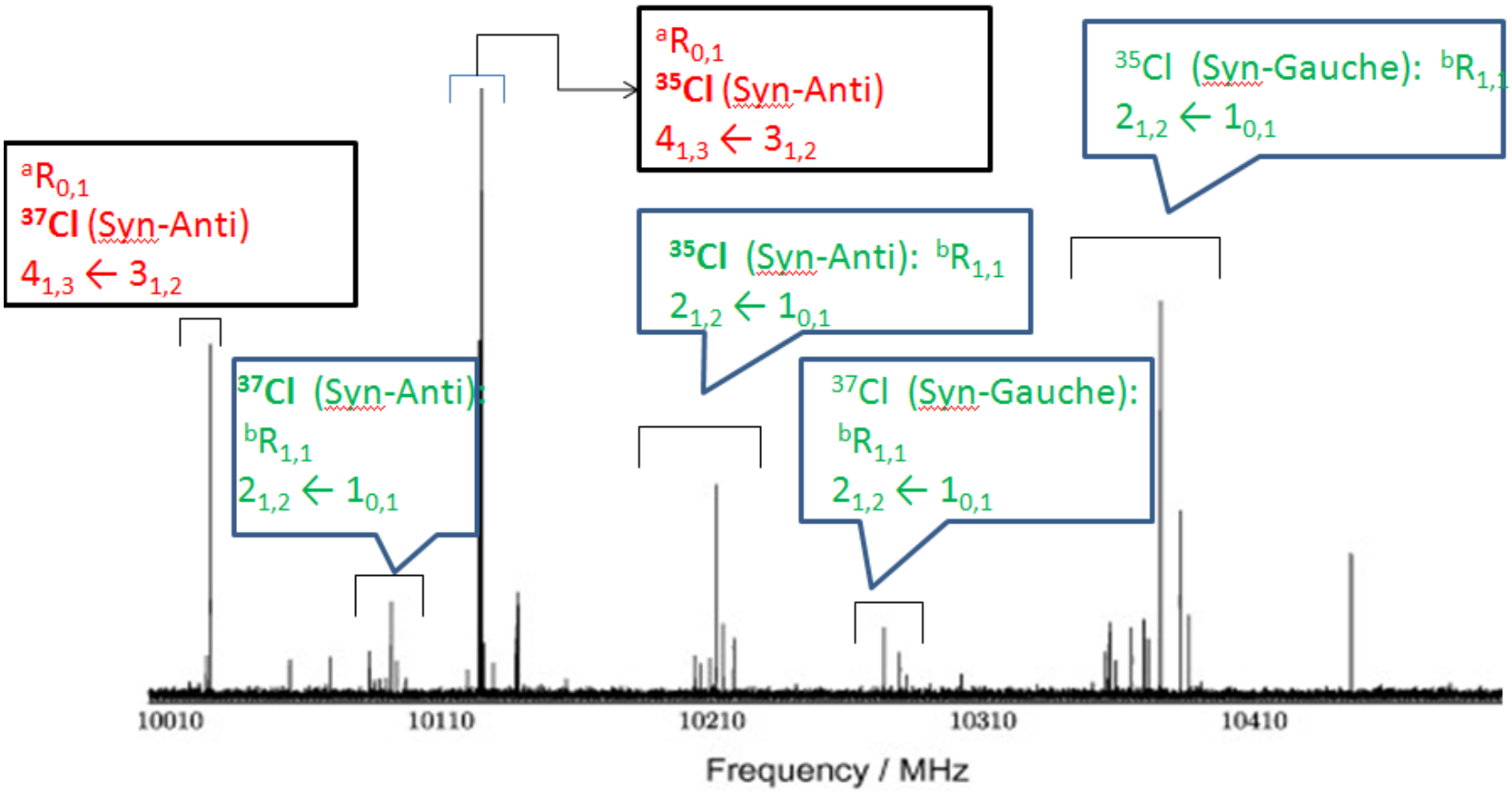

Figure 5.3: A 500 MHz portion of a 2 GHz scan of the pure rotational spectrum of butyryl chloride recorded using our CP-FTMW spectrometer. Ten-thousand averaging cycles approx 75 minutes of acquisition time. The strong grouping of transitions at ≈10,120 MHz is the $J_{KaKc} = 4_{1,3} \leftarrow 3_{1,2}$ rotational transition for syn-anti ^{35}Cl butyryl chloride. [5]

Table 5.3: Ground state spectroscopic parameters for butyryl chloride. [5]

Parameter	Syn-gauche		Syn-anti	
	^{35}Cl	^{37}Cl	^{35}Cl	^{37}Cl
A_0/MHz	6361.4602(19)[a]	6344.6913(33)	6835.9011(15)	6780.7348(76)
B_0/MHz	1466.40093(30)	1432.46721(58)	1313.97956(23)	1286.6291(14)
C_0/MHz	1338.37679(27)	1309.89117(59)	1125.24433(19)	1103.6667(13)
Δ_J/kHz	0.3518(52)	0.3416(74)	0.0775(25)	0.0835(53)
Δ_{JK}/kHz	−2.783(24)	−2.752(41)	0.031(11)	0.031[b]
Δ_K/kHz	30.20(40)	31.13(77)	13.09(33)	12.2(12)
δ_J/kHz	−0.0354(25)	−0.0395(69)	0.01410(93)	0.025(14)
χ_{aa}/MHz	−47.2245(47)	−37.442(10)	−32.1496(51)	−25.802(18)
χ_{bb}/MHz	28.7405(67)	22.769(15)	9.6649(76)	8.120(28)
χ_{cc}/MHz	18.4840(48)	14.673(11)	22.4847(56)	17.682(21)
$\lvert\chi_{ab}\rvert$/MHz	26.390(74)	20.89(62)	43.18(23)	34.44(99)
$\lvert\chi_{ac}\rvert$/MHz	16.00(24)	13.30(83)		
$\lvert\chi_{bc}\rvert$/MHz	4.8(14)	3.8[c]		
η_a[d]	−0.2171	−0.2162	0.3988	0.3706
N[e]	139	76	139	83
RMS[f]	0.21533	0.23991	0.19662	0.39473

[a] Numbers in parentheses give standard errors (1σ, 67% confidence level) in units of the least significant figure.

[b] This value was held fixed at the value obtained for the parent isotopologue.

[c] This value was held fixed at a value scaled to that obtained from the parent isotopologue.

[d] The asymmetry of the χ tensor in the principal inertial axes system, $\eta_x = (\chi_{bb}-\chi_{cc})/\chi_{aa}$.

[e] Number of observed transitions used in the fit.

[f] Root mean square deviation of the fit.

Table 5.4: Experimentally derived structural properties of butyryl chloride. [5]

Property	Syn-Gauche	Syn-Anti
I_a/amu Å^2	79.443868(24)[a]	73.930123(16)
I_b/amu Å^2	344.639038(71)	384.617099(67)
I_c/amu Å^2	377.605925(76)	449.128240(76)
P_a/amu Å^2	321.400548	379.907608
P_b/amu Å^2	56.205378	69.220632
P_c/amu Å^2	23.238491	4.70949
Δ/amu Å^{2b}	−46.47698(11)	−9.41898(10)
κ	−0.949026	−0.933901
Cl[c]		
a	2.0300(8)	2.0406(8)
b	0.260(6)	0.562(3)
c	0.207(8)	0.0[d]

[a] Numbers in parentheses give standard errors (1σ, 67% confidence level) in units of the least significant figure.
[b] Pseudo inertial defect Δ=Ic-Ia-Ib.
[c] Principal coordinates, in units of Ångstroms, of the Cl center obtained through use of Kraitchman's equation for single isotopic substitution.
[d] Imaginary value obtained.

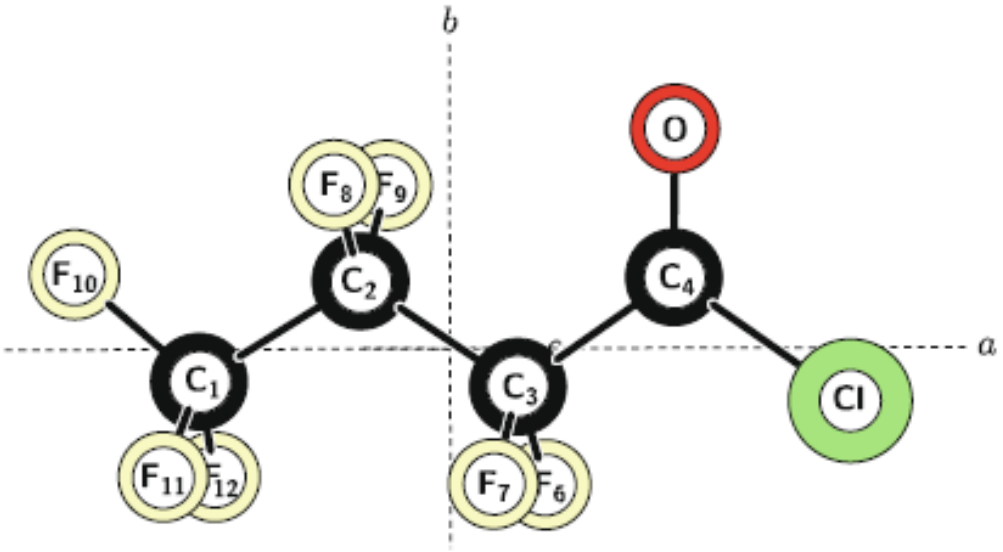

Figure 5.4: The structure of perfluorobutyryl chloride calculated at the MP2/6-311G** level. The structure shown is the syn-anti conformation. [64]

Table 5.5: The nuclear electric quadrupole coupling tensor in the principal axes system for syn-gauche and syn-anti conformers of butyryl chloride compared with comparison to propionyl chloride [6], ethanoyl chloride [10], formyl chloride [9], pivaloyl chloride [11], and perfluorobutyryl chloride [64].

Parameter	**HCOCl**[a]	**EthCl**[a]	**PropCl**[a]	**PfPropCl**	**SG–ButCl**	**SA–ButCl**	**PivCl**	**SA–PFButCl**
χ_{zz}/MHz	−59.8(7)	−59.486	−60.1	-65.41(15)	−58.02(17)	−59.22(21)	−60.05(22)	−65.427(18)[b]
χ_{xx}/MHz	39.0(2)	37.542	38.6	41.17(15)	41.23(98)	36.73(21)	37.56(22)	41.129(19)
χ_{yy}/MHz	20.8(2)	21.944	21.5	22.246(7)	16.8(11)	22.485(6)	22.4864(50)	24.298(13)
η_z[c]	−0.303(2)	−0.2622	−0.266	-0.2587(24)	−0.421(26)	−0.2406(36)	−0.2510(40)	−0.2572(4)
θ_{za}/°[d]	17.5	5.16	19.8	22.569(81)	19.30(25)	32.082(60)	31.64(7)	33.185(8)
$\theta_{(Cl–C),a}$/°[e]	17.5[g]	5.16[g]	19.8[g]	24.0[f]	22.1[f]	32.8[f]		34.68[f]

[a] Obtained from a first order perturbation analysis. No off-diagonal χ components determined. No uncertainties given.

[b] Standard errors (1σ, 67% confidence level) in units of the least significant figure.

[c] The asymmetry of the χ tensor in the principal axes system, $\eta_x = (\chi_{xx}-\chi_{yy})/\chi_{zz}$.

[d] The angle between the z and (a,b,c) axes.

[e] The angle between the C-Cl bond axis and the (a,b) axes.

[f] Taken from the calculated structure.

[g] The C-Cl bond was assumed to be coincident with the z-axis.

Table 5.6: Calculated (m06-2X/6-311G**) equilibrium structural parameters for perfluorobutyryl chloride.[a], [64]

r(C_1–C_2)	1.5450 Å
r(C_2–C_3)	1.5402 Å
r(C_3–C_4)	1.5474 Å
r(C_1–F_{10})	1.3309 Å
r(C_1–$F_{11,12}$)	1.3298 Å
r(C_2–$F_{8,9}$)	1.3455 Å
r(C_3–$F_{6,7}$)	1.3470 Å
r(C_4–O)	1.1921 Å
r(C_4–Cl)	1.7485 Å
(F10, C1, C2)	108.41°
(C_1, C_2, C_3)	115.19°
(C_2, C_3, C_4)	112.04°
(C_3, C_4, O)	124.99°
(O, C_4, Cl)	124.09°
(F_{11}, C_1, F_{12})	109.32°
(F_8, C_2, F_9)	110.08°
(F_6, C_3, F_7)	108.97°
(F_{11}, C_1, C_2)	110.62°
(F_8, C_2, C_3)	108.39°
(F_6, C_3, C_4)	108.74°
A_e/MHz	1405.307
B_e/MHz	472.159
C_e/MHz	436.872

[a] See text of reference [64] for details of the calculation and Fig. 1 for the atom labeling scheme. The atoms Cl, O, C_4, C_3, C_2, C_1, F_{10} all lie in the *ab* plane.

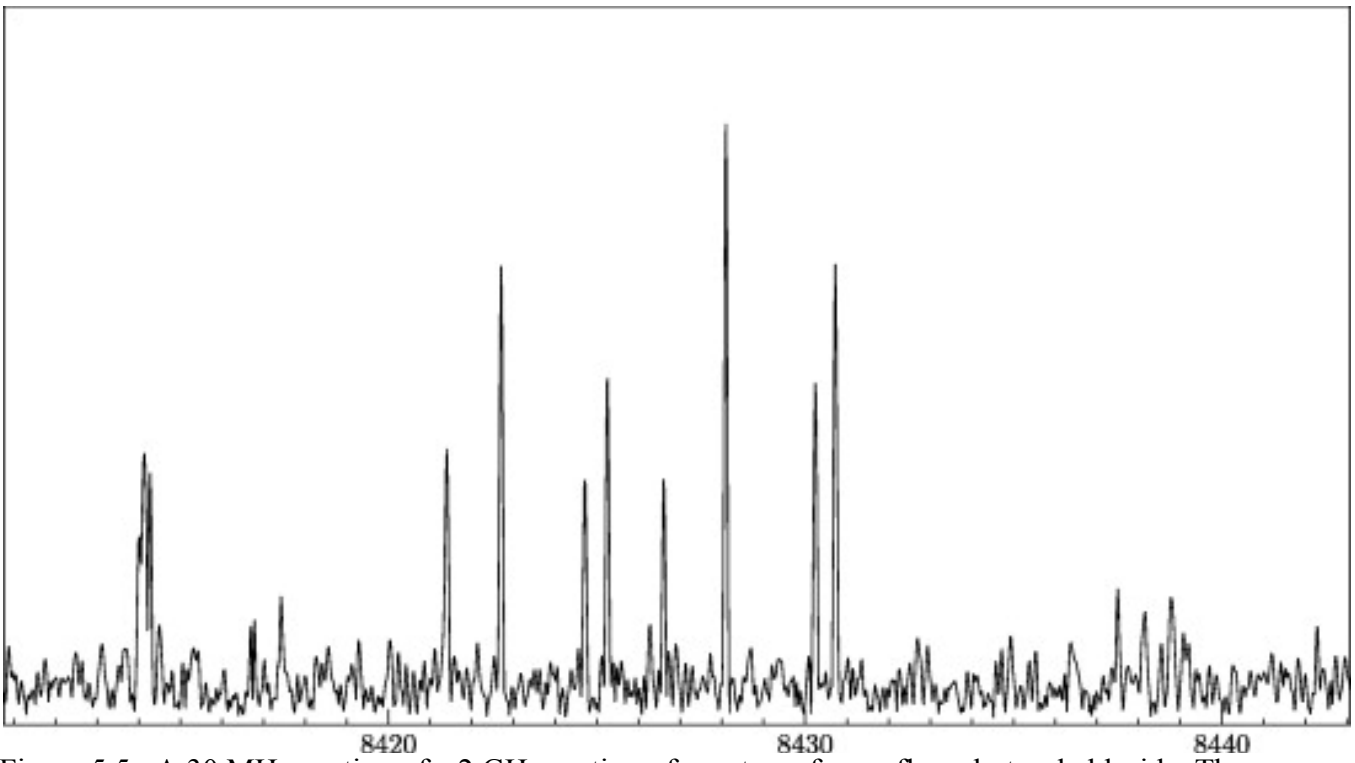

Figure 5.5: A 30 MHz portion of a 2 GHz section of spectrum for perfluorobutyryl chloride. The 2 GHz section required 10 000 averaging cycles to record, approximately 80 minutes. The group at 8414 MHz shows hyperfine splitting of the $J_{K\text{-}1K+1} = 9_{18} \leftarrow 8_{17}$ a-type rotational transition. The rest are of the $4_{32} \leftarrow 3_{21}$ and $4_{31} \leftarrow 3_{22}$ b-type rotational transitions. [64]

Table 5.9: Spectroscopic parameters for perfluorobutyryl chloride ($C_3F_7CO^{35}Cl$). [64]

Parameter	Exp.
A/MHz	1409.0159(3)[a]
B/MHz	478.4600(2)
C/MHz	442.1171(1)
Δ_J/Hz	8.7(6)
Δ_{JK}/Hz	44(2)
Δ_K/Hz	−19(8)
δ_J/Hz	0.9(2)
δ_k/kHz	−0.12(2)
χ_{aa}/MHz	−33.51(2)
χ_{bb}/MHz	9.21(2)
χ_{cc}/MHz	24.30(1)
χ_{ab}/MHz	48.8(1)
N[c]	236
RMS[d]	0.32

[a] Standard errors (1σ, 67% confidence level) in units of the least significant figure.
[b] For the signs of each experimental off-diagonal component we have followed the results of the quantum chemical calculations.
[c] Number of observed transitions used in the fit.
[d] Root mean square deviation of the fit,

CHAPTER 6

MOLECULAR STRUCTURE ANALYSIS OF VALEROYL CHLORIDE

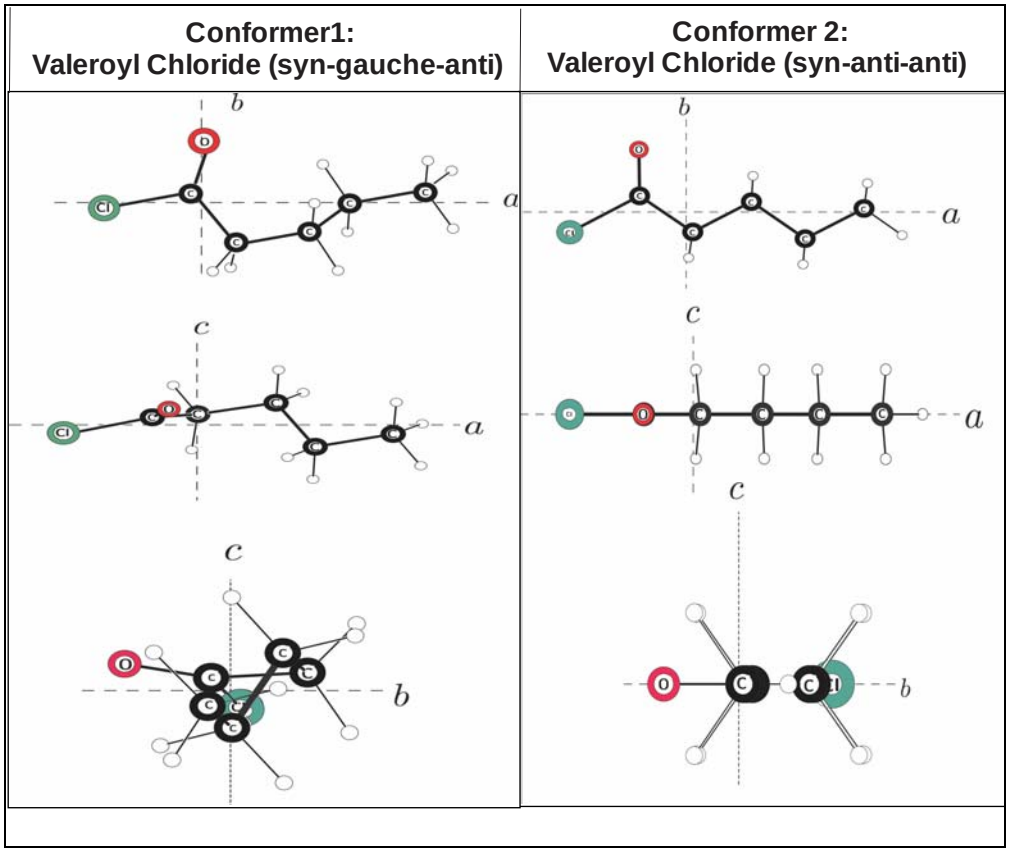

Figure 6.1: The M06-2X/6-311G** calculated structures of the syn-gauche-anti (Conformer 1) and the syn-anti-anti (Conformer 2) in the ab, ac, and bc planes of the principal inertial axis systems.

6.1 Introduction and Review

This acyl halide chapter focuses primarily on valeroyl chloride ($CH_3CH_2CH_2CH_2COCl$) compared to the shorter analogous acyl chlorides such as butyryl chloride ($CH_3CH_2CH_2COCl$) and propionyl chloride (CH_3CH_2COCl) discussed previously. The only main molecular formula difference is the added methyl CH_2 group to the parent chain, which makes it desirable to measure and compare any significant conformational and electronic changes measured relative to the following: i.) varied alkyl chain length and ii.) eventually perfluorinating; replacing the hydrogen-atoms with fluorine-atoms. The nuclear electric quadrupole coupling tensors, χ, of the

chlorine nucleus along the carbon-chlorine axis, help determine how the inductive effect changes with variation of parent chain length and after perfluorination. The data in this work comes from unpublished microwave spectra of valeroyl chloride at high resolution performed at the University of North Texas (UNT). The purpose of study is to measure the conformational structure of the molecule and to compare it to the existing microwave spectroscopic studies on other acyl halide-related compounds such as the anticipated longer parent chain and fluorinated acyl halides of hexanoyl chloride and heptanoyl chloride to be studied at the University of North Texas. [70, 10, 66, 1, 71, 68 9]

When considering the number of dihedral, or torsional angles, propionyl chloride only has one and butyryl chloride only has two dihedral angles that need to be considered. However, when considering the structure of valeroyl chloride, one must instead consider three dihedral, or torsional, angles because of the extra methyl group on the parent chain. These dihedral angles are namely that between the $C_3C_2C_1O$ centers, a second between the $C_4C_3C_2C_1$ centers, and a third between $C_5C_4C_3C_2$ centers. Therefore, valeroyl chloride is predicted to have a total of at least two or more stable conformations, because it has an additional or third dihedral angle to consider in its conformation. This study continues to apply the higher 50 kHz resolution that was done for propionyl and butyryl chloride.

6.2 Experiment

Rotational spectra were still recorded using a chirped-pulse Fourier transform microwave (CP-FTMW) spectrometer at UNT. One main modification has been made to the experimental procedure in chapter four and five: the experimental gas pulse timings were changed. Specifically, the experiment was conducted at 2 Hz gas pulse timings as opposed to the usual 4

Hz timings due to observation of greater intensities during calibration with carbonyl sulfide at lower pumping speeds. The same newly written National Instruments Labview code was used to average three sets of 10,000 acquisition cycles. This code was discussed previously in chapter 3 and in the Grubbs et al. study. [6] This allowed the spectra to be collected and deep averaged to obtain enhanced intensities of the spectra providing sufficient fitting of the molecular structural parameters, which can be and were used for analysis.

Samples of valeroyl chloride (Fluka Analytical > 98%) were used without further purification. Approximately 2-3 milliliters of the liquid sample were bubbled through 1/4" polyethylene tubing using argon backing gas at a backing pressure of approximately 2 atm.

6.3 Quantum Chemical Calculations

Quantum chemical calculations were performed the same way described previously using the GAMESS software package, Version 12 January 2009 (R1) using Gaussian via the Talon portal at the University of North Texas. The density functional method, M06-2X, with 6-311G** basis set obtained from the EMSL Basis Set Library were used without further modification to obtain a good "guess" of the rotational constants.

6.4 Experimental Results

Two valeroyl chloride conformations, each with two ^{35}Cl and ^{37}Cl isotopologues, were assigned, namely the syn-gauche-anti (conformer 1) and the syn-anti-anti (conformer 2). The Cartesian coordinates of the M06-2x/6311G** calculated structures of these two valeroyl chloride conformers are given in Table 1 for the syn-gauche-anti (conformer 1) and in Table 2 for the syn-anti-anti (conformer 2). The calculated structures are drawn in the principal inertial

planes in Figure 1. Calculated rotational constants, moments of inertia, planar moments, inertial defects, and asymmetry parameters are also given in Table 3.

6.4.1 Spectral Assignment of Transition Frequencies

A 500 MHz portion of the observed spectrum is shown in Figure 3. Transitions were assigned using the calculated spectroscopic constants. Similarly to the assignment of the butyryl chloride paper, [5] transitions of the type $^{a}R_{0,1}$ were assigned first. Fitting spectral parameters to these transitions yielded reliable values of the rotational constants A, B, C along with components of the chlorine nuclear electric quadrupole coupling tensor, χ. These constants then facilitated assignment of *b*-type transitions. *C*-type transitions were not observed for either conformer. This is most likely because of the small dipole in the c-plane for the syn-anti-anti. Comparable to butyryl chrloride, valeroyl chloride had no c-type transitions despite a slightly larger dipole in the c-plane. Again, the fitting of spectra was greatly facilitated through use of the AABS package [39] and other utilities from the PROSPE website have been used in this work such as the PLANM program, KRA program, etc. [59] A listing of the transitions recorded together with their assignments will be presented with future publication.

The parameter results of fitting the molecular spectra to the transitions recorded using the SPFIT fitting routine of Pickett [14, 59] are found in Table 4. These transitions were fitted similarly to the way butyryl chloride was fitted to the transitions recorded, using an appropriately formed Watson-A reduced Hamiltonian [57] in the I^r representation with adjustable spectroscopic parameters of the type $\hat{H} = \hat{H}_r + \hat{H}_{cd} + \hat{H}_Q$.

The centrifugal distortion constant δ_K and the chlorine nuclear electric quadrupole coupling constant χ_{bc} were not determinable for any conformer species. χ_{ac} for the syn-anti-anti

conformer was not determined nor was Δ_K for the ^{37}Cl of the syn-anti-anti conformer. Δ_K for the ^{35}Cl of the syn-anti-anti conformer was poorly defined and therefore was held fixed to it parent isotopologue with a value of zero. A scaling factor has been used before to predict the isotopologue value of quadrupole coupling constant to another by scaling with a factor of $Q(^{35}Cl)/Q(^{37}Cl) = 1.2688$. However, where this was possible, the parent was already not determined making the scale set to zero, Table 6.4.

6.4.2 Unique Lines Assigned

As usual, the fast Fourier transformations in our experiment were performed such that line widths obtained were approximately 80 kHz (FWHM) with a generous uncertainty of 25 kHz, which is the uncertainty reported as a deviation that is attributed to the location of the measured line centers. However, whenever certain spectra frequencies were relatively broader than usual, > 80 kHz, and the predicted spectra showed more than one frequency in that region, it was assumed that the resolution was too poor to resolve the multiple frequencies; and therefore, the uncertainty was slightly increased from 25 kHz, no greater than 50 kHz, to better assign the multiple frequencies. None of the fitted parameters were larger than the set uncertainty. Verification of this will be found in the supplementary listing located in future publication.

6.5 Discussion

6.5.1 Geometric Structure

Analogous to the butyryl chloride study[5], the syn-gauche conformer has a greater dipole moment along the c-plane. However, c-type transitions for either conformer were not observed

despite expecting it for the syn-gauche-anti conformer due to the larger dipole moment in the c-plane.

There are a couple of main sources of evidence to support that valeroyl chloride also prefers the cis conformation of the carbonyl and carbon group, giving an approximate dihedral angle, ∠CCCO = 0°. They are as follows: (i) agreement between the calculated rotational constants, Table 3, and observed rotational constants, Table 4 and (ii) near zero magnitudes of the c principal axes Cartesian coordinates for the CCC(=O)Cl backbone in the calculated structures of these molecules, Table 1 and Table 2.

As mentioned earlier, two conformers were observed for valeroyl chloride, the syn-gauche-anti and the syn-anti-anti, each with ^{35}Cl and ^{37}Cl isotopologues. The pseudo-inertial defects for both conformers presented with the experimentally derived moments of inertia and planar moments in Table 5 are consistent with the calculated structures in Table 3, especially for the syn-anti-anti conformer. The small value of the pseudo inertial defect for the syn-anti-anti conformer is as expected for 8 out of plane hydrogens.

Experimentally derived kraitchman substitution coordinates for the chlorine atom in both conformers have been determined and are presented in Table 5. When comparing the substitution coordinates of the Cl atom with the calculated Cartesian coordinates for the chlorine atom in Table 6.1 and Table 6.2, a good agreement is observed, especially for the syn-anti-anti conformer.

The calculated Ray's asymmetry parameter κ is in agreement with the experimentally derived parameter of around -0.98 and -0.97, respectively, found in Table 6.5 and Table 6.3. These values are negative, which implies that the molecule is more prolate in shape. From a microwave spectroscopy point of view, asymmetry is determined by having a κ value at or

closest to zero [40]. Therefore, because the magnitudes are so close to -1, these molecules are said to be only partially asymmetric.

The lack of internal rotation observed in valeroyl chloride is in agreement with the work on propionyl chloride done in 1970's [4] and butyryl chloride,[5] where no evidence of internal methyl rotation was found in the ground state spectrum, even though internal rotation was observed in a similar compound, butyronitrile. [57] A- and E-splitting were on the order of 300 kHz for butyronitrile and a barrier height to internal rotation, V_3, was determined to be ≈13 kJ mol^{-1} or ~ 3107 cal/mole for both *trans* and *cis* conformers. The failure to observe internal rotation in valeroyl chloride further indicates that the acyl chloride group produces a significantly higher barrier, > 3107 cal/mole, to methyl-group rotation than that determined in butyronitrile.

6.5.2 Electronic Structure: Chlorine Quadrupole Coupling Tensor & Effect on the Carbonyl Group

Rotating the experimentally determined, complete ^{35}Cl nuclear electric quadrupole coupling tensors, located in Table 4, into the *x*-, *y*-, *z*-axis system allows comparison of this quantity with related molecules. This comparison is presented in Table 6 and Table 7. In all cases, the *z*-axis lies very close to the axis of the C-Cl bond, and therefore, the assumption is made that χ_{zz} is a good indicator of the electric field gradient along the space fixed z-axis. A continued pattern is observed where there is an invariance of the magnitude of χ_{zz} to the length of carbon chain, branching of the carbon chain, and even to fluorination of the carbon chain. So far, χ_{zz} is approximately equal to -60 MHz for all the acyl chloride species and χ_{zz} is approximately equal to -65 MHz for all of the perfluorinated acyl chloride species studied to date. However, the chlorine-37 isotope shows smaller χ_{zz} values but is in relative agreement to its parent isotopologue, respectively, by a factor of 1.26 MHz. In summary, the electric field gradient at

the Cl center is mainly dominated by the local effects of the carbonyl group further supported by these χ_{zz} results.

The moment of inertia data results are found in Table 5. The syn-gauche-anti conformer has a larger moment of inertia than the syn-anti-anti conformer and correlates well with the rotational constants being smaller for the syn-gauche-anti conformer because moment of inertia and rotational constants are inversely proportional. The planar moment, also known as the second moment, provides useful data that support the results that most of the mass lies in the a-plane evidenced by larger P_a values when compared to P_b and P_c values.

6.6 Conclusions

An exploration and further contribution to the molecular structure and electronic structure of hydrocarbon acyl chlorides and perfluoroacyl chlorides has now been made using (CP-FTMW) spectroscopy and quantum chemical calculations. One conformer was observed for propionyl chloride and perfluoropropionyl chloride, two conformers were observed for butyryl chloride; only one was observed for perfluorobutyryl chloride [33]; and two conformers were observed for valeroyl chloride. The second syn-gauche conformer did not appear until two or more torsional angles, < CCCC, existed in the alkyl chain suggesting a three carbon minimum requirement for syn-gauche conformation. Helicity was not observed for ≤ 3 perfluorinated carbons for the perfluoroacyl chlorides in this study. Moreover, further support is now provided for the emergence of an almost "standard" χ_{zz} value for Cl in acyl chlorides suggesting that the oxygen has a stabilizing effect of the electric field gradient along the carbon-chlorine bond despite the length of the carbon chain. The χ_{zz} value averages to be about 60 MHz for the syn-anti form and 65 MHz for the syn-gauche form. The cis conformation of the CCCO dihedral

angle seems to be consistently stable among the acyl chlorides. Internal rotation stops at or ceases to be observed beyond propionyl chloride for the hydrogenated acyl chloride series. For the perfluoroacyl chloride series, internal rotation ceases beyond ethanoyl chloride so far. The perfluoroalkyl effect that is initiated by perfluorination is observed and quantified by the nuclear electric quadrupole coupling constants, χ_{zz} ,along the C-Cl bond. The isotopic substitution coordinates have determined the location of the chlorine in the principal axis system for all three categories of acyl chloride and even further for propionyl and perfluoropropionyl chloride via carbon-13 locations. Future work can be on molecular structure effects of extending the alkyl chain further, partially fluorinating the alkyl chain, replacing the chlorine atom with other halides or cyano ions, and replacing the alkyl chain with aromatic functional groups. Also, replacing the oxygen with sulfur would be interesting to compare to oxygen's perfluoroalkyl stabilizing effect and to learn more about the role of group 6 elements have in bonding.

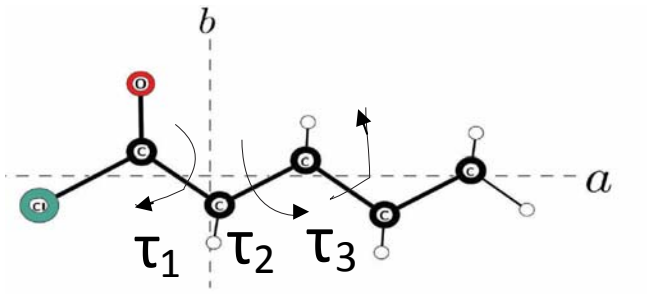

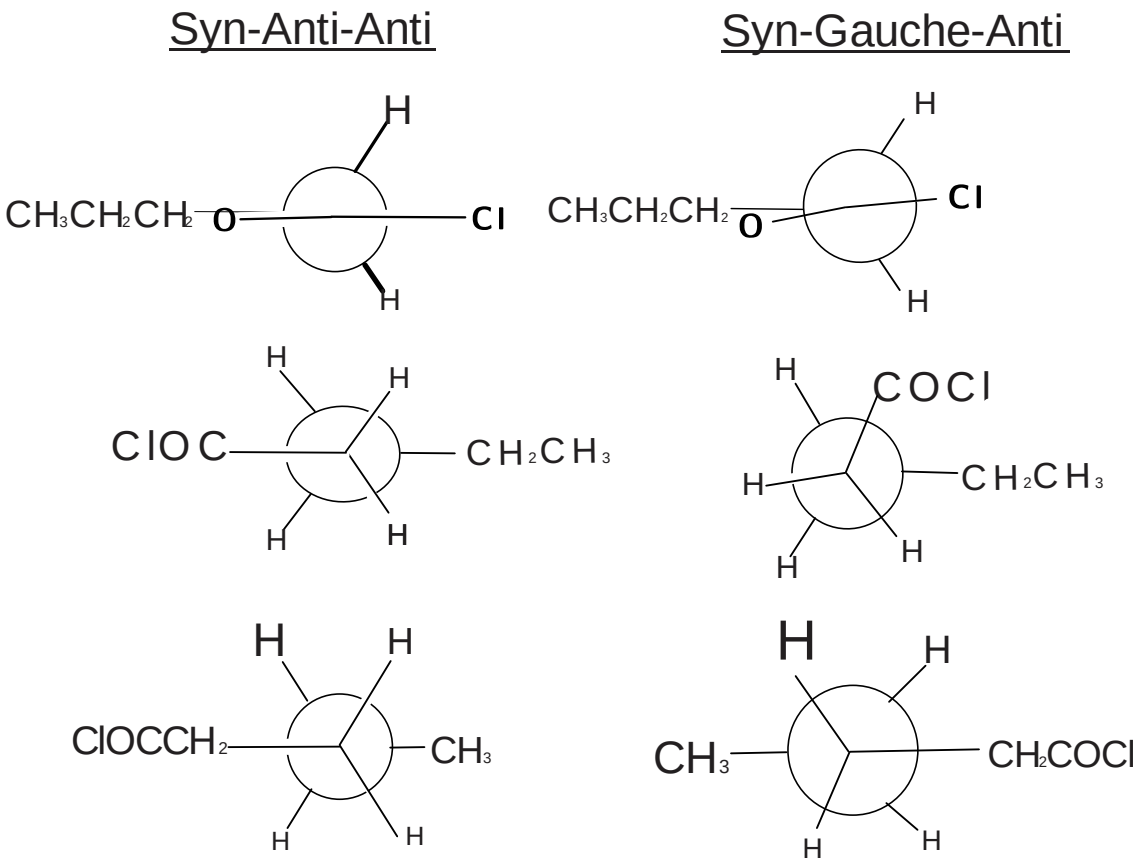

Syn-Anti-Anti
M06-2X:
T1 = 0.023^0, T2 = 179.996^0, T3 = 179.990^0

Syn-Gauche-Anti
M06-2X:
T1 = 4.930^0, T2 = 71.314^0, T3 = 179.613^0

Figure 6.1: Newman projections for the syn-anti-anti and syn-gauche-anti conformers of valeroyl chloride. The syn orientation refers to the dihedral or torsional angle between the carbonyl group and the propyl group (τ_1), $\tau_1 \sim 0^0$ and $\sim 5^0$. The anti and gauche orientation refer to the dihedral angle between the carbonyl carbon and the remaining propyl group (τ_2), $\sim 180^0$ and $\sim 70^0$. The ladder anti orientations refer to the dihedral angle between the corresponding terminal methyl group and the $ClOCCH_2$ group, (τ_3) $\sim 180^0$ and $\sim 180^0$. Diagram angles are not necessarily drawn to scale.

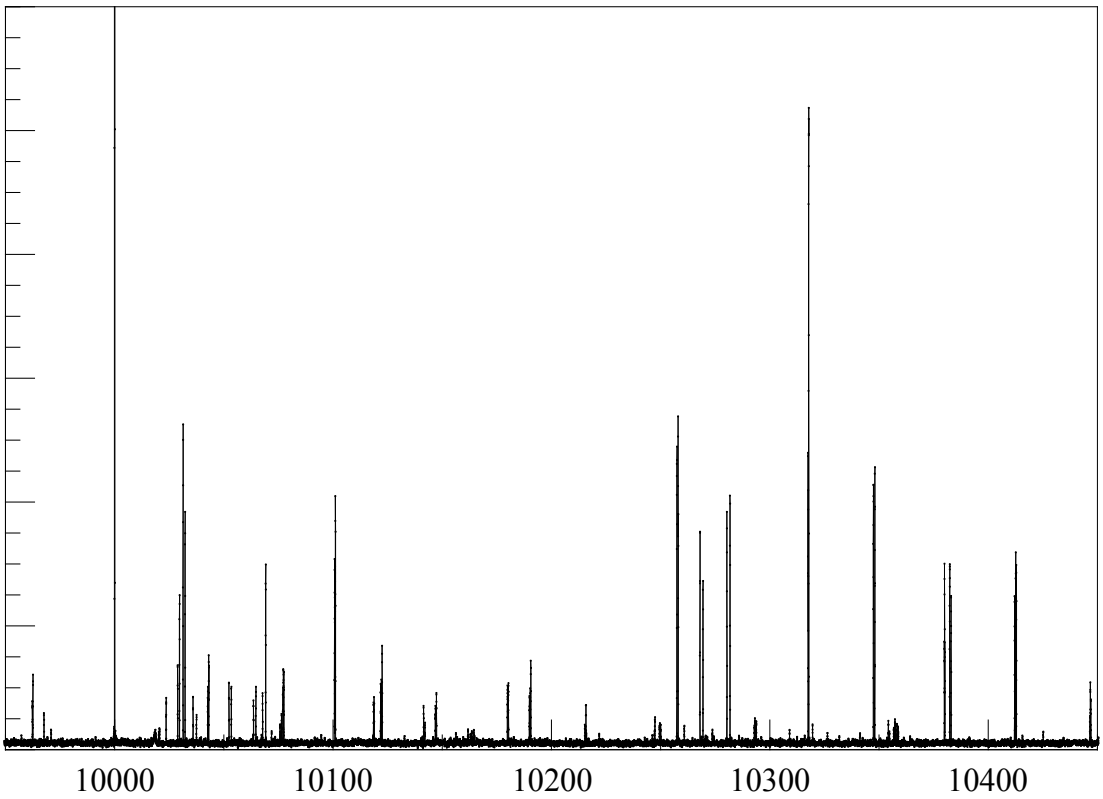

Figure 6.3: 500 MHz portion of a 2 GHz scan of the pure rotational spectrum of valeroyl chloride recorded using our CP-FTMW spectrometer. Three sequences of ten-thousand averaging cycles each at approx 150 min of acquisition time. The tall thin peak at 10,000 MHz is a man-made frequency leakage and was ignored from assignment. The strong grouping of transitions at ~ 10100 MHz is the $J_{KaKc} = 7_{17} \leftarrow 6_{16}$ rotational transition for syn-anti-anti ^{35}Cl of valeroyl chloride.

Table 6.1: M06-2x/6311G** calculated Cartesian coordinates in units of Angstroms in the principal inertial axis system for syn-gauche-anti (Conformer 1) valeroyl chloride.				Table 6.2: M06-2x/6311G** calculated Cartesian coordinates in units of Angstroms in the principal inertial axis system for syn-anti-anti (Conformer 2) valeroyl chloride.			
ATOM	A	B	C	ATOM	A	B	C
C	-3.660825	0.293931	-0.24341	C	-3.989333	0.089959	-0.000099
C	-2.20658	-0.020516	-0.582816	C	-2.669	-0.675849	0.000024
C	0.834219	0.249004	0.201423	C	-1.463452	0.261265	-0.000095
O	0.52359	1.362014	0.418629	C	-0.147279	-0.506205	0.000268
Cl	2.544223	-0.131542	-0.274687	C	1.045279	0.408438	0.000062
H	-1.688215	0.899805	-0.864699	O	1.059603	1.58379	0.000048
H	-2.164671	-0.689813	-1.44909	Cl	2.609006	-0.513938	-0.00009
H	-4.204351	-0.61402	0.030467	H	-0.055743	-1.159833	-0.873121
H	-3.719475	0.986357	0.599918	H	-0.055855	-1.159068	0.874263
H	-4.176262	0.751813	-1.089149	H	-1.499243	0.916156	-0.875722
C	-1.475055	-0.673692	0.589464	H	-1.499437	0.916636	0.875162
C	-1.523433	-0.017451	1.463488	H	-2.621245	-1.329745	-0.877275
H	-1.981135	-1.605029	0.860605	H	-2.621275	-1.329483	0.877522
C	-0.014875	-0.991513	0.282805	H	-4.066639	0.72953	0.882533
H	0.098265	-1.532492	-0.661537	H	-4.066361	0.729718	-0.88262
H	0.441342	-1.624212	1.050418	H	-4.84408	-0.588163	-0.000305

Table 6.3: Calculated equilibrium rotational constants/parameters for valeroyl chloride.

Parameter	m06-2x/6311G**	m06-2x/6311G**
	Syn-Gauche-Anti	Syn-Anti-Anti
A / MHz	5953.61104	6612.7583
B/ MHz	882.58177	773.82413
C/ MHz	831.16551	704.7467
I_a /amu Å^2	84.886131	76.424842
I_b /amu Å^2	572.61438	653.092855
I_c /amu Å^2	608.03655	717.107311
P_a /amu Å^2	547.882385	646.887634
P_b /amu Å^2	60.154152	70.21965
P_c /amu Å^2	24.731981	6.205193
Δ = Ic-Ia-Ib Å^2	-49.463963	-12.410386
κ	-0.97993	-0.97662
[a] Relative energies within each method. Zero point energies have not been taken into account.		

Table 6.4: Ground State spectroscopic parameters for valeroyl chloride

	(Syn-Gauche-Anti) CONFORMER 1 ^{35}Cl	(Syn-Gauche-Anti) CONFORMER 1 ^{37}Cl	(Syn-Anti-Anti) CONFORMER 2 ^{35}Cl	(Syn-Anti -Anti) CONFORMER 2 ^{37}Cl
A_0 /MHz	5829.4972(50) [a]	5815.4115(63)	6542.634(93)	6498.4494(93)
B_0 /MHz	880.06003(48)	860.97186(83)	774.29912(49)	758.8824(10)
C_0 /MHz	831.65614(53)	814.74626(79)	704.65566(44)	691.3660(11)
Δ_J /kHz	0.1382(20)	0.1361(34)	0.0205(23)	0.0281(37)
Δ_K /kHz	43.8(13)	45.13(47)	95.(93) [b]	[0.] c
Δ_{JK} /kHz	-3.083(11)	- 3.088 (21)	0.257(12)	0.346(72)
δ_K /kHz	-	-	-	-
δ_J /kHz	- 0.0143 (25)	- 0.0114 (40)	0.0014(18)	0.0062(45)
χ_{aa} /MHz	-48.011(12)	- 37.954 (27)	-34.540(12)	-27.770(65)
χ_{bb} /MHz	32.161 (12)	25.363 (38)	12.064(15)	9.888(88)
χ_{cc} /MHz	15.850(11)	12.591(28)	22.476(11)	17.882(59)
χ_{ab} /MHz	- 20.42 (26)	-16.02(10)	-42.16(15)	-31.82(57)
χ_{ac} /MHz	- 21.48 (45)	-16.94(60)	-	-
χ_{bc} /MHz	-	-	-	-
n_a [d]	-0.3397	-0.3365	0.301447597	0.28786
AVG	- 0.000043 MHz	-0.000068 MHz	0.000054 MHz	0.000083 MHz
RMS [f]	0.007632 MHz	0.009604 MHz	0.008149 MHz	0.010966 MHz
N [e]	128	83	130	60

[a] Numbers in parentheses give standard errors (1σ, 67% confidence level) in units of the least significant figure.
[b] This value can be held fixed at zero because it was not well defined, eventhough it is within the acceptable error.
[c] This value was held fixed at a value scaled to that obtained from the parent isotopologue
[d] The asymmetry of the χ tensor in the principal inertial axes system, $\eta_\chi = (\chi_{bb} - \chi_{cc}) / \chi_{aa}$
[e] Number of observed transitions used in the fit.
[f] Root mean square deviation of the fit, $\sqrt{\frac{\Sigma[((obs-calc)/error)^2]}{N}}$

Table 6.5: Experimentally derived structural properties of valeroyl chloride

	(Syn-Gauche-Anti) ^{35}Cl	(Syn-Gauche-Anti) ^{37}Cl	Syn-Anti-Anti ^{35}Cl	Syn-Anti-Anti ^{37}Cl
I_a /amu Å^2	86.69341(74)[a]	86.90339(94)[a]	77.243(10)[a]	77.7691(11)[a]
I_b /amu Å^2	574.2551(31)	586.9866(56)	652.6922(41)	665.9516(87)
I_c /amu Å^2	607.6778(38)	620.2900(60)	717.1999(44)	730.986(11)
P_A /amu Å^2	547.619789	560.186667	646.324099	659.584354
P_B /amu Å^2	60.05805	60.103392	70.875854	71.401847
P_C /amu Å^2	26.635363	26.800004	6.368114	6.367321
Δ /amu Å^{2}[b]	-53.2707(50)	-53.6000(83)	-12.736(12)	-12.734(14)
κ [c]	*-0.98063*	-0.981512	-0.976141	-0.976747
(A+B)/2C	4.033853	4.097216	5.19185	5.248545
2A/(B+C)	6.81129	6.940799	8.847646	8.961843
Cl[d]	Syn-Gauche-Anti (35/37)		Syn-Anti-Anti (35/37)	
a	2.52878(59)		2.59948(9)	
b	0.1534(98)		0.5103(49)	
c	0.293(51)		0.114(22)	

[a] Numbers in parentheses give standard errors (1σ, 67% confidence level) in units of the least significant figure of the least significant figure.
[b] Pseudo inertial defect, Δ = Ic - Ia - Ib, obtained from the PLANM program.
[c] Ray's asymmetry parameter [(2B-A-C)/(A-C)], obtained from the PLANM program.
[d] Principal coordinates, in units of Ångstroms, of the Cl center obtained through use of Kraitchman's equation for single isotopic substitution.

Table 6.6: The nuclear quadrupole coupling tensor in the principal axes system for syn-anti-anti (Conformer 2) and syn-gauche-anti (Conformer 1) valeroyl chloride.

Principal tensor Components	(Syn-Gauche Anti) CONFORMER 1 ^{35}Cl	(Syn-Gauche Anti) CONFORMER 1 ^{37}Cl	(Syn-Anti-Anti) CONFORMER 2 ^{35}Cl	(Syn-Anti -Anti) CONFORMER 2 ^{37}Cl
χ_{zz}	-58.77(25)[a]	-45.8(49)[a]	-59.40(13)[a]	-46.39(30)
χ_{xx}	20.30(16)	17.882(59)	22.476(11)	16.10(21)
χ_{yy}	38.47(15)	28.0(49)	36.93(13)	30.29(11)
n_z [b]	0.309(40)	0.22(10)	0.243(22)	0.3059(55)

[a]Standard errors (1σ, 67% confidence level) in units of the least significant figure.
[b] The asymmetry of the χ tensor, $\eta_z = (\chi_{xx}-\chi_{yy})/\chi_{zz}$, in the principal axes system rotated into the x, y, z system.

Table 6.7. The nuclear quadrupole coupling tensor in the principal axes system for conformers of related acyl chlorides such as propionyl chloride [1, 6], ethanoyl chloride [10], formyl chloride [9], pivaloyl chloride [11],perfluorobutyryl chloride [33], and butyryl chloride [5], valeroyl chloride

Parameter	HCOCl[a]	EthCl[a]	PropCl	SG–ButCl	SA–ButCl	PivCl	SG-ValCl [h]	SA-ValCl [h]	PF-PropCl	SA–PF-ButCl
χ_{zz}/MHz	−59.8(7)	−59.486	−59.49(35)	−58.02(17)	−59.22(21)	−60.05(22)	-58.77(25)[b]	-59.40(13)[b]	-65.41(15)	−65.427(18)[b]
χ_{xx}/MHz	39.0(2)	37.542	36.92(35)	41.23(98)	36.73(21)	37.56(22)	20.30(16)	22.476(11)	41.17(15)	41.129(19)
χ_{yy}/MHz	20.8(2)	21.944	22.569.(4)	16.8(11)	22.485(6)	22.4864(50)	38.47(15)	36.93(13)	24.246(7)	24.298(13)
η_z[c]	−0.303(2)	−0.2622	−0.2413(61)	−0.421(26)	−0.2406(36)	−0.2510(40)	0.309(40)	0.243(22)	-0.2587(24)	−0.2572(4)
θ_{za}/°[d]	17.5	5.16	19.20(27)	19.30(25)	32.082(60)	31.64(7)			22.569(81)	33.185(8)
$\theta_{(Cl–C),a}$/°[e]	17.5[g]	5.16[g]	19.5[f]	22.1[f]	32.8[f]				24. 0[f]	34.68[f]

[a] Obtained from a first order perturbation analysis. No off-diagonal χ-components determined. No uncertainties given.
[b] Standard errors (1σ, 67% confidence level) in units of the least significant figure.
[c] The asymmetry of the χ tensor in the principal axes system, $\eta_x = (\chi_{xx}-\chi_{yy})/\chi_{zz}$.
[d] The angle between the z and (a, b, c) axes.
[e] The angle between the Cl-C bond axis and the (a, b, c) axes.
[f] Taken from the calculated structure.
[g] The C-Cl bond was assumed coincident with the z-axis.
[h] Obtained from the ^{35}Cl isotopologue.

WORKS CITED

1. Karlsson, H. Microwave spectrum of propionyl chloride. *Journal of Molecular Structure* **1976,** *33,* 227-237.

2. Mata, F.; Alonso, J. L. Microwave spectrum of propionyl chloride. *Journal of Molecular Structure* **1979,** *56,* 199-205.

3. Mata, F.; Perez, J. A conformational study of butyronitrile and butyryl chloride by low resolution microwave spectroscopy. *Spectrochimica Acta, Part A: Molecular and Biomolecular Spectroscopy* **1984,** *40A*(1)*,* 109-111.

4. Lawrence, T. P.; True, N. S.; Bohn, R. K. Low resolution microwave spectroscopy. 1 1. Conformations of butyryl fluoride, chloride, and bromide. *The Journal of Physical Chemistry* **1978,** *82*(4)*,* 480-483.

5. Powoski, R. A.; Grubbs II, G. S.; Cooke, S. A. A conformational study of butyryl chloride using chirped pulse fourier transform microwave spectroscopy. *Journal of Molecular Structure* **2010,** *963,* 106-110.

6. Grubbs II, G. S.; Powoski, R. A.; Jojola, D.; Cooke, S. A. Some geometric and electronic structural effects of perfluorinating propionyl chloride. *Journal of Physical Chemistry A* **2010,** *114,* 8009-8015.

7. Grubbs II, G. S.; Cooke, S. A. The gas phase characterization of perfluorobutyryl chloride, C3F7COCl, using chirped pulse fourier transform miicrowave spectroscopy. *Chemical Physics Letters* **2009,** *483,* 21–24.

8. Grubbs II, G. S.; Dewberry, C. T.; Cooke, S. A.; Lin, W. The shape of perfluorobutyryl fluoride, C3F7COF, in the gas phase. *Journal of Molecular Structure* **2010,** *973,* 190-193.

9. Takeo, H.; Matsumura, C. Microwave spectrum of formyl chloride. *The Journal of Chemical Physics* **1976,** *64*(11)*,* 4536-4540.

10. Hayashi, M.; Inada, N.; Niide, Y. Microwave spectrum, structure, internal rotation, and nucelar quadrupole coupling constant tensor of acetyl chloride. *Journal of Molecular Structure* **1995,** *352,* 325-334.

11. Grubbs II., G. S.; Dewberry, C. T.; Etchison, K. C.; Serafin, M. M.; Peebles, S. A.; Cooke, S. A. The pure rotational spectrum of pivaloyl chloride, (CH3)CCOCl between 800 and 18800 MHz. *Journal of Molecular Spectroscopy* **2008,** *251,* 378-383.

12. Luis, A. d.; Sanz, M. E.; Lorenzo, F. J.; Lopez, J. C.; Alonso, J. L. Internal rotation and the chlorine nuclear quadrupole coupling tensor of 1-chloropropane. *Journal of Molecular Spectroscopy* **1997,** *184,* 60-77.

13. Stiefvater, O. L. Microwave spectrum of propionic acid. I. Spectrum, dipole moment, barrier to internal rotation, and low-frequency vibrations of cis-propionic acid. *The Journal of Chemical Physics* **1975,** *62*(1)*,* 233-243.

14. Pickett, H. M.; Scroggin, D. G. Microwave spectrum and internal rotation potential of propanal*. *The Journal of Chemical Physics* **1974,** *61*(10)*,* 3954-3958.

15. Nair, K. P.; Rudolph, H. D. Microwave spectrum, barrier to internal methyl rotation, dipole moment, and partial structure of dimethylketene. *Journal of Molecular Spectroscopy* **1973,** *48,* 571-591.

16. Nakagawa, J.; Hayashi, M. Internal rotation in propyl mercaptan by microwave spectroscopy. *Journal of Molecular Spectroscopy* **1981,** *85,* 327-340.

17. Vormann, K.; Dreizler, H. Microwave spectrum of butyronitrile: Methyl internal rotation and 14N quadrupole coupling. *Zeitschrift für Naturforschung. A, A Journal of Physical Sciences* **1988,** *43a,* 338-344.

18. Fournier, J. A.; Bohn, R. K.; Montgomery, J. J.; Onda, M. Helical C2 structure of perfluoropentane and the C2v structure of perfluoropropane. *Journal of Physical Chemistry A* **2010,** *114,* 1118-1122.

19. Dixon, D. A. Torsional potential about the central C-C bond in perfluoro-n-butane. *Journal of Physical Chemistry* **1992,** *96,* 3698-3701.

20. Dixon, D. A.; Van-Cadedge, F. A. A molecular model for the helicty of polytetrafluoro ethylene. *Journal of High Performance Computing Applications* **1988,** *2,* 62.

21. Woody, R. W.; Berova, N. *Circular Dicroism: Principles and Applications*, 2nd ed.*;* John Wiley & Sons: NY, 2000.

22. Munrow, M. R.; Subramanian, R.; Minei, A. J.; Antic, D.; MacLeod, M. K.; Michl, J.; Crespo, R.; Piqueras, M. C.; Izuha, M.; Ito, T.; et al. Rotational spectra of gauche perfluoro-n-butane, C4F10; perfluoro-iso-butane, (CF3)3CF; and tris(trifluoromethyl)methane, (CF3)3CH. *Journal of Molecular Spectroscopy* **2007,** *242,* 129-138.

23. Restrepo, A. A.; Bohn, R. K. Alkyl chains with CN and CCH substituents prefer gauche conformations. *Journal of Molecular Structure* **2007,** *833,* 189-196.

24. Utzat, K.; Bohn, R. K.; Michels, H. H. Four conformers observed and characterized in 1-Hexyne. *Journal of Molecular Structure* **2007,** *841,* 22-27.

25. Fournier, J. A.; Bohn, R. K.; Michels, H. H. Microwave spectroscopy and structures of two conformers of 6-methyl-3-heptyne and three of 2-methylpentane. *Journal of Molecular Spectroscopy* **2008,** *251,* 145-152.

26. Churchill, G. B.; Dombrowski, J. P.; Ma, L.; Swana, K.; Bohn, R. K.; Montgomery Jr., J. A. Microwave spectroscopy and conformations of 2-methylbutane. *Journal of Molecular Structure* **2010,** *978,* 11-13.

27. Churchill, G. B.; Milot, R. L.; Bohn, R. K. Microwave studies of 4-methyl-1-pentyne. *Journal of Molecular Structure* **2007,** *837,* 86-91.

28. Tchana, F. K.; Flaud, J. -.; Lafferty, W. J.; Manceron, L.; Roy, P. The first high-resolution analysis of the low-lying v9 band of propane. *Journal of Quantitative Spectroscopy & Radiative Transfer* **2010,** *111,* 1277-1281.

29. Gorriz, O. F.; Cadus, L. E. Supported chromium oxide catalysts using metal carboxylate complexes: Dehydrogenation of propane. *Applied Catalysis A:General* **1999,** *180,* 247-260.

30. Boutcetta, C.; Kacimi, M.; Ensuque, A.; Piquemal, J.; Bozon-Verduraz, F.; Ziyad, M. Oxidative dehydrogenation of propane over chromium-loaded calcium-hydroxyapatite. *Applied Catalysis A: General* **2009,** *356,* 201-210.

31. Lemal, D. M. Perspective on fluorocarbon chemistry. *Journal of Organic Chemistry* **2004,** *69,* 1-11.

32. Grubbs II, G. S.; Cooke, S. A. Chirped-pulse fourier transform microwave spectroscopy of perfluoroiodoethane.. *Journal of Molecular Structure* **2010,** *963,* 87-91.

33. Grubbs II, G. S.; Cooke, S. A. The gas phase characterization of perfluorobutyryl chloride, C3F7COCl, using chirped pulse fourier transform microwave spectroscopy. *Chemical Physics Letters* **2009,** *483,* 21-24.

34. *IUPAC Subcommittee on Gas Kinetic Data Evaluation: halogenated oxy radical decomposition (2000);* obtainable from http://www.iupac-kinetic.ch.cam.ac.uk/: .

35. Brown, J.; Carrington, A. *Rotational Spectroscopy of Diatomic Molecules;* Cambridge University Press: New York, The United States, 2003; 1-32, 139-176.

36. Shou-Yuan, T.; Zhi-Ning, X.; Yu-Jie, F.; Qian, G. Advances and applications of microwave spectroscopy. *Journal of Analytical Chemistry* **2008,** *36*(8)*,* 1145–1151.

37. Atkins, P.; De Paula, J. *Atkin's Physical Chemistry*, 7th ed.*;* W.H Freeman and Company: New York, The United States of America, 2002.

38. Krodo, H. *Molecular Rotation Spectra;* Dover Publications Inc.: New York, NY, 1992.

39. Pickett, H. M. SPFIT/SPCAT package. *Available from: <http://spec.jpl.nasa.gov>*

40. Gordy, W.; Cook, R. L. VII. *Microwave Molecular Spectra*, 3rd ed.*;* John Wiley & Sons: New York, NY, 1984; Vol. XVIII, 1-929.

41. Townes, C. H.; Schawlow, A. *Microwave Spectroscopy;* McGraw Hill Book Company: New York, NY, 1955.

42. Oka, T. On negative inertial defect. *Journal of Molecular Structure* **1995,** *352,* 225-233.

43. Brown, G. G.; Dian, B. C.; Douglass, K. O.; Geyer, S. M.; Shipman, S. T.; Pate, B. H. A broadband Fourier transform micorwave spectrometer based on chirped-pulse excitation. *Review of Scientific Instruments* **2008,** *79,* 1-13.

44. Houston, P. L. Chapter 7. *Chemical Kinetics and Reaction Dynamics;* Dover Publications: Mineola, NY, 2001; 207-209.

45. Skoog, D. A.; Holler, J. F.; Crouch, S. E. Chapter 1. In *Principles of Instrumental Analysis*, 6th ed.*;* Kiselica, S., Ed.; Thomson Brooks/Cole: Canada, 2007; 64-67.

46. Lemal, D. M.; Dunlap, L. H. Kinetics and thermodynamics of (CCF3)6 valence isomer interconversions. *Journal of American Chemical Society* **1972,** *94,* 6562.

47. Wiberg, K. B.; Morgan, K. M.; Maltz, H. Thermochemistry of carbonyl reactions. 6. A study of hydration equilibriia. *Journal of American Chemical Society* **1994,** *116*(24)*,* 11067-11077.

48. Guthrie, J. P. Carbonyl addition reactions: Factors affecting the hydrate-hemiacetal-acetal equilibrium constants. *Canada Journal of Chemistry* **1974,** 898-906.

49. Hart, H.; Rappoport, Z.; Biali, S. E. In *The Chemistry of Enols;* Rappoport, Z., Ed.; Wiley: Chichester, 1990; 502.

50. Schmidt, M. W.; Baldridge, K.; Boatz, J. A.; Elbert, S. T. et al. General atomic and molecular electronic structure system. *Journal of Computational Chemistry* **1993,** *14,* 1347-1363.

51. Zhao, Y.; Truhlar, D. G. The M06 suite of density functionals for main group thermochemistry, thermochemical kinetics, noncovalent interactions, excited states, and transition elements.. *Accounts of Chemical Research* **2008,** *41*(157)*,*

52. Zhao, Y.; Truhlar, D. G. Density functionals with broad applicability in chemistry. *Theoretical Chemistry Accounts* **2007,** *41*(2)*,* 157-167.

53. Krishnan, R.; J., B. S.; Seeger, R.; Pople, J. A. Self-consistent molecular orbital methods. XX. A basis set for correlated wave functions. *Jounral of Chemical Physics* **1980,** *72*(1)*,* 650-654.

54. Glukhovtsev, M. N.; McGrath, M. P.; Radom, L. Extension of Gaussian-2 (G2) theory to bromine- and iodine-containing molecules: Use of effective core potentials. *Journal of Chemical Physics* **1995,** *103*(5)*,* 1878-1885.

55. Feller, D. The role of databases in support of computational chemistry calculations. *Journal of Computational Chemistry* **1996,** *17*(13)*,* 1571-1586.

56. Schuchardt, K. L.; Didler, B. T.; Elsethagen, T.; Sun, L.; Gurumoorthi, V.; Chase, J.; Li, J.; Windus, T. L. Basis set exachange: Acommunity database for computational sciences. *Journal of Chemical Information and Modeling* **2007,** *47,* 1045-1052.

57. Kisiel, Z.; Pszczolkowski, L.; Medvedev, I. Rotational spectrum of trans-trans diethyl ether in the ground and three excited vibrational states. *Journal of Molecular Spectroscopy* **2005,** *233,* 231-243.

58. Kisiel, Z. PROSPE Programs for rotational spectroscopy available from. *<http://info.ifpan.edu.pl/kisiel/prospe.htm>*

59. Pickett, H. M. The fitting and prediction of vibration-rotation spectra with spin interactions. *Journal of molecular spectroscopy* **1991,** *148,* 371-377.

60. Watson, J. K. In *Vibrational Spectra and Structure;* Durig, J. R., Ed.; , 1978; Vol. 6.

61. Hatwig, H.; Dreizler, H. Z. The microwave spectrum of trans-2,3-dimethyloxirane in torsional excited states. *Naturforsch* **1996,** *51a,* 923.

62. Kraitchman, J. Determination of molecular structure from microwav spectroscopic data. *American Journal of Physics* **1952,** *21*(1)*,* 17-24.

63. Dewberry, C. T.; Cooke, S. A.; Grubbs II, G. S. A molecule with small rotational constants containing an atom with a large nuclear quadrupole moment: The microwave spectrum of trans-1-iodoperfluoropropane. *Journal of Molecular Spectroscopy* **2009,** *257,* 66-73.

64. Grubbs II, G. S.; Cooke, S. A. The gas phase characterization of perfluorobutyryl chloride, C3F7COCl, using chirped pulse fourier transform microwave spectroscopy. *Chemical Physics Letters* **2009,** *483,* 21-24.

65. Butcher, S. S.; Wilson, E. B. Microwave spectrum and internal rotation potential of propanal. *Journal of Chemical Physics* **1974,** *61,* 3954.

66. Stiefvater, O. L.; Wilson, E. B. Microwave spectrum, rotational isomerism, and internal barrier functions in propionyl fluoride . *Journal of Chemical Physics* **1969,** *50,* 5385.

67. de Luis, A.; Sanz, M. E.; Lorenzo, F. J.; Lopez, J. C.; Alonzo, J. L. Internal rotation and the chlorine nuclear quadrupole coupling tensor of 1-chloropropane. *Journal of Molecular Spectroscopy* **1997,** *184,* 60-77.

68. Grubbs II, G. S.; Cooke, S. A. The gas phase characterization of perfluorobutyryl chloride, C3F7COCl, using chirped pulse fourier transform miicrowave spectroscopy. *Chem. Phys. Lett.* **2009,** *483,* 21–24.

69. Milot, R. L.; Bohn, R. K.; Churchill, G. B. Microwave studies of 4-methyl-1-pentyne. *Journal of Molecular Structure* **2007,** *837,* 86-91.

70. Sinnott, K. M. Microwave spectrum of acetyl chloride. *Journal of Chemical Physics* **1961,** *34,* 851-861.

71. Grubbs II, G. S.; Dewberry, C. T.; Etchison, K. C.; Serafin, M. M.; Peebles, S. A.; Cooke, S. A. The pure rotational spectrum of pivaloyl chloride, (CH3)CCOCl between 800 and 18800 MHz. *J. Mol. Spectrosc.* **2008,** *251,* 378-383.

72. Grubbs II, G. S.; Dewberry, C. T.; Etchison, K. C.; Kerr, K. E.; Cooke, S. A. A search accelerated correct intensity fourier transform microwave spectrometer with pulsed laser ablation source. *Review of Scientific Instruments* **2007,** *78,* 1-3.

73. Moller, M. P. Note on an approximation treatment for many-electron systems. *Physical Review* **1934,** *46*(7)*,* 618-622.

74. Watson, J. G. Determination of centrifugal distortion coefficients of asymmetric-top molecules . *Journal of Chemical Physics* **1967,** *46,* 1935-1949.

75. Pyykko, P. Year-2008 nuclear quadrupole moments. *Molecular Physics* **2008,** *106*(16)*,* 1965-1974.

76. Harmony, M. D. *Vibrational, Rotational & Raman Spectroscopies Methods and Instrumentation;* Copyright (c) 1999 Academic Press: Lawrence, KS, 1999; 1308-1314.

78. Adkins, H.; Quentin, T. E. Diacylation of water and of hydrogen sulfide with acyl chloride-Pyridine. *A communication from the laboratory of organic chemistry of the university of wisconsin* **1949,** *71,* 2242-2244.

79. Jagod, M.; Oka, T. Inertial defects of planar symmetric top molecules. *Journal of Molecular Spectroscopy* **1990,** *139,* 313-327.

80. Wilson, J. E. Determination of molecular structure with microwave spectroscopy. *Microwave Spectroscopy* **1950,** 108-114.

81. Truhlar, D. G.; Zhao, Y. The M06 suite of density functionals for main group thermochemistry, thermochemical kinetics, noncovalent interactions, excited states, and transition elements: two new functionals and systematic testing of four M06-class functionals and 12 other function. *Theoerical Chemistry Accounts* **2008,** *120,* 215-241.

82. Truhlar, D. G.; Zhao, Y. Density functionals with broad applicibility in chemistry. *Accounts of chemical research* **2007,** *41*(2)*,* 157-167.

83. Dziewatkoski, M. P.; Boss, C. B. A study of hydrocarbon dissociation in a microwave induced plasma sustained in Ar gas. *Spectrochimica Acta* **1994,** *49B*(2)*,* 117-135.

84. Grubbs II, G. S.; Long, B. E.; Powoski, R. A.; Cooke, S. A. Chirped-pulse fourier transform microwave spectroscopy of the simple chiral compound bromofluoroacetonitrile, CHBrFCN. *Journal of Molecular Spectroscopy* **2009,** *258,* 1-5.

85. Lemal, D. M. Perspective on fluorocarbon chemistry. *Journal of Organic Chemistry* **2004,** *69,* 1-11.

86. Li, Z.; Bohn, R. K.; Sweedler, J. V. Comparison of sample pre-treatments for laser desorption ionization and secondary ion mass spectrometry imaging of miscanthus x giganteus. *Bioresource Technology* **2010,** *101,* 5578-5585.

87. Mollendal, H. Chapter 2. *Microwave Spectroscopy;* Kluwer Academic Publishers: Netherlands, 2002; 11-29.

88. Novick, S. E. Extended townes-dailey analysis of the nuclear quadrupole coupling tensor. *Journal of Molecular Spectroscopy* **2011,** *In Press,*

89. Fournier, J. A.; Bohn, R. K. *Talk RH10. 65th International Symposium on Molecular Spectroscopy*, Columbus Ohio, 2010;